# Engineering Optical Properties of Doped Quantum Dots by Chemical Reactions

A thesis submitted by

**Raihana Begum**

to

**Indian Institute of Technology Guwahati**

for the award of the degree of

**Doctor of Philosophy**


Department of Chemistry
Indian Institute of Technology Guwahati
Guwahati-781039, Assam, India

December, 2013

*Dedicated to*
*My beloved Parents*

# Declaration

I hereby declare that the matter embodied in the thesis entitled "**Engineering Optical Properties of Doped Quantum Dots by Chemical Reactions**" is the result of investigations carried out by me in the Department of Chemistry, Indian Institute of Technology Guwahati, India under the supervision of Prof. Arun Chattopadhyay, Head, Department of Chemistry.

In keeping with the general practice of reporting observations, due acknowledgements have been made wherever the work described is based on the findings of other investigators.

Date: 20th December, 2013
Place: Guwahati

Raihana Begum
Roll No. 08612210
Department of Chemistry
IIT Guwahati

**Indian Institute of Technology Guwahati**
Assam- 781 039, INDIA
Tel: (+91) 361-258 2304
Fax: (+91) 361-2690762
**Email: arun@iitg.ernet.in**

Arun Chattopadhyay
Professor and Head
Department of Chemistry

# CERTIFICATE

This is to certify that the thesis entitled "**Engineering Optical Properties of Doped Quantum Dots by Chemical Reactions**" submitted by **Ms. Raihana Begum** for the award of the degree of Doctor of Philosophy, is an authentic record of the results obtained from the research work carried out under my supervision in the Department of Chemistry, Indian Institute of Technology Guwahati, India, and this work has not been submitted elsewhere for a degree.

Date: 20th December, 2013
Place: Guwahati

Prof. Arun Chattopadhyay
(Thesis Supervisor)

# Engineering Optical Properties of Doped Quantum Dots by Chemical Reactions

By

**Raihana Begum**

Submitted to the Indian Institute of Technology Guwahati on 20th December, 2013 in partial fulfillment of the requirements for the degree of Doctor of Philosophy

## Abstract

Understanding the origin of emitting species and the contribution of the surface ions in quantum dots (Qdots) towards the overall photoluminescence are important and much remains to be explored. The current thesis primarily deals with the decisive role of the surface ions in doped Qdots and their potential to react with external chemical species, thereby tuning their optical properties.

This was approached with three different binary quantum dots (Qdots); having the same host but different dopants. Experimental results reveal that systematic removal (via chemical means) of the surface ions as well as ions present in the immediate vicinity, resulted in reproducible changes in emission quantum yield as well as emission energy, which ascertained their contribution towards the overall emission.

Furthermore, significance of electronic state of the dopant ions in the emission of the Qdots has been successfully demonstrated. When they react with redox reagents such as sodium borohydride and potassium peroxodisulfate, anticipated change in their oxidation state is reflected through significant changes in their emission spectra. This thus implies that the Qdots could be used as potential redox probes for local oxidation/redox milieu in mammalian cells.

Thesis Supervisor: Arun Chattopadhyay

Title: Professor of Chemistry

# Preface

The following chapters of the thesis have appeared in previously published articles. Copyright approval has been obtained for the figures and text.

**Chapter 2**

Reproduced with permission from *Langmuir* **2012**, 28, 9722–9728.
Copyright 2012 American Chemical Society.

**Chapter 3**

Reproduced with permission from *Langmuir* **2011**, 27, 6433-6439.
Copyright 2011 American Chemical Society.

**Chapter 4**

Reproduced with permission from *Nanoscale* **2014** (DOI: 10.1039/C3NR05280J)
Copyright 2013 Royal Society of Chemistry.

**Chapter 5**

Reproduced with permission from *Journal of Physical Chemistry Letters* **2014**, 5, 126–130. Copyright 2013 American Chemical Society.

# Acknowledgement

At the outset, I would like to express my heart-felt regards and profound sense of gratitude to my supervisor, Prof. Arun Chattopadhyay for his motivation and unflinching support. This interesting piece of work would have never been possible but for his mentoring. One would really be blessed to have such an inspiring guide who gave us the desired freedom in research and practicals to cultivate a proper scientific temperament among us. His in-depth knowledge and original thinking has immensely guided this work. A mere word of thanks seems insufficient to express my indebtedness towards him.

I would like to extend my sincere thanks to Dr. B. Mandal, chairman and other members; Dr. S. S. Bag and Dr. Biplob Bose, of the doctoral committee for their guidance and evaluation through my research progress.

I also take this opportunity to thank Dr. Anumita Paul and Prof. S. S. Ghosh for their collaborative support and proving us with the best facilities. Also, my sincere thanks to all other faculty members and the non-teaching staff of Chemistry Department for valuable involvement in this work. Thanks also goes to the staff of Central Instruments Facility and particularly, Centre for Nanotechnology. Special thanks to Mr. Indrajit Talukdar for the transmission electron microscopic measurements. I sincerely acknowledge CSIR, Delhi and IIT Guwahati for fellowships.

I express my gratitude to my senior labmates Dr. B. R. Panda, Dr. J. Deka, Dr. S. K. Gogoi and Dr. S. Mallick for mentoring me and introducing me to the new instruments and techniques, particularly Dr. A. Murugadoss for his initial help in working with zinc sulphide quantum dots. I would also like to thank our present group members –Nirmala, Subhojit, Rumi, Palash, Satya, Rama, Sunil, Anushree, Shilaj, Upashi, Uday, Sabya and Kafeel- for the friendly working atmosphere and their nice company that was really important for the completion of the thesis. I had the privilege to collaborate with my collegue Amaresh K. Sahoo from Centre for Nanotechnology for biological cell imaging experiments. It was really nice working with him.

Thanks to all my fellow research scholars of Chemistry Department, specially Krishnamurthy group members with whom I have interacted over the past few years.

I acknowledge the invaluable friendship of Priyanka, Sujata, Bapan, Prasenjit, Nilamoni and many of my school freinds. Heartfelt thanks to Anasuya who helped keep my composure during the tough times. Special thanks to two of my wonderful friend Bandana and Lim for their unwavering support all the way till the finale of thesis submission. I am truly blessed to have such trustworthy and lovable friends and wish for a lifelong friendship.

I also acknowledge the constant support and motivation I recieved from my local guardians at Guwahati- Syed S. Rahman, Dr. I. S. Mumtaza, Syed A. Shah and their family.

Heartfelt thanks goes to my parents and siblings-Farhana, Tahshina and Zahid for their endless love and affection. Today I am what because of the innumerable sacrifices they have made for me. I truly appreciate their understanding and constant support for my higher studies. This dissertation is affectionately dedicated to them.

At the end, I would like to thank the Almighty Allah, for all His mercy and blessings throughout my life and career….!!

Raihana Begum
Guwahati

# Table of Contents

# List of Abbreviations

| | |
|---|---|
| AAS | Atomic Absorption Spectroscopy |
| AcAc | Acetyl Acetonate |
| AR | Auger Recombination |
| CB | Cation Beads |
| DLS | Dynamic Light Scattering |
| DNA | Deoxyribonucleic Acid |
| FFT | Fast Fourier Transform |
| FTIR | Fourier Transform Infrared Spectroscopy |
| FWHM | Full Width at Half Maximum |
| GSH | Glutathione |
| HDA | Hexadecylamine |
| HNs | Hetero-Nanostructures |
| HOMO | Highest Occupied Molecular Orbital |
| KPS | Potassium Peroxodisulfate |
| LED | Light Emitting Diodes |
| LUMO | Lowest Unoccupied Molecular Orbital |
| MPA | Mercapto Propionic Acid |
| NCs | Nanocrystals |
| NIR | Near Infra-Red |
| NPs | Nanoparticles |
| PL | Photoluminescence |
| QDLED | Qdots Based Light Emitting Diodes |
| Qdots | Quantum Dots |
| QE | Quantum Efficiency |
| QY | Quantum Yield |
| ROS | Reactive Oxygen Species |
| SAED | Selected Area Diffraction |
| TEM | Transmission Electron Microscopy |
| TOPO | Trioctylphosphine Oxide |
| TPP | Sodium Tripolyphosphate |
| TSC | Trisodium Citrate |
| XPS | X-Ray Photoelectron Spectra |
| XRD | X-Ray Diffraction |

# List of Schemes

# List of Figures

# Chapter 1

## Introduction

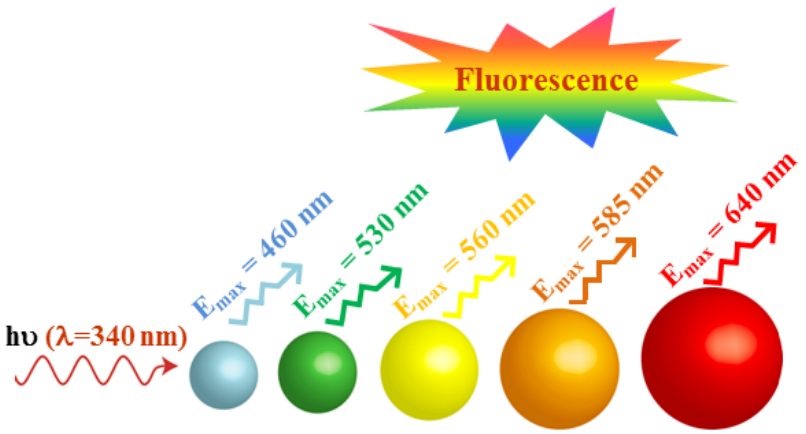

# Chapter 1

## Introduction

Fluorophores are ubiquitous in nature and in materials world. Traditionally natural and synthetic dyes have represented fluorophores for use in human civilization. With the advancement of science various inorganic complexes and organic polymers have also been realized to be of potential use as fluorophores. Typical uses of the fluorophores have been in the fields of biological imaging, agricultural research, optoelectronics, and so on. The area of optoelectronics has witnessed immense developments with the generation of numerous energy efficient devices, namely, organic dye lasers, dye sensitized solar cells, organic light emitting diodes, etc.[1-12]

Notwithstanding the advantages of the conventional fluorophores, there was a need for a new material that would provide high photostability, thermal and chemical stability, and high quantum yield (QY), that are otherwise not realized in most fluorophores. This need was fulfilled with the advent of quantum dots (Qdots) that are light-emitting quantum-sized particles found to be promising alternatives to many of the known organic and inorganic fluorophores. The present thesis is based upon such Qdots, primarily ways to tuning their photo-physical properties.

## 1.1. Quantum Dots

Qdots are known to be 20 times brighter and 100 times more stable than organic dyes.[13-14] These are zero dimensional semiconducting nanocrystals (NCs) of size range 1- 10 nm. The discovery of size dependent behaviour in semiconductors took place in the year 1981 by Alexei Ekimov and his co-workers, while they were working on CuCl crystals grown on a glass matrix.[15] Later in 1983, Louis E. Brus introduced colloidal CdS nanocrystals.[16-17] The term 'Quantum dot' is believed to be coined by Mark Reed in the year 1988.[18] Qdots are also known as 'artificial atoms' because of their atom-like discrete density of electronic states.[19-22]

Though, zero dimensional, a Qdot is considered as a box in quantum mechanics. The electron-hole pair formed upon photo-irradiation i.e. the excited electron in

the conduction band (CB) and the hole subsequently left behind in the valence band (VB), also called 'exciton' is the quasi-particle which is confined within the box. Exciton is a neutral particle, where the electron ($e^-$) and hole ($h^+$) pair is held together by Coulombic interactions, similar to a hydrogen atom. Because of the three dimensional confinement of the charge carriers ($e^-$ or $h^+$), they only can occupy very specific energy levels i.e. the energy levels become discrete, unlike continuous bands of bulk semiconductor (shown in Figure 1-1). 'Quantum confinement' makes the exciton very energetic, especially when the size of the nanocrystal is very small. The exciton can either reemit a photon with energy equivalent to $E_g$ or undergo non-radiative recombination.[23-25]

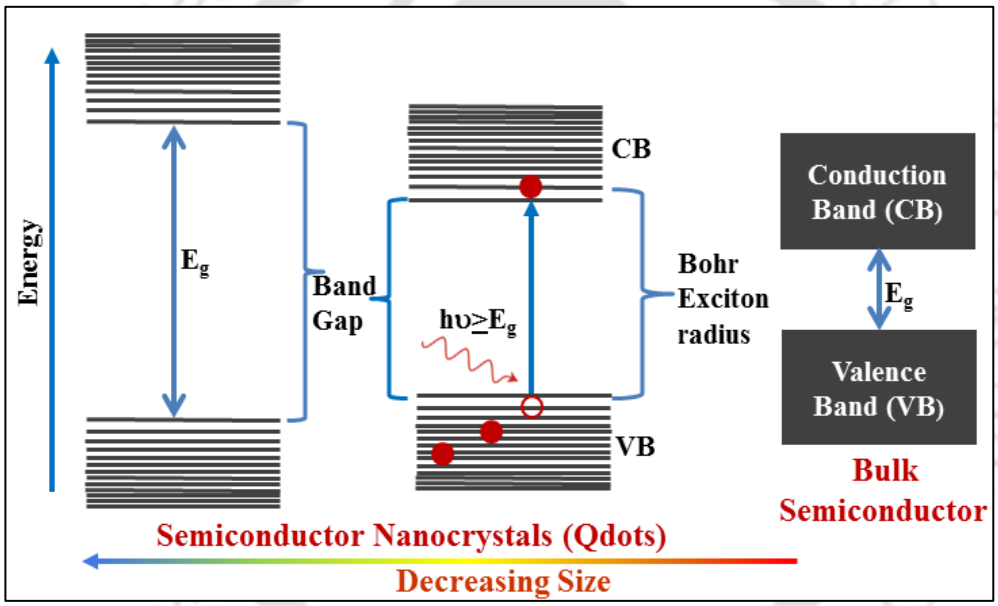


**Figure 1-1.** Schematic representation of quantum confinement showing effect of reduced dimension on band gap energy.

### 1.1.1. Optical Properties and applications of Qdots

Quantum confinement assigns many important properties to Qdots. The most important being size dependent emission profile i.e. the band gap energy increases with decrease in size of the nanocrystal. Qdots have high extinction coefficient and high QY. They have large absorption window and can be excited over a broad excitation window. Another important property is their narrow

emission (full width at half maximum (FWHM) which is practically 20-30 nm), thereby showing small Stokes shift, whereas conventional fluorophores have FWHM larger than 50 nm. Organic dyes absorb in a narrow spectral window and show a reasonable Stokes shift requiring spectral filters. Furthermore, unlike organic dyes, which tend to photobleach easily, Qdots have better photostability against photobleaching and thermal stability too.[14, 25-27] Arguably, with these fascinating properties, Qdots have surmounted the constraints of organic fluorophores and have replaced them to a great extent.[28]

Qdots have wide applications in diverse fields. For example, Qdots have been successfully used in biomedical industry like bioimaging, as biological marker, fluorescent probe and biosensor, in immunoassays, optical barcoding, etc. With longer lifetime up to hours, Qdots allow data collection or imaging over long times with continuous excitation without a filter. Interference due to autofluorescence in the visible spectrum by biological cells could also be avoided by use of Qdots, as their emission could be tuned by varying size or using Qdots that emit in the near infra-red (NIR) region.[29-38]

Because of surface dependent properties of Qdots, they have also been used as photocatalytic material for hydrogen evolution and decomposition of dyes, detection of organic compounds, other pollutants and heavy metal sensing, thereby helping in environmental remediation.[39-43]

Qdots have technological uses too and have been able to overcome two major constrictions- energy conversion and cost of production of conventional photovoltaic cells. In this regards, with Qdots incorporated into conducting polymer, such photovoltaic cell can be made cheaper and more efficient with multiple exciton generation, resulting in higher photocurrent.[44-46] Qdots based light emitting diodes (QDLED) with improved color saturation and high color rendering index have already been put to commercial use. In addition, Qdots films have been used for QDLED displays, photonics, highly efficient lasers, optical sensors and fabrication of many other optoelectronic devices.[47-55]

### 1.1.2. Type of Quantum Dots

Qdot nanocrystals basically comprise elements from the II-VI, III-V or IV-VI of the periodic table. The II-VI Qdots like CdSe, CdS, ZnS and ZnSe possess high

fluorescence because of their direct band-gap. III-V Qdots like InP, InAs and IV-IV Qdots like PbS, PbSe, PbTe with small band gap energy also have been reported.[56-61]

Apart from these binary Qdots, ternary I–III–VI Qdots like $CuInS_2$, $CuInSe_2$, $AgInS_2$, $GaInP_2$ etc. have been introduced in the recent past.[62-66] Depending on their composition and structure, they are either called core shell or alloyed Qdots. Ternary alloyed core/shell Qdots like $InAs_xP_{1-x}$/InP/ZnSe and $CuInS_2$/ZnS Qdots, which also emit in the NIR region have been reported in the literature.[67-69] Very recently, binary alloy of $Bi_{1-x}Sb_x$ and quaternary I-II-III-VI $CuZnInS_3$, Zn–Ag–In–Se Qdots were also introduced.[70-72]

Various transitional, as well as rare earth metal ions like $Mn^{2+}$, $Cr^{3+}$, $Co^{2+}$, $Ni^{2+}$, $Cu^{2+}$, $Ag^{+}$, $Pb^{2+}$, $Eu^{3+}$, $Tb^{3+}$, $Sm^{3+}$ and $Er^{3+}$ have been doped into the above mentioned binary Qdots, as well as most of the ternary core shell/alloyed Qdots.[73]

## 1.2. Synthesis and Surface Passivation

Synthesis of Qdots has been categorized as top-down and bottom-up method. 'Top-down' methods include electron beam lithography, reactive-ion etching, focused ion beam technique etc.; however such Qdots often have poor reproducibility and develop crystal imperfection during patterning and have reduced optical emission. Qdots prepared by 'bottom-up' processes like micro-emulsion, sol-gel, aqueous co-precipitation method, hot-solution decomposition, hydrothermal/solvothermal method have advantages like control over size, shape and monodispersity.[74-77]

Colloidal synthesis is comparatively easier and needs only three components-solvent, precursor materials and a capping agent- usually a long chain molecule.[77] A stabilizing agent is always wisely chosen as it controls growth of nanocrystals and prevents them from further aggregation by charge neutralization. Also, it determines size, shape and solubility of NCs in a polar or non-polar medium. Characteristic properties of Qdots largely depend on its synthesis conditions like-precursor materials, solvents, reagent concentrations, temperature, growth time, etc.[78-84]

In a perspective article on Qdots, [85] Luther and Pietryga stated that "Qdots can be a double-edged sword, as Qdots are inherently surface dominated". As size of

Qdot decreases, its surface-to-volume ratio increases and thus a large fraction of surface atoms, having low coordination number become highly reactive or remain unsaturated.[86-87] Thus it is very important that during growth of the Qdots, those surface ions are chemically well passivated so that the surface is nearly inert to the charge carriers. Presence of defects in the form of vacancies, non-stoichiometry or local lattice mismatches, dangling bonds or loosely bonded atoms simply as adsorbates at the surface may act as trap states.[26-27] Such trap states can capture electron or hole and following radiative recombination produces defect (trap) emission-via pathway '(B)', shown in Figure 1-2. In absence of trap states, the exciton decay through radiative pathway '(A)' producing band-edge emission.[26]

Alternatively the exciton may recombine nonradiatively via pathway '(C)' with extra charge carriers formed as result of separation of photo excited electron-hole pair (under the condition when $kT$ is greater than exciton binding energy[88]), a process known as Auger recombination (AR). 'Blinking', also called 'on/off' behaviour is known to cause by AR. It is observed as fluctuations in photoluminescence (PL) intensity with time under constant excitation. Blinking is often followed by 'spectral diffusion', also known as 'blueing'. Spectral shift (up to ~ 15 nm) is attributed to change in charge distribution around the Qdots due to photoionization/photooxidation process.[89-93]

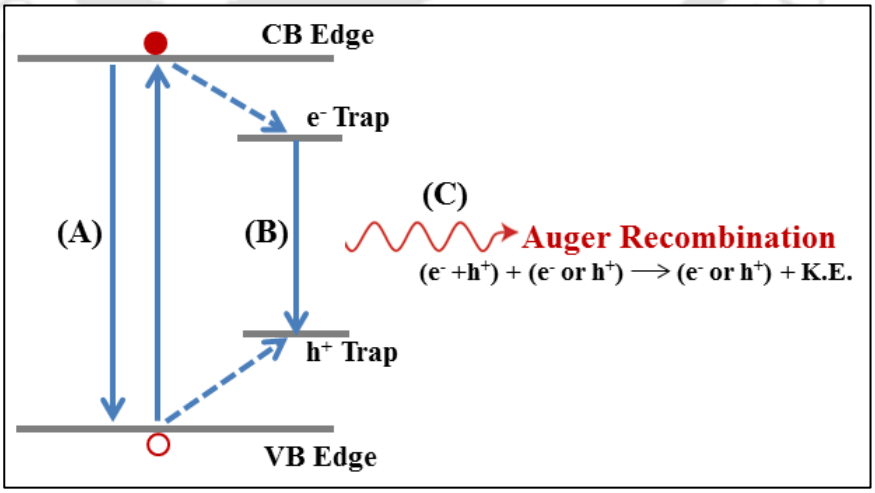


**Figure 1-2.** Energy level diagram showing trapping of electrons and holes and possible radiative and nonradiative recombination.

As passivation plays an important role in deciding quantum efficiency (QE) of the Qdots by eliminating the surface traps and confining the charge carriers; one can literally expect near unity QY in absence of the defects and trap states. Chemical passivation is usually done either during synthesis of Qdots or post synthesis via two ways - ligand capping/exchange and epitaxially growing inorganic shell structures.

### 1.2.1. Organic Capping Structures

Generally, coordinating organic molecule with large HOMO-LUMO gap like trioctylphosphine oxide (TOPO), dodecylamine (DDA), hexadecylamine (HDA), etc. are used as capping ligand.[94] The choice of ligand is based on surface stoichiometry of Qdots, whether the surface of Qdots is anion or cation rich. For example, phosphine ligands are used for anion rich surface, while ligand containing oxygen and nitrogen like alkylamine or alkylphosphine oxide ligands are used for cation rich surface of Qdots.[95-96] The coordinating ligand determines the inter-particle distance, electron transport and more importantly decides the compatibility of the Qdots with chemical environment. For example, a well-established method for synthesizing high quality CdSe Qdots is organometallic route[79-80] that uses coordinating solvent TOPO at high temperature ~$290^0$-$350^0$C. Since alkyl chain facing outward makes the Qdots insoluble in polar solvent, so removal of the top layer of TOPO and then replacing those by organic ligands with polar end group makes the Qdots hydrophilic.[87]

Another way is to replace with a linker which is amphiphilic i.e. hydrophobic on one end and hydrophilic on the other. Silane derivatives of thiol, aminopropyl-silanes or phospho-silanes serve best for this purpose, ensuring solubilisation in aqueous buffer and allow further functionalization.[97-100] Biolinkers like oligopeptide, oligonucleotide,[101] serum albumins, bifunctional thiol ligands are also often attached to the surface of Qdots via biomolecules like DNA, glycoprotiens, transferrin, etc. for use in biosensing.[101-105] Further, optical properties especially PL intensity and emission peak wavelength have been reported to be tuned via post-synthetic ligand exchange. For example, upon ligand exchange with 3-mercaptopropionic acid (MPA) of as grown TOPO/DDA capped

CdS Qdots, the emission wavelength was changed from blue to red along with increase in QY by varying concentration of MPA.[106]

However, post surface modification or functionalization increases the overall size of the Qdot inducing steric hindrance and thus not preferred for bio-applications. Furthermore, use of a long alkyl chain ligand, makes the Qdots insulating in nature and thus as-synthesized Qdots cannot be used for fabrication of optoelectronic devices.[107-109] Therefore, long chain capping ligands are often exchanged with small molecules like hydrazine, ethanedithiol, ammonium thiocyanate, etc., which are more conductive and facilitate charge transport.[109]

### 1.2.2. Inorganic Capping Structures

Organic ligands being more labile may get detached from the surface of Qdots or photo-degraded during photoexcitation causing photobleaching.[110] In that case, the unpassivated Qdots may try to saturate the resulting dangling bonds via surface reconstruction.[111] Defects may re-appear leading to non-radiative recombination. This motivated researchers to look for inorganic ligand capping agents.[112]

#### 1.2.2.1. Inorganic ligand

It was the Talapin group who first introduced the concept of using metal chalcogenide complexes, which provide better stability to the colloidal Qdots through chalcogenide bridges and does not affect its conductivity. A stable colloidal solution of CdSe Qdots capped by $In_2Se_4^{2-}$, $Sn_2S_6^{4-}$ etc. having approximate size length of 0.7 nm were reported. However, such metal complex were found to affect other chemical and physical properties of the Qdots, for example, their redox properties.[113-114]

Later the same research group reported use of metal free ligands like $S^{2-}$, $HS^-$, $Se^-$, $HSe^-$, $Te^{2-}$, $HTe^-$, $OH^-$ and $NH_2^-$ etc. [115] Similar to this, they proposed atomic ligand capping. Ammonium salt of the halide ions like $Cl^-$, $Br^-$ and $I^-$ having average size 0.1 nm were used for the purpose since these ions have strong affinity for the cations on the surface of Qdots. Cation rich PbS and CdS Qdots were passivated with monolayers of halide ions to render n-type behaviour.[116-117]

### 1.2.2.2. Inorganic core-shell

Apart from ligand capping of Qdots, another prevalent method is inorganic shell capping. Inorganic shell passivated Qdots have been found to be more robust with high QY and better thermal and photochemical stability. Optical properties of the core are not affected by the presence of oxygen or water molecules in the local chemical environment, making them ideal candidates for versatile use. Depending on the alignment of respective VB and CB of core and shell material, core-shell Qdots were classified as- type-I, reverse type- I and type-II (Figure 1-3).[118]

In type-I Qdots, the bandgap of shell is larger than that of the core and both electron and hole are confined in the core, e.g. CdS/ZnS, CdSe/ZnS core-shell Qdots.[119] By increasing the size of the core, the emission could be tune towards red region. In the case of reverse type-I Qdots, bandgap of the shell is smaller than that of the core and thickness of the shell decides the PL emission, example includes CdS/CdSe, ZnSe/CdSe Qdots, etc.

While in type-II Qdots, either of VB and CB of the shell is located in the band gap of the core. As a result, either of electron or hole is confined in the core, while the other in the shell, e.g. CdTe/CdSe, CdSe/ZnTe Qdots, etc. Emission in type-II Qdots results from the radiative recombination of the exciton across the core and shell boundary. By increasing the size of core (4.5 nm to 6 nm), emissions have been reported to be tuned from 460 nm to 630 nm, in case of type II ZnSe/CdS core-shell Qdots.[120] On the other hand, by varying the number of monolayers of shell material, as well as core size, emission in type-II CdTe/CdSe Qdots was reported to be tuned from 700 nm to 1000 nm.[121]

Multi-shell growth is known to suppress photoblinking and AR by separating the charge carriers between core and shell.[122-124] Lately Viswanatha group has showed near unity QY (> 90%) with high stability, reduced AR and suppressed blinking by growing thick shell of CdS over CdSe Qdots.[125] Further, shell also reduce toxicity of Qdots by not allowing release of toxic cations like Cd and Pb into the medium.[34, 119]

### 1.2.2.3. Alloyed composition

Though core-shell Qdots have advantages like thermal and photochemical stability, [126-128] but because of lattice mismatch on the core and shell interface

induced during the shell growth, they give rise to interfacial defects. To overcome this stress, alloyed Qdots- homogeneous alloy and gradient type were suggested (Figure 1-3). Interfacial defects have been avoided in absence of an abrupt boundary by a gradual transition from core to shell materials. Some examples of alloyed Qdots are $Zn_xCd_{1-x}Se$, $Zn_xCd_{1-x}S$, $CdSe_xSe_{1-x}$, $CdSe_xTe_{1-x}$, ZnCdSSe, etc.[129-130]

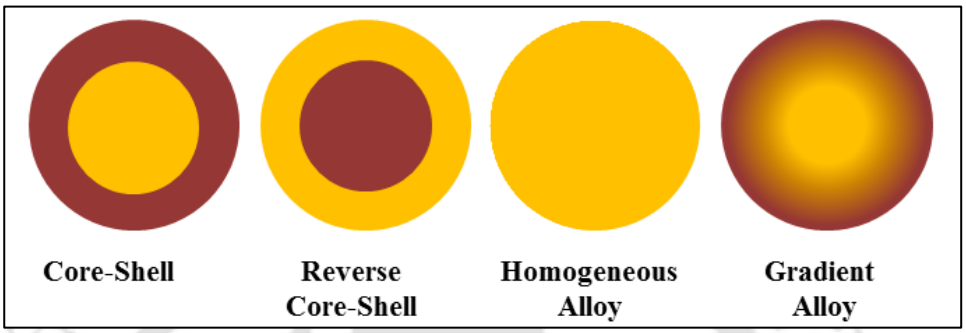


**Figure 1-3.** Schematic representation of Qdots of different compositions. Redrawn from J. Am. Chem. Soc. 2003, 125, 7100-7106. Copyright 2003 American Chemical Society.

Depending on the composition of the alloyed Qdots, emission could be tuned covering whole of the visible spectral window. Nie group had demonstrated tuning of optical emission by varying the constituent stoichiometries and internal structure of CdSeTe alloyed Qdots without changing the particle size.[131] Similar composition based tuning- high QY and tunable emission from 500 nm to 950 nm has also been demonstrated with I-III-VI Qdots like $CuInS_2$ and ZnS-$CuInS_2$ alloyed Qdots.[64, 132] Size independent tunable emission in the blue-yellow region have been reported with $(Zn_{1-x}Cd_x)Se$ alloyed Qdots. Of late it was reported by Groeneveld et al. that reaction temperature plays a key role in deciding the composition- core/shell, gradient or alloyed Qdots.[133] Further, Smith and Nie have reported synthesis of alloyed $Hg_xCd_{1-x}Te$ Qdots from CdTe binary Qdots via partial replacement of $Cd^{2+}$ by $Hg^{2+}$ in CdTe nanocrystals.[134] This allowed tuning of band gap energy without changing the lattice parameters.

### 1.2.3. Ion exchange reactions

In addition to size and compositional tunable emissions of Qdots, shape tunable optical properties have also been widely studied. By controlling reaction

conditions like temperature, monomer precursor concentration or by addition of surfactants, one dimensional disk, quasi-two dimensional platelets, also various elongated shapes including, rod shaped, rice shaped, pencil, arrow and tree-shaped NCs have been reported.[135-137] Octahedral, star-shaped, cubic and truncated octahedral shaped PbS nanocrystals have also been reported in the recent past.[138] Even more complex hetero-nanostructures (HNs) like hetero-nanorods, hetero-dumbbells, barbell, heterodimers, tetrapods and octapods have been introduced.[77, 139-147] Such branched nanocrystals have enormous applications in optoelectronic industry and for catalysis purpose too.[148] HNs allow tailoring of optical properties since they are known to interact less with the surface states and thus charge carriers trapping could be inhibited.[140-141]

HNs are synthesized by ion exchange reactions which otherwise could not be synthesized by conventional methods.[141] Nanocrystal of a given shape and crystal structure could be transformed via post synthetic cation exchange reaction into another nanocrystal that retains the original characteristics. For example, wurtzite CdSe nanocrystals were transformed in ZnSe, following two cation exchange steps involving Cu ions and Zn ions.[149] Similarly ZnS Qdots were chemically transformed to stable colloidal solution of $Ag_2S$, PbS and HgS nanocrystals by direct cation exchange with the respective ions.[150] Cation exchange reaction process can give rise to improved magnetic properties.[151] It has also been used to introduce dopants into binary Qdots, for example, ZnTe: Mn, InAs: Cu, Ag or Au, and CdSe: Ag.[152-155]

### 1.3. Doped Quantum Dots

Doped Qdots in the form of impurity ions present in the semiconductor NCs have added to their eminence via tuning their emission properties. Dopant introduces atomic states within the band gap of the host, which being confined within a small volume; strongly influence the optical properties of the host.[156-157] For example, QE of doped Qdots is found to be higher, because of greater overlap of the exciton of the host with the localized dopant states, further emission of the host could be red-shifted via doping. The lifetime of dopant emission is longer compared to band-edge emission or defect related emission and is often not perturbed by change in environmental condition, unlike host emission. Another advantage is

their less self-quenching due to large Stokes shift. Optical properties of the host could be tuned by doping with different elements; concentration, location and nature of the dopant element play important role in this regard. Doping is indeed an effective way to modify the functionality of Qdots.[158]Apart from binary Qdots, ternary, core-shell, alloyed Qdots and HNs having suitable band gap have also been doped. For example, Cu: InP/ZnSe core/shell Qdots, Cu-doped $Zn^{II}$–$In^{III}$–$Se^{VI}$, Cu-Zn-In-S ternary alloys[71] Mn doped $Zn_{1-x}Mn_xSe$/ZnCdSe core/shell Qdots, etc. have been reported.[156-166]

### 1.3.1. Doping Methods

Different methods to introduce dopant into host Qdots have been proposed till date. Reaction conditions as well as timing of addition of dopant are decisive factors for QE. Two methods that are reported to have yield high quality Qdots are 'nucleation-doping' and 'growth-doping' methods proposed by Peng group (Figure 1-4).[167]

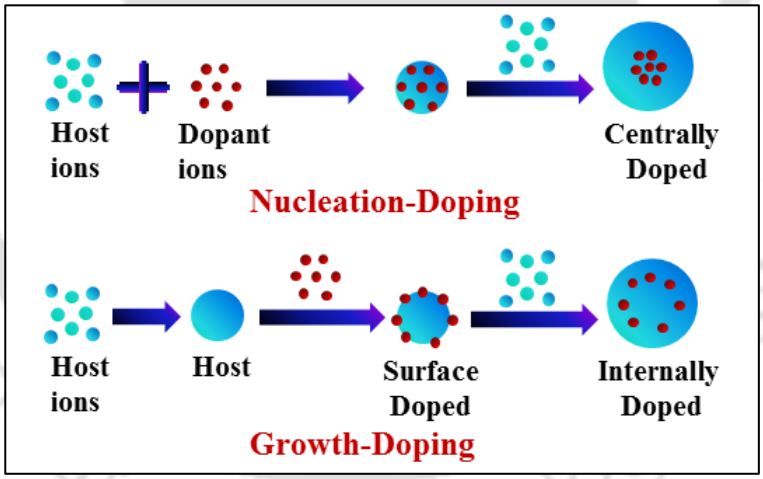


**Figure 1-4.** Schematic representation of nucleation and growth doping. Redrawn from J. Am. Chem. Soc. 2005, 127, 17586-17587. Copyright 2005 American Chemical Society.

Nucleation doping method involves addition of dopant and host precursor together, while growth doping method involves addition of dopant at low temperature subsequent to host growth, which results into surface doped Qdots. Other popular methods includes 'doping through ion diffusion', 'trapped-dopant model', 'radial-position controlled dopant model', etc.[168-172]

A conventional method like aqueous co-precipitation method however involves addition of dopant and host precursor together, while remote doping method involves introducing extra electrons into host Qdots with the help of a molecule attached to the surface or electrochemically. Irrespective of the route, doping is a means to increase concentration of charge carriers; that dramatically changes the optical, electronic, magnetic and conductivity of the host.[157]

### 1.3.2. Electrochemical Doping

Conductivity of semiconductor NCs is traditionally measured by applying an electrochemical potential. By applying electric current, electrons could be injected into the quantum-confined states of the nanocrystal that changes the oxidation number of the nanocrystal, leading to changes in PL properties of the Qdots. The injected electron gets localized in the surface states or delocalized in the conduction band of the nanocrystal, thus facilitating optical transition and causing chromic changes.[173] Sionnest group for the first time introduced this concept and has demonstrated reversible 'on/off' emission upon variation in the electrochemical potential in CdSe/ZnS core shell Qdots.[174] In the presence of a free electron in the CB, the exciton energy is transferred to it, which hinders radiative recombination, resulting quenching of the band edge emission. They have also reported voltammetric and electrochromic response in CdSe nanocrystal thin film and hole injection in PbSe Qdot films.[175-176] Similar observations were also made by Gamelin group in case Mn doped CdS Qdots. It was then proposed that electron injection leads to decrease in PL QY through electron-exciton Auger recombination.[177]

Lately electrobrightening by applying cathodic bias to the Qdots was reported by Gamelin group. They have demonstrated electrobrightening up to ~ 40 fold in ZnSe Qdots, which according to them could be possibly due to reductive passivation of surface traps, when reducing potential higher than ZnSe conduction band potential was applied. They also reported electrobrightening in case of doped Qdots too, especially Mn doped ZnSe.[178]

### 1.3.3. Photoluminescence mechanism

Understanding the luminescence mechanism of doped Qdots is important as it is very different from their undoped counterpart and varies depending on the dopant and host.[157] Although CdS and CdSe Qdots are commonly employed as host, ZnS with wider band gap of 3.6 eV has special advantage of being nontoxic and allows longer dopant emission lifetime. Among all transition metal ions, doping with Mn and Cu have been widely studied.[179-182] Emission could be tuned corresponding to different metal ions doped in the same host. For example, Mn doped ZnSe emits yellow-orange color, while Cu doped ZnSe emits green (Figure 1-5).[183]


**Figure 1-5.** Fluorescence image of Mn and Cu doped ZnSe Qdots. Reprinted with permission from J. Phys. Chem. Lett. 2011, 2, 2818–2826. Copyright 2009 American Chemical Society.

Bhargava et al first reported Mn doped ZnS having QY~ 18%, the Qdots were prepared in organic medium by using diethyl zinc, diethylmanganese and hydrogen sulphide stabilized by methacrylic acid.[184]

#### 1.3.3.1. Mn doped Qdots

Among 3d transitional metals Mn has highest magnetic moment, when introduced into a host, it induces magnetic behaviour. Mn doped ZnS Qdots thus have found important applications in magneto-optical devices. When a Mn doped ZnS Qdot absorbs a photon of light, radiative recombination takes place at the band edge, accompanied by energy transfer to the Mn d states. As a result, it emits dual colour, blue and orange with emission peak centred at 420 nm and 590 nm. The

1st peak is due to band-edge emission (blue), while the peak at 590 nm (orange) is due to a transition from $^4T_1$ to $^6A_1$ Mn d- states (Figure 1-6).[182, 185]

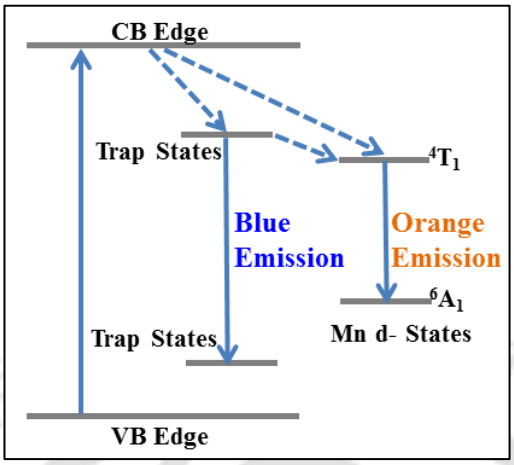


**Figure 1-6.** Energy level diagram of Mn doped ZnS Qdots.

Although Mn d-d transition is spin forbidden, but hybridization between Mn d states with s-p states of the host is responsible for its relaxation. This hybridization causes faster energy transfer from ZnS host to Mn dopant and therefore increased QE. Bol and Meijerink reported decay time of $^4T_1$ - $^6A_1$ Mn transition in the range of millisecond (~ 1.9 ms).[184, 186]

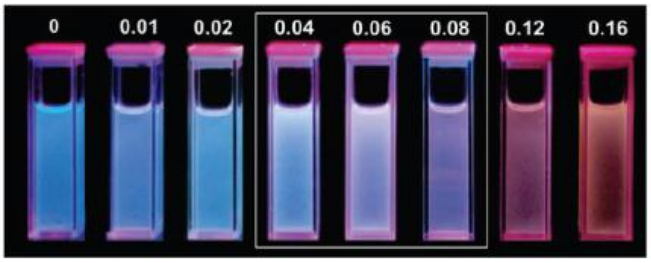


**Figure 1-7.** Digital images of Mn doped ZnS Qdots under UV excitation. The numerical value indicates the concentration of the dopant. Reprinted with permission from Langmuir, 2009, 25, 10259-10262. Copyright 2009 American Chemical Society.

The emission intensity due to $^4T_1 \rightarrow {}^6A_1$ transition emission intensity at 590 nm increases with subsequent decrease in band edge emission with increasing doping

concentration, but up to an optimum level, beyond which it may contribute to quenching.[182, 185-187]

The Mn atomic emission is widely accepted to be independent of size, shape and nature of host.[188-191] However, Chen et al.[192] reported size dependent emission shift of Mn doped ZnS grown in zeolite-Y. The authors stated that emission shift from 591 nm to 570 for a large size variation of 10 nm to 3.5 nm is because of electron-phonon coupling. Sarma group[193] also reported size dependent emission shift of 40 nm for a size variation from 1.9 nm to 2.6 nm, for Mn doped CdS Qdots, the reason being change in crystal field corresponding to the location (core versus surface) of the dopant. Dopant ions present in the core are known to have tetrahedral geometry; while subsurface ones have distorted tetrahedral and surface adsorbed dopants ions have octahedral geometry.[180] While Peng group has observed that Mn atomic emission to be dependent on the shape of the nanocrystal. PL intensity is less when the shape of the nanocrystal deviates from nearly spherical.[194]

Multicolour tuning (from blue to orange) in Mn doped ZnS has been reported by varying Mn concentration (Figure 1-7).[187] Pradhan and Peng have reported highly efficient (QY~40-70 %) and thermally stable Mn doped ZnSe via growth doping method, where they have demonstrated PL tuning from 565 nm to 610 nm by changing reaction conditions.[195]Colour tunable dual emission has been reported in case of Mn doped in type-I core-shell Qdots like CdS/ZnS upon exciting at a single wavelength but different excitation intensity.[196] Synthesis temperature is also a key factor in deciding QE of Qdots.[181] Chen et al. have demonstrated temperature dependent lattice diffusion of dopant. Their experimental results suggested four elementary steps in the process of doping- “surface adsorption”, “lattice incorporation”, “lattice diffusion”, and “lattice ejection” each of which is temperature dependent. Pressure also has been reported to affect the PL properties, with increase in pressure the emission shift to lower energy.[197]

#### 1.3.3.2. Cu doped Qdots

Cu doping is important as depending on the size and nature of host, the emission could be tuned covering the entire visible spectrum. For example, Cu doped in ZnSe emits green; Cu doped ZnS emits bluish green.[191] While in Cu doped CdS,

emission could be tuned from 550 nm to 650 nm by varying the concentration of the dopant and QY maximized up to 50%.[198] On the other hand Cu doped in InP and coated by ZnSe shell, emit in the red and NIR region (between 630 nm and 1100 nm) depending on the size of the InP host.[199] PL tuning also has been demonstrated with Cu doped ZnSe Qdots synthesized by growth doping method, where the emission wavelength has been tuned from 470 nm to 550 nm, along with QY increase up to 30% through 10%.[167] Cu doping is bit complex than Mn doping because of stability problems. Copper when present as a dopant has the possibility of existing in either of +2 or +1 oxidation states in the as synthesized Qdots and PL mechanism is still under debate.

### 1.4. Challenges

Apart from the blinking and associated issues of AR, discussed briefly in the beginning of this chapter, there are issues that need special attention. For example, toxicity and difficulties related to doping.

#### 1.4.1. To dope or not to dope

P. V. Kamat stated in one of his editorial articles of JPC Letters, "Hence, the question remains, to dope or not to dope!"[200] Doping in semiconductor NCs is indeed a challenging task. One of the concerns is controlling the dopant concentration and its location in the Qdots- core, interstitial sites, surface and near-surface. Further, due to longer dopant lifetime, doped Qdots are found to be more sensitive to Auger quenching than their undoped counterparts.

Doping could be control by reaction kinetics, bond strength between capping ligand and dopant metal. The ligand itself may bind to the dopant, preventing it's adsorption on the surface of Qdots and subsequent diffusion into the Qdots. Besides, doping efficiency is also determined by the solubility limit of the precursor material. When solubility is much lower, NCs undergo 'self-purification', an intrinsic mechanism whereby impurities are expelled to the surface due to thermodynamic reasons.[172, 201-202]

Further, crystal structure of NCs is also an important factor for doping. For example, CdSe in zinc blende structure could be easily doped than its wurtzite form. Any irregularities in the lattice structure in the form of lattice mismatch or

lattice strain caused by dopant ions, site symmetry and valence state of the dopant can hamper the growth doping process. Lattice strain could be avoided by choosing the dopant element wisely; it is always preferred that ion radii of host and dopant are nearly equal.[154]

### 1.4.2. Toxicity

Another issue with Qdots- doped and undoped - is toxicity. Though, cadmium and lead based Qdots are most widely used material, however because of environmental concern, elements listed under class-A, such as cadmium, lead, mercury etc. being toxic, and their usage has always been disputable.[158]

Majority of the people ambiguously believe that all Qdots are toxic- because of higher surface to volume ratio; most of the ions are exposed so Qdots are likely to be deleterious to the biological cells. However, in reality, it is not the Qdots itself- size and shape, but the physicochemical properties of the Qdots that determine its toxicity level. Nature of the capping material, charge and reactivity of its functional groups and mechanical stability of the surface ligand mainly decide toxicity. For example, Cd-based Qdots are found to be cytotoxic only after oxidative and photodegradation of their surface ligands. Upon exposure to air or UV light sulphur/selenium may get oxidized, releasing free $Cd^{2+}$ ions and ultimately causing cell death via reactive oxygen species (ROS) generation. Additionally, the surface of Qdots may get oxidized in presence of hydrogen peroxide present in the biological medium. While TOPO itself is known to be genotoxic, cysteamine or thioglycerol are also weakly genotoxic. In this regard, coating the core Qdots with multiple ZnS shells proved successful, however the resulting large hydrodynamic diameter as well as such a robust coating have raised concern. Failure in renal clearance and persistence of the injected Qdots in internal parts of the body for months may lead to acute metal toxicity again. Moreover, dose, mode of delivery, duration and frequency of exposure, mechanisms of action are a few factors that determine toxicity in Qdots. In this regard, bio-friendly Qdots like ZnS, InP, ZnSe and Cu-In-S are found to be useful as substitutes for Cd-based Qdots.[203-211]

Although brief and challenging, the evolutionary history of Qdots is impressive and remarkable for their large scale use as ideal fluorophore. Their intensive and

innovative uses in nanochemistry in collaboration with other multidisciplinary sciences hold a promising future.

### 1.5. Thesis Outline

The thesis has been divided into six chapters each of which has been described briefly below-

**Chapter 1:**

The first chapter of this thesis is an introductory chapter on Qdots. It reviews briefly the advent of Qdots, their general importance and how they have replaced the use of organic molecules and inorganic complex as fluorophores. A brief account of the advances made to achieve high quality luminescent Qdots through synthetic approaches and also, the involvement of surface traps (emission quencher) in non-radiative radiation and hence methods adopted so far for their elimination have been primarily discussed. Towards the end it gives a general idea of doped Qdots and challenges associated with Qdots.

**Chapter 2:**

The report about the experimental works of this thesis begins in the chapter 2. We have chosen to use the principles of chemistry in tuning the emission properties of doped Qdots and learn more about the contribution of the surface states. Since photoluminescence properties of Qdots depend largely on the surface traps, therefore, explicit knowledge about the nature of surface traps and control of their exact location (surface versus crystal Lattice) in the Qdots are important. It becomes more important in case of doped Qdots, where dopant itself act as emissive trap. Thus, engineering the surface dopant ions following synthesis could become an easier way of tuning their properties.

This has been demonstrated using $Mn^{2+}$-doped ZnS Qdots, where excess surface ions present in the form of clusters or individual ions on the surface and in its immediate vicinity have been systematically removed by using cation-exchange resin beads. It was observed that treatment of the Qdots with resin beads caused significant changes in the emission properties without any significant change in the particle size.

**Chapter 3:**

Realizing the significant role played by the surface ions towards the overall photoluminescence of the Qdots and their reactivity with cation resin beads, chapter 3 presents a new way of reversibly tuning the photoluminescence of doped Qdots by use of principles of redox chemistry. The primary contribution of the chapter is that emission due to the dopant element is not only dependent on its concentration but also on its electronic state. For example, when $Mn^{2+}$-doped ZnS Qdots were treated with an oxidizing agent such as potassium peroxodisulfate (KPS), it was observed that emission due to the dopant reduced systematically with increase in concentration of KPS and the lost intensity could be recovered by treatment with sodium borohydride, a common reductant. This has been attributed to oxidation and subsequent reduction of $Mn^{2+}$ ions present on the surface and in the immediate vicinity. Thus, the doped Qdots could be used as redox probe. This was pursued in the next chapter.

**Chapter 4:**

The objective of the work reported in chapter 4 is to use the photoluminescence properties of doped quantum dots in probing the reductive mammalian cellular environment. To our surprise, it was observed that as-synthesized $Cu^{2+}$-doped ZnS Qdots are weakly emitting in the blue region upon UV excitation. On the other hand, when the Qdots were treated with a reducing agent they emitted green fluorescence. Composite nanoparticles of chitosan (a biopolymer) and the Qdots were also found to be weakly-fluorescent and when added to mammalian cells, green fluorescence could be observed. The results indicated a new way of probing reducing nature of mammalian cells using the emission properties of the doped Qdots, based on the redox state of its dopant.

**Chapter 5:**

During my work with single doped Qdots ($Mn^{2+}$-doped ZnS Qdots and $Cu^{2+}$-doped ZnS Qdots), there was a wish to work with double doped Qdots- to study the optical properties of ZnS Qdots when doped simultaneously with $Mn^{2+}$ and $Cu^{2+}$. It was found that as-synthesized double-doped Qdots emitted orange upon excitation with UV light. However, upon treatment with reducing agent, a new

peak appeared in the green region, accompanied by increase in overall quantum yield. Finally, the emission appeared to be yellow. Further, upon addition of excess amount of oxidizing agents to the as-synthesized Qdots they emitted blue color.

Thus the contribution reported in of the 5$^{th}$ chapter is about achieving tricolour emission in double ($Mn^{2+}$ and $Cu^{2+}$) doped ZnS Qdots under different redox chemical environment. The results in addition supported the conclusions drawn in the previous chapters.

**Chapter 6:**

The last chapter deals with the synopsis of the current thesis summarizing its important findings and concluding remarks. That follows brief discussion about prospective and allied works which can be carried out in future or to address the limitations encountered during the course of this study.

## References


1) Hagberg, D. P.; Edvinsson, T.; Marinado, T.; Boschloo, G.; Hagfeldt, A.; Sun. L. *Chem. Commun*. **2006**, 2245–2247.
2) Thomas, K. R. J.; Hsu, Y. C.; Lin, J. T.; Lee, K. M.; Ho, K. C.; Lai, C. H.; Cheng, Y. M.; Chou. P. T. *Chem. Mat*. **2008**, 20, 1830–1840.
3) Gonçalves. M. S. T. *Chem. Rev*. **2009**, 109, 190–212.
4) Yang, C. H.; Mauro, M.; Polo, F.; Watanabe, S.; Muenster, I.; Fröhlich, R.; Cola, L. D. *Chem. Mater.* **2012**, 24, 3684–3695.
5) Nazeeruddin, M. K.; Zakeeruddin, S. M.; Baker, R. H.; Jirousek, M.; Liska, P.; Vlachopoulos, N.; Shklover, V.; Fischer, C. H.; Gratzel. M. *Inorg. Chem*. **1999**, 38, 6298-6305.
6) Nazeeruddin, M. K.; Kay, A.; Rodicio, I.; Baker, R. H.; Miiller, E.; Liska, P.; Vlachopoulos, N.; Gratzel, M. *J. Am. Chem. Soc*. **1993**,115, 6382-6390.
7) Gong, S.; Zhong, C.; Fu, Q.; Ma, D.; Qin, J.; Yang. C. *J. Phys. Chem. C* **2013**, 117, 549–555.
8) Duarte, F. J. *Optics & Photonics News* **2003**, 20-25.
9) Samuel, I. D. W.; Turnbull, G. A. *Chem. Rev.* **2007**, 107, 1272-1295.
10) Zhao, Q.; Huang, C.; Li, F. *Chem. Soc. Rev.* **2011**, 40, 2508-2524.
11) Giepmans, B. N. G.; Adams, S. R.; Ellisman, M. H.; Tsien, R. Y. *Science* **2006**, 312, 217-224.
12) Gonçalves, M. S. T. *Chem. Rev*. **2009**, 109, 190–212.
13) Walling, M. A.; Novak, J. A.; Shepard, J. R. E. *Int. J. Mol. Sci.* **2009**, 10, 441-491
14) Chan, W. C. W.; Nie, S. *Science* **1998**, 281, 2016-2018.
15) Ekimov, A. I.; Onushchenko, A. A. *JETP Lett.* **1981**, 84, 345-348.
16) Rossetti, R.; Nakahara, S.; Brus, L. E. *J. Chem. Phys*. **1983**, 79, 1086-1088.
17) Brus, L. E. *J. Chem. Phys.*, **1983**, 79, 5566-5571.
18) Reed, M. A.; Randall, J. N.; Aggarwal, R. J.; Matyi, R. J.; Moore, T. M.; Wetsel, A. E. *Phys Rev Lett*. **1988**, 60, 535–537.
19) Alivisatos, A. P. *Science* **1996**, 217, 933-977.
20) Bratschitsch, R.; Leitenstorfer, A. *Nat. Mat.* **2006**, 5, 855 - 856.
21) Ashoori, R. C. *Nature* **1996**, 379, 413-419.
22) Banin, U.; Cao, Y. W.; Katz, D.; Millo, O. *Nature* **1999**, 400, 542-544.
23) Brus, L. E. *J. Chem. Phys*. **1984**, 80, 4403.

24) Wang, Y.; Herron, N. *J. Phys. Chem*. **1991**, 95, 525-532.

25) Alivisatos, A. P. *J. Phys. Chem*. **1996**, 100, 13226-13239.

26) Murphy, C. J.; Coffer, J. L. *Appl. Spectros.* **2002**, 56, 16-27.

27) Murphy, C. J. *Anal. Chem.* **2002**, 520-526.

28) Gerion, D.; Pinaud, F.; Williams, S. C.; Parak, W. J.; Zanchet, D.; Weiss, S.; Alivisatos, A. P. *J. Phys. Chem. B* **2001**, 105, 8861-8871

29) Genger, U. R.; Grabolle, M.; Jaricot, S. C.; Nitschke, R.; Nann. T. *Nat. Methods* **2008**, 5, 763-775.

30) Bera, D.; Qian, L.; Tseng, T. K.; Holloway, P. H. *Materials* **2010**, 3, 2260-2345

31) Algar, W. R.; Susumu, K.; Delehanty, J. B.; Medintz, I. L. *Anal. Chem.* **2011**, 83, 8826–8837.

32) Kairdolf, B. A.; Smith, A. M.; Stokes, T. H.; Wang, M. D.; Young, A. N.; Nie, S. *Annu. Rev. Anal. Chem*. **2013**, 6, 143–162.

33) Frasco, M. F.; Chaniotakis, N. *Sensors* **2009**, 9, 7266-7286

34) Medintz, I. L.; Uyeda, H. T.; Goldman, E. R.; Mattoussi, H. *Nat. Mat*. **2005**, 4, 435-446.

35) Hildebrandt, N. *ACS Nano* **2011**, 5, 5286-5290.

36) Jaiswal, J. K.; Mattoussi, H.; Mauro, J. M.; Simon, S. M. *Nat. Biotechnol*. **2003**, 21, 47-51.

37) Alivisatos P. A. *Nat. Biotechnol*. **2004**, 22, 47-52.

38) Liu, W.; Choi, H. S.; Zimmer, J. P.; Tanaka, E.; Frangioni, J. V.; Bawendi, M. *J. Am. Chem. Soc.* **2007**, 28, 129, 14530-1.

39) Han, Z.; Qiu, F.; Eisenberg, R.; Holland, P. L.; Krauss, T. D. *Science*, **2012**, 338, 1321.

40) Amirav, L.; Alivisatos, A. P. *J. Am. Chem. Soc*. **2013**, 135, 13049–13053.

41) Zhang, W.; Zhong, X. *Inorg. Chem.* **2011**, 50, 4065–4072.

42) Han, Z.; Qiu, F.; Eisenberg, R.; Holland, P. L.; Krauss, T. D. *Science* **2012**, 338, 1321-1324.

43) Amirav, L.; Alivisatos, A. P. *J. Phys. Chem. Lett.* **2010**, 1, 1051–1054.

44) Klimov, V. I. *Annu. Rev. Phys. Chem*. **2007**, 58, 635–673.

45) Nozik, A. J. *Inorg. Chem.* **2005**, 44, 6893–6899.

46) Matthew, C. B. *J. Phys. Chem. Lett*. **2011**, 2, 1282–1288.

47) Polina O. A.; Jonathan E. H.; Bawendi, M. G.; Bulović, V. *Nano Lett.* **2009**, 9, 2532–2536

48) Colvin, V. L.; Schlamp, M. C.; Alivisatos, A. P. *Nature* **1994**, 370, 354–357.

49) Mashford, B. S.; Stevenson, M.; Popovic, Z.; Hamilton, C.; Zhou, Z.; Breen, C.; Steckel, J.; Bulovic, V.; Bawendi, M.G.; Sullivan, S. C.; Kazlas, P. T. *Nat. Photon.* **2013**, 7, 407–412.

50) Qian, L.; Zheng, Y.; Xue, J.; Holloway, P. H. *Nat. Photon.*, **2011**, 5, 543–548

51) Klimov, V. I.; Mikhailovsky, A. A.; Xu, S.; Malko, A.; Hollingsworth, J. A.; Leatherdale, C. A.; Eisler, H.-J.; Bawendi, M. G. *Science*, **2000**, 290, 314-317.

52) Kazes, M.; Lewis, D. Y.; Ebenstein, Y.; Mokari, T.; Banin, U. *Adv. Mater*. **2002**, 14, 317.

53) Anikeeva, P. O.; Halpert, J. E.; Bawendi, M. G.; Bulovic. V. *Nano Lett.* **2007**, 7, 2196-2200.

54) Kamat. P. V. *J. Phys. Chem. C* **2008**, 112, 18737–18753

55) Kongkanand, A.; Tvrdy, K.; Takechi, K.; Kuno, M.; Kamat. P. V. *J. Am. Chem. Soc.*, **2008**, 130, 4007-4015.

56) Hines, M.A.; Sionnest, P. G. *J. Phys. Chem. B* **1998**, 102, 3655-3657.

57) Chen, H. S.; Lo, B.; Hwang, J. Y.; Chang, G. Y.; Chen, C. M.; Tasi, S. J.; Wang. S. *J. Phys. Chem. B* **2004**, 108, 17119-17123.

58) Peng, Z. A. Peng, X. *J. Am. Chem. Soc*. **2001**, 123, 183-184.

59) Lucey, D. W.; MacRae, D. J.; Furis, M.; Sahoo, Y.; Cartwright, A. N.; Prasad, P. N. *Chem. Mater*. **2005**, 17, 3754–3762.

60) Micic, O. I.; Sprague, J. R.; Curtis, C. J.; Jones, K. M.; Machol, J. L.; Nozik, Giessen, H.; Fluegel, B.; Mohs, G.; Peyghambarian, N. *Phys. Chem*. **1995**, 99, 7754–7759

61) Moreels, I.; Justo, Y.; Geyter, B. D.; Haustraete, K.; Martins, J. C.; Hens, Z. *ACS Nano*, **2011**, 5, 2004–2012.

62) Zhong, H.; Bai, Z.; Zou, B. *J. Phys. Chem. Lett.* **2012**, 3, 3167–3175.

63) Yarema, O.; Bozyigit, D.; Rousseau, I.; Nowack, L.; Yarema, M.; Heiss, W.; Wood, V. *Chem. Mater*. **2013**, 25, 3753–3757.

64) Xie, R.; Rutherford, M.; Peng, X. *J. Am. Chem. Soc*. **2009**, 131, 5691–5697.

65) Pan, D.; An, L.; Sun, Z.; Hou, W.; Yang, Y.; Yang, Z.; Lu, Y. *J. Am. Chem. Soc*. **2008**, 130, 5620–5621.

66) Mao, B.; Chuang, C. H.; Wang, J.; Burda, C. *J. Phys. Chem. C* **2011**, 115, 8945–8954.

67) Kim, S. W.; Zimmer, J. P.; Ohnishi, S.; Tracy, J. B.; Frangioni, J. V.; Bawendi, M. G. *J. Am. Chem. Soc*. **2005**, *127*, 10526-10532.

68) Xie, R.; Rutherford, M.; Peng, X. *J. Am. Chem. Soc*. **2009**, 131, 5691–5697.

69) Chen, Y.; Li, S.; Huang, L.; Pan, D. *Inorg. Chem*. **2013**, 52, 7819–7821.

70) Zhang, H.; Son, J. S.; Jang, J.; Lee, J. S.; Ong, W. L.; Malen, J. A.; Talapin, D. V. *ACS Nano*, **2013**, 7, 10296–10306.

71) Zhang, J.; Xie, R.; Yang, W. *Chem. Mater*., **2011**, 23, 3357–3361.

72) Deng, D.; Qu, L.; Zhang, J.; Ma, Y.; Gu, Y. *ACS Appl. Mater. Interfac*. **2013**, 5, 10858–10865.

73) Shen, S.; Wang, Q. *Chem. Mater*., **2013**, 25, 1166–1178.

74) Bera, D.; Qian, L.; Tseng, T. K.; Holloway, P. H. *Materials* **2010**, 3, 2260-2345

75) Tsutsui, K.; Hu, E. L.; Wilkinson, C. D. W. *Jpn. J. Appl. Phys. Part 1* **1993**, 32, 6233–6236.

76) Burda, C.; Chen, X. B.; Narayanan, R.; El-Sayed, M. A. *Chem. Rev*. **2005**, 105, 1025–1102.

77) Yin, Y.; Alivisatos, A. P. *Nature* **2005**, 437, 664-670.

78) Murray, C.B.; Norris, D.J.; Bawendi, M.G. *J. Am. Chem. Soc*. **1993**, 115, 8706-8715.

79) Talapin, D.V.; Rogach, A.L.; Kornowski, A.; Haase, M.; Weller, H. *Nano Lett.* **2001**, 1, 207-211.

80) Mikulec, F. V.; Kuno, M.; Bennati, M.; Hall, D. A.; Griffin, R. G.; Bawendi, M. G. *J. Am. Chem. Soc.* **2000**, 122, 2532-2540.

81) Yu, W.W.; Peng, X. *Angew. Chem.* **2002**, 41, 2368-2371.

82) Norris, D. J.; Yao, N.; Charnock, F. T.; Kennedy, T. A. *Nano Lett*. **2001**, 1, 3-7.

83) Peng, Z. A.; Peng, X. *J. Am. Chem. Soc.* **2001**, 123, 183-184.

84) Green, M.; Brien, P. O' *Chem. Commun*. **1999**, 2235-2241.

85) Luther, J. M.; Pietryga, J. M. *ACS Nano* **2013**, 7, 1845-1849.

86) Roduner, E. *Chem. Soc. Rev*., **2006**, 35, 583–592.

87) Alivisatos, A. P. *J. Phys. Chem*. **1996**, 100, 13226-13239.

88) Nirmal, M.; Brus, L. E. *Acc. Chem. Res*. **1999**, 32, 407-414.

89) Neuhauser, R. G.; Shimizu, K. T.; Woo, W. K.; Empedocles, S. A.; Bawendi, M. G. *Phys. Rev. Lett*. **2000**, 85, 3301.

90) Empedocles, S. A.; Bawendi, M. G. *Science* **1997**, 278, 2114.

91) Efros, A. L.; Rosen, M. *Phys. Rev. Lett.* **1997**, 78, 1110.

92) Banin, U.; Bruchez, M.; Alivisatos, A. P.; Ha, T.; Weiss, S.; Chemla, D. S. *J. Chem. Phys.* **1999**, 110, 1195.

93) Klimov, V. I.; Mikhailovsky, A. A.; McBranch, D. W.; Leatherdale, C. A.; Bawendi, M. G. *Science* **2000**, 287, 1011–1013.

94) Kilina, S.; Ivanov, S.; Tretiak, S. *J. Am. Chem. Soc*., **2009**, 131 7717-7726.

95) Soni, U.; Sapra, S. *J. Phys. Chem. C* **2010**, 114, 22514–22518.

96) Jasieniak, J.; Mulvaney, P. *J. Am. Chem. Soc*. **2007**, 129, 2841-2848.

97) Dubertret, B.; Skourides, P.; Norris, D.J.; Noireaux, V.; Brivanlou, A.H.; Libchaber, A. *Science* **2002**, 298, 1759-1762.

98) Larson, D. R.; Zipfel, W.R.; Williams, R.M.; Clark, S.W.; Bruchez, M.P.; Wise, F.W.; Webb,W. W. *Science* **2003**, 300, 1434-1436.

99) Wu, X.; Liu, H.; Liu, J.; Haley, K.N.; Treadway, J.A.; Larson, J.P.; Ge, N.; Peale, F.; Bruchez, M.P. *Nat. Biotechnol*. **2003**, 21, 41-46.

100) Dubois, F.; Mahler, B.; Dubertret, B.; Doris, E.; Mioskowski, C. *J. Am. Chem. Soc.* **2007**, 129, 482-483.

101) Algar, W. R.; Krull. U. J. *Langmuir* **2008**, 24, 5514-5520.

102) Clapp, A. R.; Medintz, I. L.; Uyeda, H. T.; Fisher, B. R.; Goldman, E. R.; Bawendi, M. G.; Mattoussi, H. *J. Am. Chem. Soc*. **2005**, 127, 18212-18221

103) Mattoussi, H.; Mauro, J. M.; Goldman, E. R.; Anderson, G. P.; Sundar, V. C.; Mikulec, F. V.; Bawendi, M. G. *J. Am. Chem. Soc.* **2000**, 122, 12142-12150.

104) Frasco, M. F.; Chaniotakis, N. *Sensors* **2009**, 9, 7266-7286

105) Mazumder, S.; Dey, R.; Mitra, M. K.; Mukherjee, S.; Das, G. C. J. *Nanomaterials* **2009**, 2009, Article ID 815734, doi:10.1155/2009/815734.

106) Baker, D. R.; Kamat, P. V. *Langmuir* **2010**, 26, 11272–11276.

107) Kim, S.; Bawendi, M. G. *J. Am. Chem. Soc*. **2003**, 125, 14652-14653.

108) Dubertret, B.; Skourides, P.; Norris, D. J.; Noireaux, V.; Brivanlou, A. H.; Libchaber, A. *Science* **2002**, 298, 1759-1762.

109) Koh, W.; Saudari, S. R.; Fafarman, A. T.; Kagan, C. R.; Murray, C. B. *Nano Lett*. **2011**, 11, 4764–4767.

110) Hollingsworth, J. A. *Chem. Mater*. **2013**, 25, 1318−1331

111) Inerbaev, T. M; Masunov, A. E.; Khondaker, S. I.; Dobrinescu, A.; Plamadă, A.-V.; Kawazoe, Y. *J. Chem. Phys*. **2009**, 131, 044106.

112) Puzder, A.; Wlliamson, A. J.; Gygi, F.; Galli, G. *Phys. Rev. Lett*. **2004**, 92, 217401.

113) Kovalenko, M. V.; Bodnarchuk, M. I.; Zaumsei, J.; Lee, J. S.; Talapin, D. V. *J. Am. Chem. Soc.* **2010**, 132, 10085−10092.

114) M. V. Kovalenko, M. Scheele, D. V. Talapin. *Science*, **2009**, 324, 1417-1420.

115) Nag, A.; Kovalenko, M. V.; Lee, J. S.; Liu, W.; Spokoyny, B.; Talapin, D. V. *J. Am. Chem. Soc.*, **2011**, 133, 10612−10620

116) Tang, J.; Kemp, K. W.; Hoogland, S.; Jeong, K. S.; Liu, H.; Levina, L.; Furukawa, M.; Wang, X.; Debnath, R.; Cha, D.; Chou, K. W.; Fischer, A.; Amassian, A.; Asbury, J. B.; Sargent, E. H. *Nat. Mat.*, **2011**, 10, 765-771.

117) Zhitomirsky, D.; Furukawa, M.; Tang, J.; Stadler, P.; Hoogland, S.; Voznyy, Ol.; Liu, H.; Sargent, E. H. *Adv. Mater*. **2012**, 24, 6181−6185.

118) Reiss, P.; Protiere, M.; Li. L. *Small* **2009**, 5, 154−168.

119) Dabbousi, B. O.; Rodriguez-Viejo, J.; Mikulec, F. V.; Heine, J. R.; Mattoussi, H.; Ober, R.; Jensen, K. F.; Bawendi, M. G. *J. Phys. Chem. B* **1997**, 101, 9463-9475.

120) Nemchinov, A.; Kirsanova, M.; Hewa-Kasakarage, N. N.; Zamkov, M. *J. Phys. Chem. C* **2008**, 112, 9301−9307.

121) Kim, S.; Fisher, B.; Eisler, H. J.; Bawendi, M. *J. Am. Chem. Soc.* **2003**, 125, 11466-11467.

122) Chen, Y.; Vela, J.; Htoon, H.; Casson, J. L.; Werder, D. J.; Bussian, D. A.; Klimov, V. I.; Hollingsworth, J. A. *J. Am. Chem. Soc*. **2008**, 130, 5026.

123) Garcia-Santamaria, F.; Chen, Y.; Vela, J.; Schaller, R. D.; Hollingsworth, J. A.; Klimov, V. I. *Nano Lett.* **2009**, 9, 3482−3488.

124) García-Santamaría, F.; Brovelli, S.; Viswanatha, R.; Hollingsworth, J. A.; Htoon, H.; Crooker, S. A.; Klimov, V. I. *Nano Lett*. **2011**, *11*, 687−693.

125) Saha, A., Chellappan, K. V.; Narayan, K. S.; Ghatak, J.; Datta, R.; Viswanatha, R. *J. Phys. Chem. Lett.* **2013**, 4, 3544−3549.

126) Li, J. J.; Wang, Y. A.; Guo, W.; Keay, J. C.; Mishima, T. D.; Johnson, M. B.; Peng, X. *J. Am. Chem. Soc.* **2003**, 125, 12567−12575.

127) Guo, W.; Li, J. J.; Wang, Y. A.; Peng, X. *J. Am. Chem. Soc*. **2003**, 125, 3901–3909.

128) Peng, X.; Schlamp, M. C.; Kadavanich, A. V.; Alivisatos, A. P. *J. Am. Chem. Soc*. **1997**, 119, 7019–7029.

129) Winnik, F. M.; Maysinger D. *Acc. Chem. Res.* **2013**, 46, 672-680.

130) Regulacio, M. D.; Han, M. Y. *Acc. Chem. Res.* **2010**, 43, 621-630.

131) Bailey, R. E.; Nie, S. *J. Am. Chem. Soc*. **2003**, 125, 7100-7106.

132) Zhang, W.; Zhong, X. *Inorg. Chem*. **2011**, 50, 4065–4072.

133) Groeneveld, E.; Witteman, L.; Lefferts, M.; Ke, X.; Bals, S.; Tendeloo, G. V.; Donega, C. M. *ACS Nano* **2013**, 7, 7913–7930.

134) Smith, A. M.; Nie, S. *J Am Chem Soc*. **2011**, 133, 24–26.

135) Ithurria, S.; Dubertret, B. *J. Am. Chem. Soc*. **2008**, 130, 16504–16505.

136) Peng, X. G. *Adv. Mater*. **2003**, 15, 459–463.

137) Scher, E. C.; Manna, L.; Alivisatos, A. P. *Philos. Trans. R. Soc. London, Ser. A* **2003**, 361, 241–255.

138) Wang, Y.; Tang A, Li K, Yang C, Wang M, Ye H, Hou Y, Teng F. *Langmuir* **2012**, 28, 16436–16443.

139) Miszta, K.; Dorfs, D.; Genovese, A.; Kim, M. R.; Manna, L. *ACS Nano* **2011**, 5, 7176-7183.

140) Son, D. H.; Hughes, S. M.; Yin, Y.; Alivisatos A. P. *Science* **2004**, 306,1009-1012.

141) Beberwyck, B. J.; Surendranath, Y.; Alivisatos, A. P. *J. Phys. Chem. C* **2013**, 117, 19759–19770.

142) Halpert, J. E.; Porter, V. J.; Zimmer, J. P.; Bawendi, M. G. *J. Am. Chem. Soc*. **2006**, 128, 12590.

143) Robinson, R. D; Sadtler, B.; Demchenko, D. O.; Erdonmez, C. K.; Wang, L. W.; Alivisatos, A. P. *Science*. **2007**, 317, 355-358

144) Manna, L.; Milliron, D. J.; Meisel, A.; Scher, E. C.; Alivisatos, A. P. *Nat. Mater.* **2003**, 2, 382–385.

145) Fu, W.; Qin, S.; Liu, L.; Kim, T.-H.; Hellstrom, S.; Wang, W.; Liang, W.; Bai, X.; Li, A.-P.; Wang, E. *Nano Lett.* **2011**, 11, 1913–1918.

146) Deka, S.; Miszta, K.; Dorfs, D.; Genovese, A.; Bertoni, G.; Manna, L. *Nano Lett.* **2010**, 10, 3770–3776.

147) Huang, X.; Zhao, Z.; Fan, J.; Tan, Y.; Zheng, N. *J. Am. Chem. Soc*. **2011**, 133, 4718–4721.

148) Khon E, Lambright K, Khnayzer RS, Moroz P, Perera D, Butaeva E, Lambright S, Castellano FN, Zamkov M. *Nano Lett.* **2013**, 13, 2016-2023.

149) Li, H.; Zanella, M.; Genovese, A.; Povia, M.; Falqui, A.; Giannini, C.; Manna, L.; *Nano Lett*. **2011**, 11, 4964–4970.

150) Jaiswal, A.; Ghosh, S. S.; Chattopadhyay, A. *Langmuir* **2012**, *28*, 15687–15696

151) Sytnyk, M.; Kirchschlager, R.; Bodnarchuk M. I.; Primetzhofer, D.; Kriegner, D.; Enser, H.; Stangl, J.; Bauer, P.; Voith, M.; Hassel, A. W.; Krumeich, F.; Ludwig, F.; Meingast, A.; Kothleitner, G.; Kovalenko, M. V.; Heiss, W. *Nano Lett*. **2013**, 13, 586-593.

152) Groeneveld, E.; Witteman, L.; Lefferts, M.; Ke, X.; Bals, S.; Van Tendeloo, G.; de-Mello D. C. *ACS Nano* **2013**, 7, 7913–7930.

153) Eilers, J.; Groeneveld, E.; Donega, C. d. M.; Meijerink, A. *J. Phys. Chem. Lett.* **2012**, 3, 1663–1667.

154) Mocatta, D.; Cohen, G.; Schattner, J.; Millo, O.; Rabani, E.; Banin, U. *Science* **2011**, 332, 77–81.

155) Sahu, A.; Kang, M. S.; Kompch, A.; Notthoff, C.; Wills, A. W.; Deng, D.; Winteren, M.; Frisbie, C. D.; Norris, D. J. *Nano Lett*. **2012**, 12, 2587–2594.

156) Buonsanti, R.; Milliron, D. J. *Chem. Mater*. **2013**, 25, 1305–1317.

157) Norris, D. J.; Efros, A. L.; Erwin, S. C. *Science* **2008**, 319, 1776-1779.

158) Peng, X. *Nano Res.* **2009**, 2, 425 447.

159) Stouwdam, J. W.; Janssen, R. A. J. *Adv. Mater*. **2009**, 21, 2916–2920.

160) Xie, R.; Peng, X. *J. Am. Chem. Soc.* **2009**, 131, 10645–10651.

161) Sarkar, S.; Karan, N. S.; Pradhan, N. *Angew. Chem. Int. Ed.* **2011**, 50, 6065 – 6069.

162) Manna, G.; Jana, S.; Bose, R.; Pradhan, N. *J. Phys. Chem. Lett*. **2012**, 3, 2528–2534.

163) Quan, Z.; Wang, Z.; Yang, P.; Lin, J.; Fang, J. *Inorg. Chem*. **2007**, 46, 1354-1360.

164) Shen, S.; Zhang, Y., Liu, Y.; Peng, X. Chen, and Q. Wang. *Chem. Mater*., **2012**, 24, 2407–2413.

165) Vlaskin, V. A.; Janssen, N.; Rijssel, J.; Beaulac, R.; Gamelin, D. R. *Nano Lett.* **2010**, 10, 3670–3674.

166) Hsia, C. H.; Wuttig, A.; Yang, H. *ACS Nano*, **2011**, 5, 9511–9522.

167) Pradhan, N.; Goorskey, D.; Thessing, J.; Peng, X. *J. Am. Chem. Soc*. **2005**, 127, 17586-17587.

168) Du, M. H.; Erwin, S. C.; Efros, A. L. *Nano Lett.* **2008**, 8, 2878-2882

169) Zeng, R.; Rutherford, M.; Xie, R.; Zou, B.; Peng, X. *Chem. Mater*. **2010**, 22, 2107–2113.

170) Vlaskin, V. A.; Barrows, C. J.; Erickson, C. S.; Gamelin, D. R. *J. Am. Chem. Soc*, **2013**, 135, 14380–14389.

171) Yang, B.; Shen, X.; Zhang, H.; Cui, Y.; Zhang, J. *J. Phys. Chem. C* **2013**, 117, 15829–15834.

172) Chen, D.; Viswanatha, R.; Ong, G. L.; Xie, R.; Balasubramaninan, M.; Peng, X. *J. Am. Chem. Soc*. **2009**, 131, 9333–9339.

173) Shim, M.; Sionnest, P. G. *Nature* **2000**, 407, 981-983.

174) Wang, C. Shim, M.; Sionnest, P. G. *Science* **2001**, 291, 2390-2392.

175) Sionnest, P. G.; Wang, C. *J. Phys. Chem. B* **2003**, 107, 7355-7359.

176) Wehrenberg, B. L.; Sionnest, P. G. *J. Am. Chem. Soc*. **2003**, 125, 7806-7807.

177) White, M. A.; Weaver, A. L.; Beaulac, R.; Gamelin, D. R. *ACS Nano* **2011**, 5, 4158-4168.

178) Weaver, A. L.; Gamelin, D. R. *J. Am. Chem. Soc*. **2012**, 134, 6819–6825.

179) Nag, A.; Sarma, D. D. *J. Phys. Chem. C* **2007**, 111, 13641-13644.

180) Norman, T. J.; Magana, D.; Wilson, T.; Burns, C.; Zhang, J. Z. *J. Phys. Chem. B* **2003**, 107, 6309-6317.

181) Suyver, J. F.; Wuister, S. F.; Kelly, J. J.; Meijerink, A. *Nano Lett*. **2001**, 1, 429-433.

182) Sapra, S.; Prakash, A.; Ghangrekar, A.; Periasamy, N.; Sarma, D. D. *J. Phys. Chem. B* **2005**, 109, 1663-1668.

183) Pradhan, N.; Sarma, D. D. *J. Phys. Chem. Lett*. **2011**, 2, 2818–2826.

184) Bhargava, R. N.; Gallagher, D.; Hong, X.; Nurmikko, *Phys. Rev. Lett*. **1994**, 72, 416–419.

185) Sooklal, K.; Cullum, B. S.; Angel, S. M.; Murphy, C. J. *J. Phys. Chem*. **1996**, 100, 4551-4555.

186) Bol, A. A.; Meijerink, A. *Phys. Rev. B* **1998**, 58, R15997-R16000.

187) Quan, Z.; Yang, D.; Li, C.; Kong, D.; Yang, P.; Cheng, Z.; Lin, J. *Langmuir* **2009**, 25, 10259-10262.

188) Srivastava, B. B.; Jana, S.; Karan, N. S.; Paria, S.; Jana, N. R.; Sarma, D. D.; Pradhan, N. *J. Phys. Chem. Lett*. **2010**, 1, 1454–1458.

189) Zheng, J.; Yuan, X.; Ikezawa, M.; Jing, P.; Liu, X.; Zheng, Z.; Kong, X.; Zhao, J.; Masumoto, Y. *J. Phys. Chem. C* **2009**, 113, 16969–16974.

190) Acharya, S.; Sarma, D. D.; Jana, N. R.; Pradhan, N. *J. Phys. Chem. Lett*. **2010**, 1, 485–488.

191) Karan, N. S.; Sarma, D. D.; Kadam, R. M.; Pradhan, N. *J. Phys. Chem. Lett*. **2010**, 1, 2863–2866.

192) Chen, W.; Sammynaiken, R.; Huang, Y.; Malm, J. O.; Wallenberg, R.; Bovin, J. O.; Zwiller, V. N.; Kotov, A. *J. App. Phys*. **2000**, 88, 1120-1129.

193) Nag, A.; Cherian, R.; Mahadevan, P.; Gopal, A. V.; Hazarika, A.; Mohan, A.; Vengurlekar, A. S.; Sarma, D. D. *J. Phys. Chem. C* **2010**, 114, 18323–18329.

194) Viswanatha, R.; Battaglia, D. M.; Curtis, M. E.; Mishima, T. D.; Johnson, M. B.; Peng, X. *Nano Res*. **2008**, 1, 138-144.

195) Pradhan, N.; Peng, X. *J. Am. Chem. Soc*. **2007**, 129, 3339-3347.

196) Chen, O., Shelby, D. E., Yang, Y., Zhuang, J., Wang, T., Niu, C., Omenetto, N. and Cao, Y. C. *Angew. Chem*. **2010**, 122: 10330–10333.

197) Su, F.H.; Fang, Z.L.; Ma, B.S.; Ding, K.; Li, G.H.; Chen, W. *J. Phys. Chem. B* **2003**, 107, 6991–6996.

198) Stouwdam, J. W.; Janssen, R. A. J. *Adv. Mater*. **2009**, 21, 2916–2920.

199) Xie, R.; Peng, X. *J. Am. Chem. Soc*. **2009**, 131, 10645–10651.

200) Kamat, P. V. *J. Phys. Chem. Lett*. **2011**, 2, 2832–2833.

201) Galli, G. *Nature* **2005**, 436, 32-33.

202) Dalpian, G. M.; Chelikowsky, J. R. *Phys. Rev. Lett.* **2006**, 96, 226802-1-4.

203) Derfus, A. M.; Chan, W. C. W.; Bhatia, S. N. *Nano Lett*. **2004**, 4, 11-18.

204) Choi, H. S.; Liu, W.; Misra, P.; Tanaka, E.; Zimmer, J. P.; Ipe, B.I.; Bawendi, M.G. Frangioni, J. V *Nat. Biotechnol.* **2007**, 25, 1165-1170.

205) Hardman, R. *Environ. Health Perspect*. **2006**, 114,165-172.

206) Shiohara, A.; Hoshino, A.; Hanaki, K.; Suzuki, K.; Yamamoto, K. *Microbiol. Immunol*., **2004**, 48, 669-675.

207) Kirchner, C.; Liedl, T.; Kudera, S.; Pellegrino, T.; Javier, A. M.; Gaub, H. E.; Stollzle, S.; Fertig, N.; Parak, W. J. *Nano Lett*. **2005**, 5, 331-338.

208) Hoshino, A.; Fujioka, K.; Oku, T.; Suga, M.; Sasaki, Y. F.; Ohta, T.; Yasuhara, M. Suzuki, K.; Yamamoto, K. *Nano Lett.* **2004**, 4, 2163-2169.

209) Bradburne, C. E.; Delehanty, J. B.; Gemmill, K. B.; Mei, B. C.; Mattoussi, H.; Susumu, K.; Blanco-Canosa, J. B.; Dawson, P. E.; Medintz, I. L. *Bioconjug. Chem*. **2013**, 24, 1570−1583.

210) Mancini, M. C.; Kairdolf, B. A.; Smith, A. M.; Nie, S. *J. Am. Chem. Soc*. **2008**, 130, 10836−10837.

211) Fitzpatrick, J. A. J.; Andreko, S. K.; Ernst, L. A.; Waggoner, A. S.; Ballou, B.; Bruchez, M. P. *Nano Lett*. **2009**, 9, 2736-2741.

# Chapter 2

## Surface Ion Engineering of $Mn^{2+}$-doped ZnS Quantum Dots

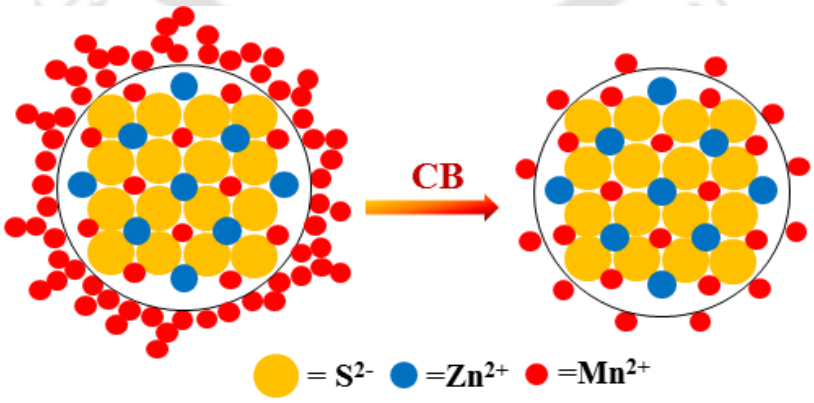

# Chapter 2

**Abstract:** This chapter describes post-synthesis engineering of surface ions present as defects in doped quantum dots (Qdots). Aqueous dispersion of $Mn^{2+}$-doped ZnS Qdots, when treated with different amounts of cation exchange resin beads (CB) resulted in two kinds of changes in the emission due to $Mn^{2+}$ ions. Initially, intensity increased in the presence of smaller amount of CB, to the extent of doubled quantum yield. With increased CB as well as incubation time the intensity of emission decreased systematically, accompanied by increasing blue shift of peak emission wavelength. The results have been explained based on the removal of $Mn^{2+}$ (and also $Zn^{2+}$) ions present on the surface of Qdots in the forms of clusters as well as individual ions. Electron spin resonance (ESR) results indicated removal of clusters of $Mn^{2+}$ present in the Qdots by the CB, which has been attributed to the changes in the emission characteristics.

## 2.1. Introduction

Doping of Qdots by incorporation of atomic impurities is routinely used to modify their electrical and optical properties.[1-4] The dopants function as emissive traps, as the trap energy levels lie between the valence and conduction bands of the host crystal. The trap states thus change optical and electronic properties of the host. For example, the emission wavelengths of wide band gap Qdots of ZnS or ZnSe could be significantly red shifted by introducing $Mn^{2+}$ ions as dopants.[5, 6] The widely accepted hypothesis is that following excitation, which occurs through the host lattice, non-radiative energy transfer takes place to the $Mn^{2+}$ d-states, leading to Qdot size independent emission from the atomic states.[7-10]

While there is a general consensus on the nature of emissive states in the doped Qdots, there remains considerable room for investigating the exact location and the nature of the emitting dopants in the host crystals. In $Mn^{2+}$-doped ZnS Qdots, the available experimental evidences suggest the presence of $Mn^{2+}$ ions deep inside the crystals as well as on the surface and in its immediate vicinity.[10, 11] The location, of course, is dependent on the experimental condition of synthesis of the crystal.[12-15] It is anticipated that a better knowledge and control of the location of

the dopant, its environment and extent of agglomeration of the ions would result in superior design of the crystal with high stability, photocatalytic efficiency and luminescence quantum yield (QY). For example, in the case of $Mn^{2+}$-doped ZnS Qdots, it has been demonstrated that emission intensity due to $^4T_1$ to $^6A_1$ transition initially increases with $Mn^{2+}$ concentration.[16-19] However, beyond a certain concentration of $Mn^{2+}$ dopant the QY goes down. The lowering of QY has been attributed to the presence of surface trap states, where the $Mn^{2+}$ could form pairs or clusters and also MnS, which individually or collectively contribute to the quenching of fluorescence.[20] Thus, a better control over the formation of the surface trap states (or elimination for that matter) following synthesis, would possibly provide an alternative way of enhancing the performance of Qdots.

In this chapter, it has been demonstrated that the photoluminescence of $Mn^{2+}$-doped ZnS Qdots could be modulated following their synthesis, by systematically removing the cations (especially $Mn^{2+}$) using CB. The Qdots used were synthesized in water, given the importance of aqueous based Qdots for which a significant number of synthetic methods are available.[21-24] It was observed that when a lower amount of CB was used with a shorter duration of incubation, intensity of emission increased. For a longer incubation time, the intensity of emission decreased comparatively, though it was still higher than the original intensity. On the other hand, in the presence of a larger amount of CB the intensity of emission decreased in a shorter time. Interestingly, the maximum wavelength of emission shifted to blue with increasing amount of beads and with longer duration of incubation. Transmission electron microscopy (TEM) studies indicated that use of smaller amount of beads or shorter incubation time did not change the size of the particles significantly. However, when the Qdots were incubated with higher amount of beads for longer time the particle size decreased. Electron spin resonance (ESR) studies indicated that treatment of Qdots with CB did not only remove $Mn^{2+}$ ions but also reduced the extent of clustering on the surface. Results also suggested that clustering of $Mn^{2+}$ was present at all doping concentrations of $Mn^{2+}$ (produced during synthesis), which could be systematically removed using CB.

## 2.2. Experimental section

### 2.2.1. Materials

Zinc acetate dihydrate (98%), manganese acetate tetrahydrate (99%), sodium sulfide (55-58%), acetyl acetone (98%), and Amberlite IR 120. All chemicals were procured from Merck Limited, Mumbai, India.

### 2.2.2. Synthesis of Acetyl-acetone Stabilized $Mn^{2+}$-doped ZnS Qdots

For the synthesis of Mn doped zinc sulphide Qdots, a simple aqueous method has been developed using zinc acetate dihydrate, manganese acetate tetrahydrate and sodium sulphide as the starting materials. Acetyl acetone was used as the capping agent and Milli-Q grade water as the solvent. Zinc acetate and sodium sulphide (1:1 ratio with 5 mM each) were added to 50 mL of water (containing 400 uL acetylacetone), followed by addition of manganese acetate. The reaction mixture was heated to 85 $^0$C. The mixture was allowed to stir for 3 h under refluxing condition. Finally, the colloidal dispersion so obtained was centrifuged at a speed of 22,000 rpm for 20 min; the pellet was washed with water, redispersed in 50 mL water and the same cycle was repeated. The pellet so obtained was again redispersed in 250 mL water and sonicated for 1 h.

Four sets of Qdots with different Mn precursor concentrations (7 mM, 4 mM, 0.5 mM and 0.15 mM) were prepared and used for ESR measurements. However, for all fluorescence measurements Qdots with 7 mM precursor concentration of Mn were used. The actual concentrations of Zn and Mn in the Qdots as determined by Atomic absorption spectroscopic (AAS) were however far less than the amount used during synthesis.

### 2.2.3. Activation of the Cation Exchange Resin Beads (CB)

About 3.0 g of commericially available cation exchange resin beads (Amberlite IR 120 as purchased) were at first kept in 20 mL of 3.0 M hydrochloric acid solution for 1 h. These were then washed thoroughly with plenty of water to remove the excess acid. This was further confirmed by checking the pH of the water for which a pH equal to 6.5 was obtained finally. This activation is important so as to replace the $Na^+$ ions in the beads by $H^+$ ions, which would again to be replaced with the metal ions present in the Qdots.

### 2.2.4. Treatment of Activated CB with Qdots

A weighed amount of CB, which varied between 0.6 mg and 25 mg, was added separately to 10 mL Qdots taken in each vial and incubated for a maximum time of 3 h prior to measurements.

### 2.2.5. Sample preparation for analytical measurements

Solid powder samples of Qdots were used for powder X-ray diffraction (XRD) and ESR spectroscopic measurements. For these, Qdots were prepared in large scale keeping the ratio of precursor materials the same as mentioned above. The prepared samples were tested for quality by photoluminescence measurements at room temperature. As-synthesized Qdots as well as Qdot dispersion treated with CB were then centrifuged and dried to obtain powdered form of Qdots. About 10.0 mg of powdered sample was used for ESR and 120.0 mg for recording XRD.

TEM samples were also prepared from the redispersed medium. About 3 μL of diluted liquid sample of Qdots dispersion was drop-cast on a carbon-coated copper grid for TEM measurements.

### 2.2.6. Characterization

Absorption spectra were recorded using a Perkin Elmer Lambda 45 UV-vis spectrophotometer. Fluorescence spectra were recorded in a Horiba Fluoromax-4 spectrofluorometer. Liquid samples were used for the measurements. The powder XRD measurements were carried out using a CuKα radiation (λ=1.542 Å) on a using a Bruker D8 Advance X-ray diffractometer. ESR spectra of the powder samples were recorded using a JEOL FA 200 ESR spectrometer. Elemental analysis was done using a Fast Sequential atomic absorption spectrometer (VARIAN AA240FS model).

TEM measurements were performed using a JEOL JEM 2100 electron microscope operating at a maximum accelerating voltage of 200 KV. Liquid dispersions of samples were deposited on carbon coated copper grids followed by drying; which were then used for TEM imaging. For size calculations, TEM images of each Qdot sample were recorded at different locations. Then from the clearly observed spherical particles (for each image), their sizes have been calculated

considering sizes of 100 such particles. The reported value (discussed later) is an average of those numbers.

### 2.3. Results and Discussion

When an aqueous dispersion of the Qdots, with an absorbance value of 0.03 (Figure 2-1A), was excited by 340 nm light a broad emission in the visible region with a peak maximum at 598 nm was observed (Figure 2-1B-i). The photoluminescence QY was found to be 6%. AAS study evidenced the presence of 11% (mole %) of Mn (relative to Zn) in the crystal. TEM studies indicated that the average particle size of the as-synthesized Qdots was 3.5 $\pm$ 0.3 nm. When 10 mL dispersions were incubated with 0.6 mg and 1.5 mg activated CB for 10 min, the intensity of emission increased to values of QY of 10% and 12% respectively. The increase in emission intensity (in comparison to emission of as-synthesized Qdots) was observed for addition of CB of amount up to 10.5 mg (Figure 2-1B). There was no further significant change when 15 mg of CB was added. Additionally, for the same Qdot dispersions when incubated for 3 h, the intensity of emission decreased comparatively and there was significant decrease for larger amount of CB (Figure 2-1C). It was observed that QY could be as low as 4% in the presence of 23 mg of bead, when incubated for 3 h. Higher amount of CB led to significant change in pH and hence the addition was limited to smaller amount of CB.

Measurements of the pH of the medium indicated that upon addition of any of the above amounts of CB, the pH of the medium remained the same at 6.4. In other words, the increase in intensity of emission of the Qdots might have been resulted due to their interactions with the CB. A plot of change in the intensity of emission peak at 598 nm with CB (Figure 2-1D) indicated that increase in emission intensity peaked at small amount of CB. However, there was no net increase in intensity beyond a certain concentration of CB; furthermore the presence of additional amount led to an eventual decrease in the intensity. Also, it was observed that longer incubation time led to less increase in the emission intensity in comparison to that for shorter times. More interestingly, there was a gradual blue shift in the maximum emission wavelength with increase in the amount of CB (incubated for a fixed period of time). A plot of the emission peak wavelength

versus the amount of bead indicated a step wise decrease, as shown in Figure 2-2A.

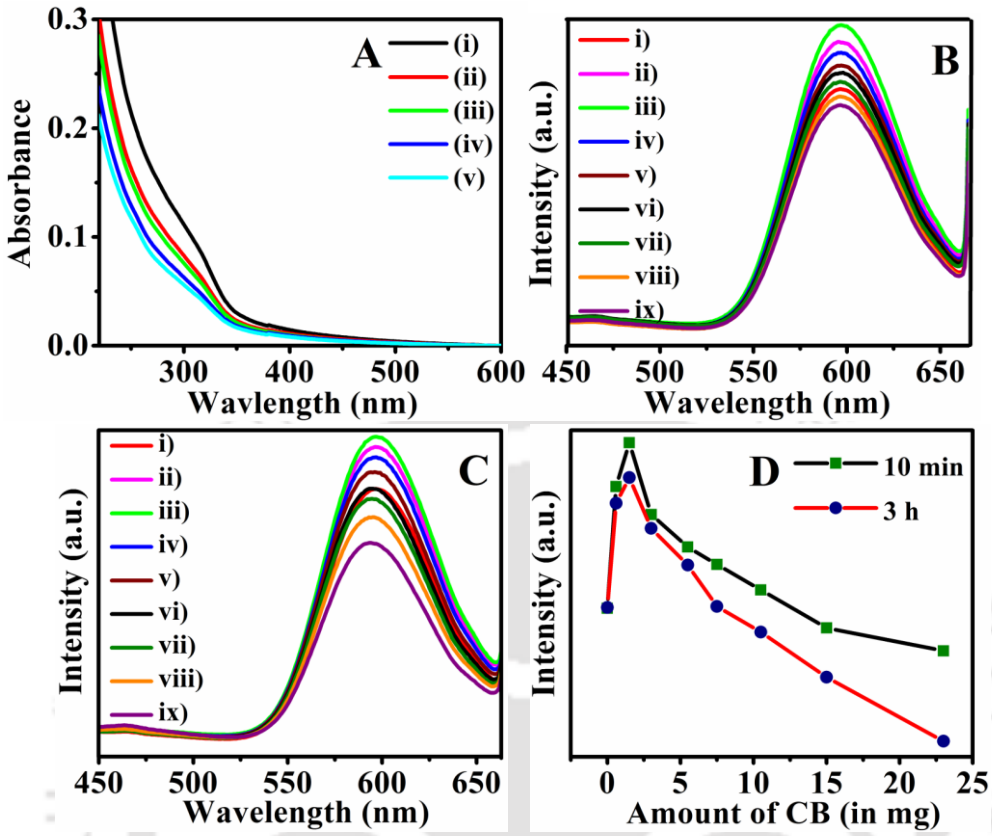


**Figure 2-1.** (**A**) Absorption spectra of Qdots treated with increasing amount of CB (7-23 mg). Fluorescence emission spectra of $Mn^{2+}$-doped ZnS Qdots recorded after (**B**) 10 min and (**C**) 3 h incubation of fixed amount of CB addition. The spectra were for (**i**) as synthesized Qdots and those of Qdots treated with (**ii**) 0.6 mg (**iii**) 1.5 mg (**iv**) 3 mg (**v**) 5.5 mg (**vi**) 7.5 mg (**vii**) 10.5 mg (**viii**) 15 mg (**ix**) 23 mg each separately with 10 mL of Qdots. The excitation wavelength for all the samples was fixed at 340 nm. (**D**) Change in emission intensity of samples incubated for (**i**) 10 min, as calculated from data in Figure (**B**) and for (**ii**) 3 h, as calculated from data in Figure (**C**).

For example, while the peak wavelength for as-synthesized Qdots was at 598 nm, addition of 0.6 mg or 1.5 mg of the beads changed the peak to 597 nm. When the amount of bead was 3 mg the wavelength shifted to 597-596 nm. Additionally, when the bead amount was 5.5 mg the peak was at 595 nm, and with 7.5 mg or 10.5 mg the emission peak shifted to 595-594 nm. Furthermore, an addition of 15 mg and 23 mg of the beads led to change in the peak position to 594 nm. It is important to point out here that a shift in emission peak wavelength of 4 nm

although apparently small, given the nature of the emission being atomic (ion) the shift may be considered as significant.

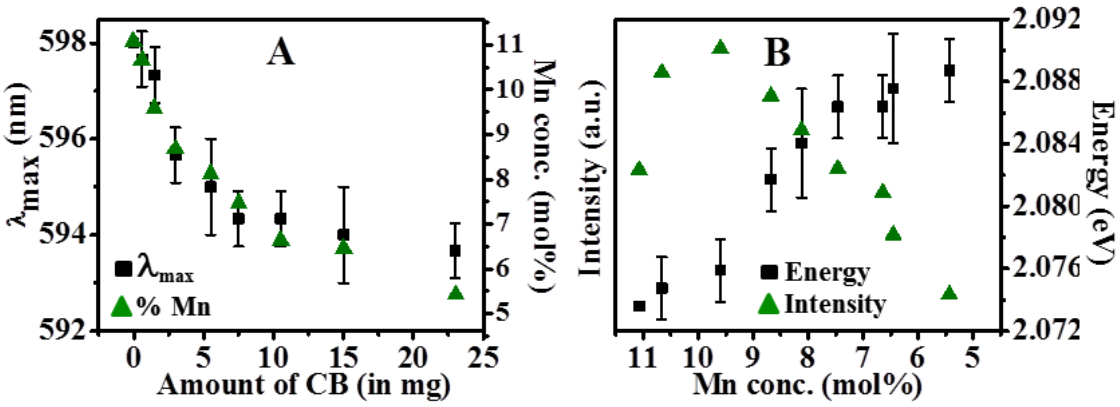


**Figure 2-2.** (**A**) Change in emission peak wavelength and % Mn against the amount of bead as calculated from data in Figure 2-1C. (**B**) Change in emission intensity and emission energy gap with respect to change in % Mn. Here, % Mn represents mole percentage with respect to Zn and the error is the standard deviation.

Atomic absorption spectroscopic studies of the Qdots treated with CB and incubated for 3 h indicated loss of both $Mn^{2+}$ and $Zn^{2+}$ ions from the Qdots. The loss increased with the increase in amount of CB. With the addition of beads to the Qdots both $Mn^{2+}$ and $Zn^{2+}$ ions were systematically removed (Figures 2-3, A and B). Sharp decrease in the $Mn^{2+}$ concentrations could be observed first followed by a slower process of removal, with $Mn^{2+}$ ions being removed at a faster rate for all concentrations of CB. Further, $Mn^{2+}$ ions were removed from a concentration of 11% to 5.5 % (Figure 2-2A). It is also interesting to note the correlation between the emission intensity and $Mn^{2+}$ concentration as shown in Figure 2-2B. The intensity of emission increased initially as the concentration of $Mn^{2+}$ decreased (from 11% to 9.5%); beyond this the removal of ions led to lowering of emission QY. The results indicated that the emission efficiency of a doped Qdots could be tuned by systematic removal of ions present in the Qdot. The initial increase in intensity indicated that the presence of excess dopant ions in the crystal may decrease the emission efficiency, which has also been observed earlier via synthesis of Qdots with different dopant concentrations.[18, 19] On the other hand, the decrease in intensity with the increase in the concentration of CB supported

the conventional knowledge of concentration dependent emission, i.e. decrease in $Mn^{2+}$ decreased the emission intensity. Overall, the experiments indicated that the Qdots reacted with CB and the ions present in the crystals could be removed systematically by the ion exchange resin beads, leading to controllable changes in emission quantum yield.

Also, in Figure 2-2B, the plot of energy difference between $^4T_1$ and $^6A_1$ states of $Mn^{2+}$ in the crystal lattice of ZnS as a function of decreasing dopant concentration indicated step - wise increase. The increase in energy could be attributed to the loss of clustering of $Mn^{2+}$ ions especially those present on the surface. The trend indicated that the as - synthesized crystals consisted of larger number of clusters of $Mn^{2+}$ ions. The treatment of the Qdots with CB led to systematic removal of clusters of ions. This, consequently led to increase in the energy gap between the atomic states till it finally reached the level where clustering was minimum.

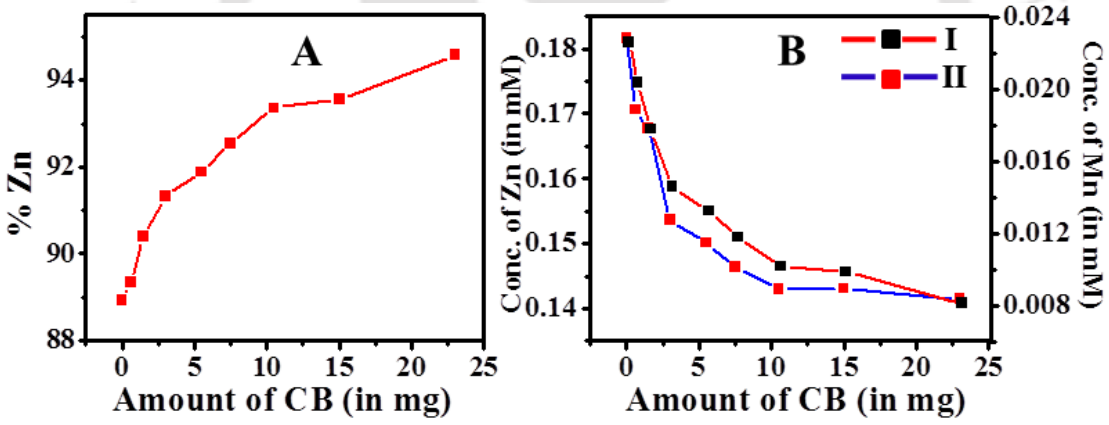


**Figure 2-3.** (**A**) The relative increase in $Zn^{2+}$ ion population with removal of $Mn^{2+}$ ions against amount of CB used and (**B**) Change in concentration (in mM) of $Zn^{2+}$ ions (**I**) and $Mn^{2+}$ ions (**II**) against amount of CB used.

It is also important to mention here that the word 'cluster' has been used here in a general sense. For example, it could be that there would be different extent of clustering of $Mn^{2+}$ ions in the same crystal or in different crystals. Now, when the number of ions in a cluster is large there may not be any emission from the cluster. However, when the numbers of ions are sufficiently small the cluster may contribute to the emission (albeit with lower efficiency). It could be that clusters of ions present on the surface of the crystal shifts the emission maximum to the

red. Thus when the ions from the smaller clusters are selectively removed, there would be changes in the emission characteristics with concomitant blue shift of emission peak from the original value. This is what has been observed herein. That the presence of clusters in the crystals was significant and their removal using CB was obvious has been demonstrated by the ESR results.

The systematic loss of $Mn^{2+}$ ions from the Qdots due to the treatment with CB was further corroborated by ESR measurements. The results are shown in Figure 2-4. Qdots with four different $Mn^{2+}$ precursor concentrations were prepared and actual concentration of Mn present in the Qdots increased with increase in the amount of precursor used during synthesis, which was clearly reflected in the ESR spectra. Figure 2-4A and 2-4B, which are the ESR spectra of the Qdots with high Mn content (11% Mn), exhibited six weak peaks along with strong background signal due to Mn-Mn interactions, possibly due to the presence of clusters of $Mn^{2+}$. With the addition of smaller amount of CB (0.6 mg to 5 mg) the sharpness of the peaks increased as shown in Figures 2-4 A (I) to A (IV), indicating slight reduction in the clustering. The same was observed for Qdots with intermediate concentration of Mn (7 % Mn in the Qdot), shown in Figure 2-4C. With increasing CB amount added to the Qdots, the sharpness of the peaks increased significantly as shown in Figures 2-4B(I) to B(IV). The reduction of the background signal accompanying the enhancement of the sharpness of the peaks was also apparent from the spectra. It may be mentioned here that the ESR spectra mentioned above (Figure 2-4A) corresponded to the samples in which emission intensity increased upon addition of the CB. Further, Figure 2-4B shows the ESR spectra of the samples in which more amount of CB (7.5 mg to 25 mg) were added and in which the intensities of emission decreased upon addition of the beads. As is clear from Figure 2-4, the addition of CB enhanced the sharpness of the peaks and also decreased the background signal significantly. The above results indicated that upon addition of CB to the Qdots, the clustering of the Mn ions was reduced. Also the background signal usually observed due to clustered ions decreased and the prominence of the six ESR peaks that corresponds to the presence of isolated $Mn^{2+}$ ions increased.

When Qdot samples with low Mn content (3% and 1.2 % Mn) were treated with CB, similar observations were made. Figures 2-4D (I) and E (I) are ESR spectra of

the as- synthesized Qdots, whereas D (II) and E (II) are those of the samples after CB (7.5 mg) treatment. Thus at lower $Mn^{2+}$ concentrations the ESR signals were sharper to begin with and with low background signal, due to absence of significant clustering of $Mn^{2+}$ ions. Even then treatment of the Qdots with CB led to further lowering of background and enhanced clarity of the peaks. This means that clustering of the ions on the surface of the Qdots could occur at all concentrations of the dopant; although lowering of prevalence of occurrence with lower impurity concentration took place. It is important to mention here that the weak peaks at the edges of Figure 2-4E(I), which corresponds to Mn present on the surface, were greatly diminished upon treatment with CB as shown in Figure 2-4E(II).

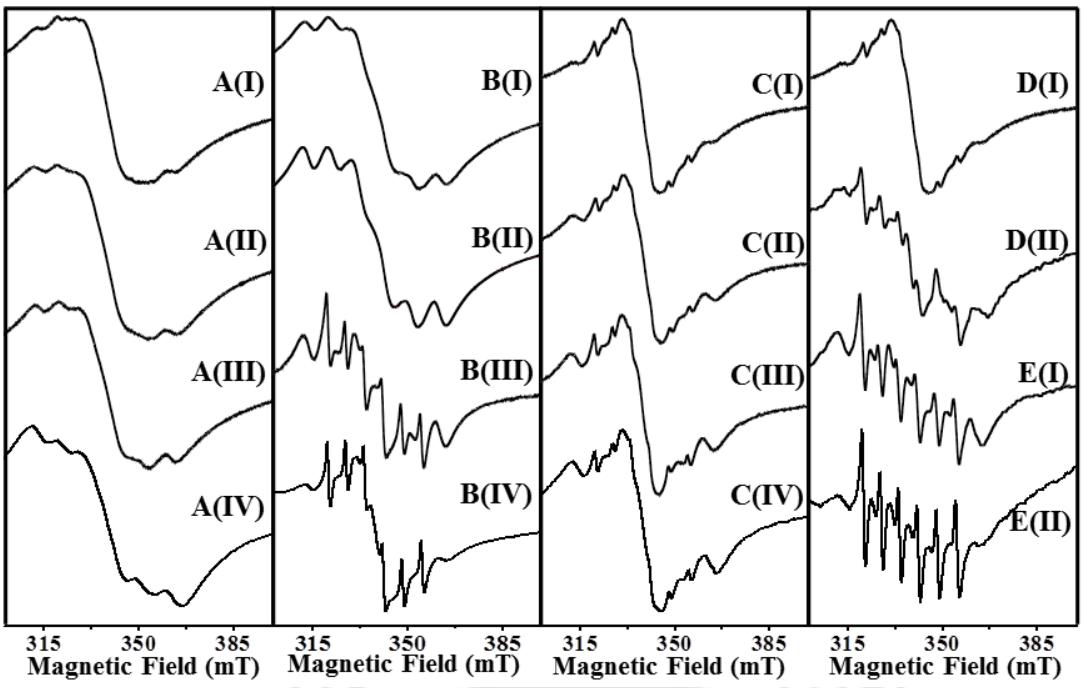


**Figure 2-4.** ESR spectra of Mn doped ZnS Qdots treated with cation beads. (**A**) is for Qdots with high Mn content (11%) treated with smaller amounts of CB (**i**) 0 mg CB; (**ii**) 0.6 mg (**iii**) 3 mg (**iv**) 5.5 mg; (**B**) is for the same Qdots but treated with higher amounts of CB (**i**) 7.5 mg CB; (**ii**) 10.5 mg (**iii**) 15 mg (iv) 25 mg; (**C**) is for Qdots with intermediate concentration of Mn (7%) treated with smaller amounts of CB (0.6 mg to 5.5 mg); (**DI**) and (**EI**) are of Qdots with very less Mn content (3% and 1.2% respectively) and (**DII**) and (**EII**) are the spectra recorded after treatment with 7.5 mg of CB.

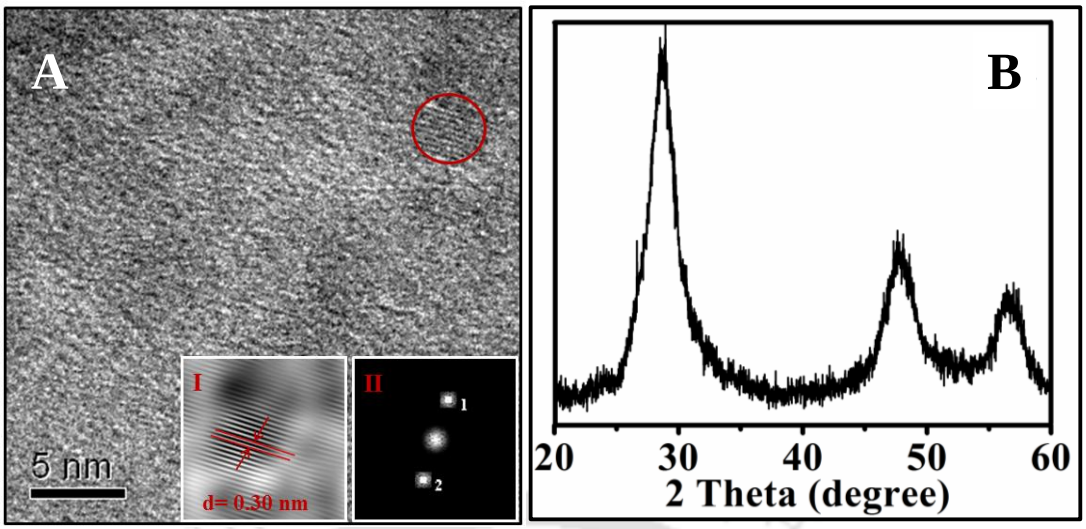


**Figure 2-5.** (**A**) High resolution TEM image with (**I**) Inverse Fast Fourier Transform (IFFT) image of the selected region and (**II**) the corresponding FFT image in the inset; (**B**) Powder X-ray diffraction pattern of as-synthesized $Mn^{2+}$- doped ZnS Qdots.

This clearly indicated the removal of surface $Mn^{2+}$ ions by the beads. It may be mentioned here that the ESR measurements were performed with solid samples of Qdots, obtained following incubation with CB for 3 h.

The average particle size of the as-synthesized Qdots was found to be 3.5 $\pm$ 0.3 nm as calculated from TEM images (Figure 2-6) with d-spacing equal to 0.30 nm (Figure 2-5A). Size calculated from powder XRD pattern (Figure 2-5B) also matched with the TEM results. TEM measurements of the Qdots treated with CB indicated that at lower amounts of the beads there was no discernible change in the average size of the particles. For example, when the as-synthesized Qdots with size of 3.5 $\pm$ 0.3 nm were treated with 1.5 mg or 10.5 mg of the CB the particle sizes remained the same (Figure 2-6B). However, when the amount of bead was further increased the particle size was reduced (following addition of 25 mg of beads) to 2.8 $\pm$ 0.2 nm (Figure 2-6C). UV-vis spectroscopic measurements indicated that the particle size changed by modest amount from 3.9 nm to 3.5 nm upon treatment with the beads (Figure 2-1A). Further, it was observed that the PL QY of samples of diameter 3.9 $\pm$ 0.14 nm was 6%, while that of size 3.5 $\pm$ 0.15 nm was 4%.

The above results were further complemented by performing etching of the Qdots using a strong acid (HCl), following a literature procedure. Upon etching of

the Qdots, the Mn% content was substantially reduced at a faster rate than Zn%. Thus, majority of $Mn^{2+}$ ions were present on the surface of the Qdots and in its immediate vicinity (refer to Appendix).

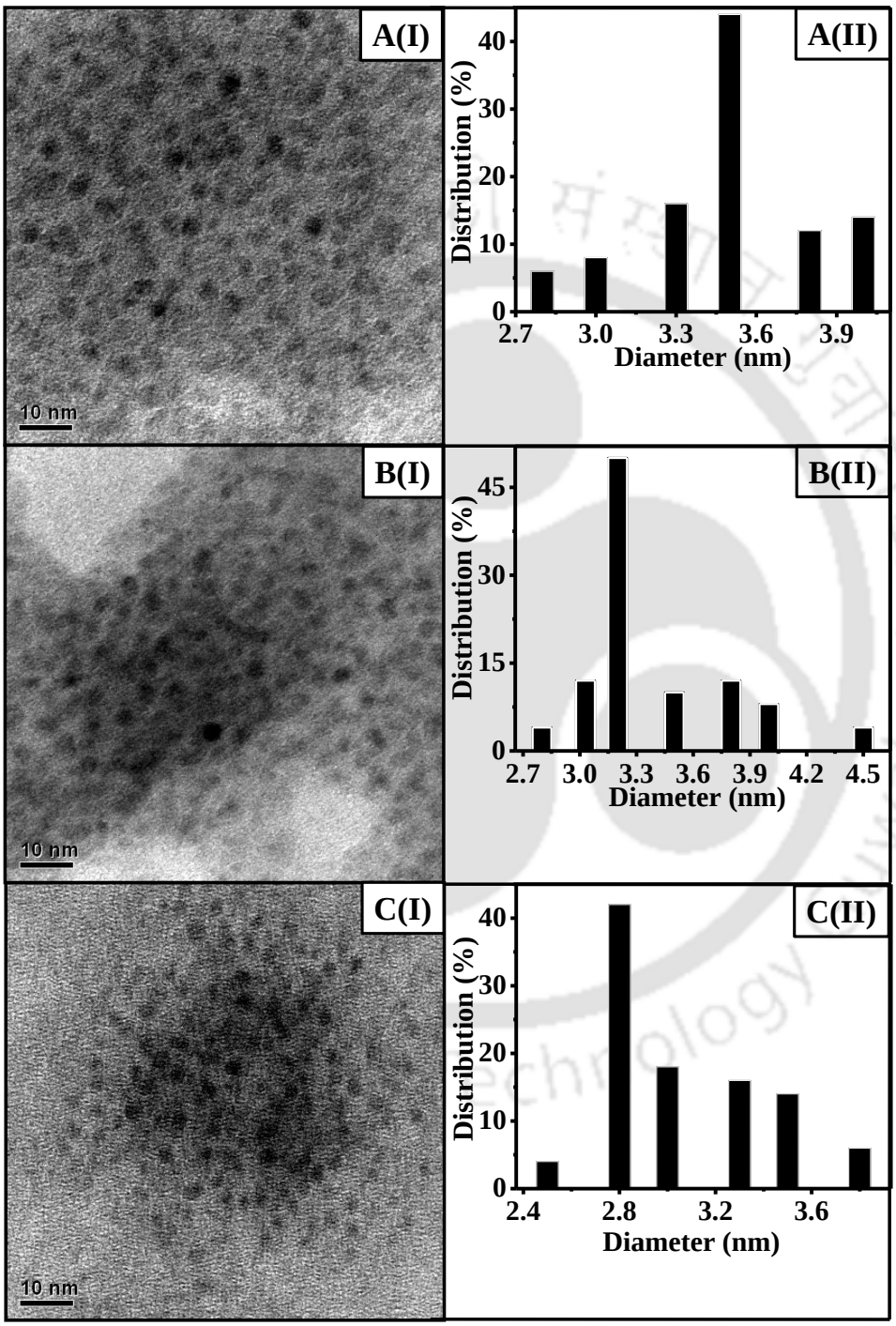


**Figure 2-6.** TEM image and their corresponding particle size distribution of (**A**) as-synthesized Qdots, (**B**) Qdots treated with smaller amount of CB and (**C**) Qdots treated with higher amount of CB.

Based on the results as above, the following process may be concluded to be responsible for the observed changes in the emission characteristics of the $Mn^{2+}$-ZnS in the presence of CB. A general representation of the Qdots and their fate upon treatment with CB is shown in Scheme 2-1.

First of all, it is clear that the $Mn^{2+}$-doped ZnS Qdots reacted with CB to release both the $Mn^{2+}$ and $Zn^{2+}$ ions to the beads. This is the primary reason for the observed changes in the intensity and wavelength of the photoluminescence of the Qdots. Also, there seems to be the presence of $Mn^{2+}$ ions on the surface of the Qdots at all dopant ($Mn^{2+}$) concentrations, in addition to their possible presence in the immediate vicinity of the surface and deep inside the crystal. The dopant ions (in the form of clusters) could be present on the surface of the Qdot as defects. While ions present in the subsurface could be bonded in octahedral geometry and are labile. Thus they could be removed by ion exchange resins with relative ease, even at room temperature. Similar would be the case with loosely bonded $Zn^{2+}$ ions present on the surface as defects.

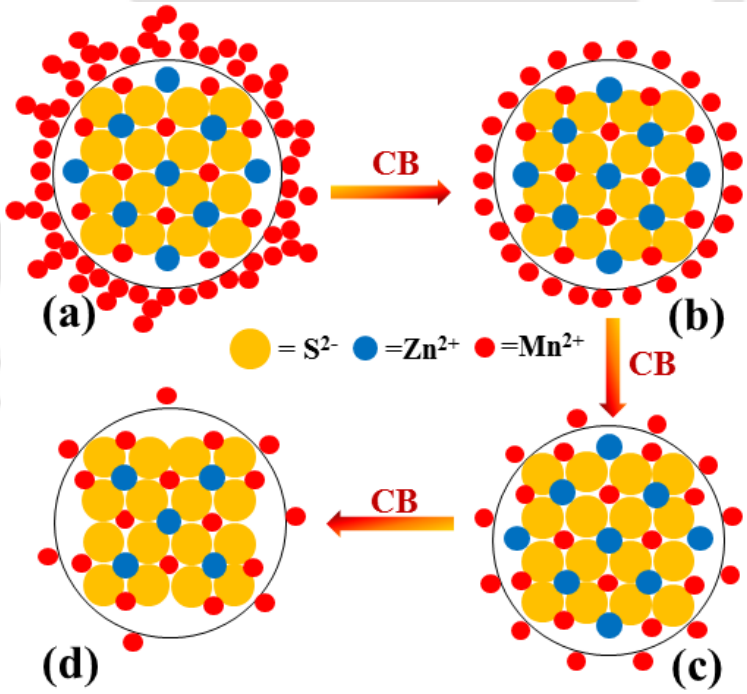


**Scheme 2-1.** A pictorial representation of the Qdots and their fate upon treatment with CB.

Also, there is substantial clustering of ions present on the surface of the Qdots. It could be that the population of the clusters in the Qdots synthesized herein was generally high to have resulted in the observed ESR signals consisting of high background with weakly resolved peaks, especially at higher concentrations of the dopants. With removal of clusters of $Mn^{2+}$ ions, the quality of ESR signal due to the individual $Mn^{2+}$ ions was improved as has been observed herein.

In other words, the systematic decrease in the background signal and enhancement of clarity of the peaks due to $Mn^{2+}$ ions for all the samples indicated the presence of clusters of $Mn^{2+}$ ions and their removal in the presence of CB. In the presence of small amount of CB, the $Mn^{2+}$ ions present in the clusters were preferentially (over other $Mn^{2+}$ ions present in the crystal) removed by the CB. Since the $Mn^{2+}$ ions in the form of clusters act as defects, their removal led to increase in the emission intensity. On the other hand, with further increase in the addition of CB individual $Mn^{2+}$ ions present on the surface and subsurface would be removed. This would have led to net decrease in the emission quantum yield. In general loosely bonded $Zn^{2+}$ ions present on the surface through dangling bonds or as clusters would also be removed along with the $Mn^{2+}$ ions. However, increase in the amount of CB led to further removal of surface $Zn^{2+}$ ions resulting in the reduction of particle size systematically. This would lead to exposure of the inner $Mn^{2+}$ ions to the medium which would again be removed by the CB. This process would continue in the presence of increasing amount of CB. However, we have used CB up to a particular concentration; so that pH of the medium did not change and also that the changes due to emission from $Mn^{2+}$ ions could be probed. Further, one cannot also discount the contribution of the new defect centers, which could possibly have been created on the surface following removal of ions resulting in additional quenching of fluorescence.

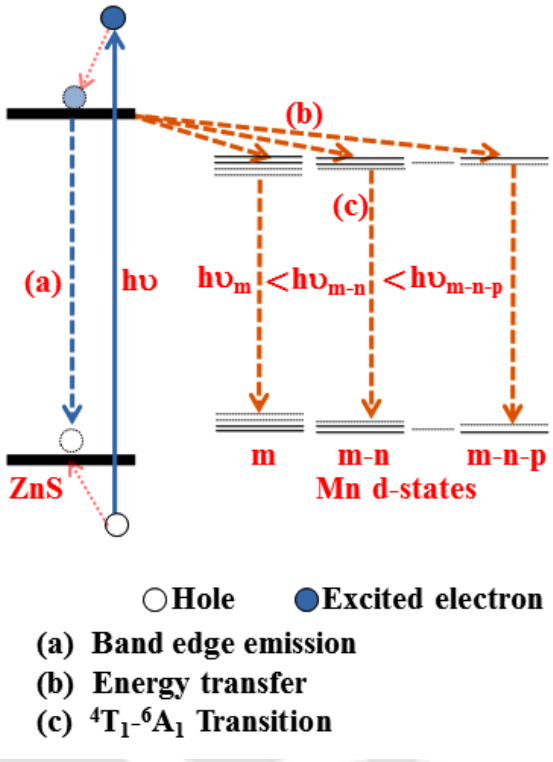


**Scheme 2-2.** Schematic diagram illustrating the energy gap between the $^4T_1$ - $^6A_1$ of $Mn^{2+}$ in the (ZnS) crystals, in the presence of increasing amount of CB

It is known that Mn-Mn interaction leads to the decrease in the energy between $^4T_1$ - $^6A_1$ states of the emitting $Mn^{2+}$ ions present as a dopant in ZnS Qdots.[25-27] Thus with increased doping, the emission wavelength shifts to longer wavelength due to formation of larger clusters or large number of smaller clusters. Upon treatment with small amount of CB although the sizes and numbers of the clusters might have been reduced, their presence was persistent. Thus at the lower amount of CB the intensity of emission increased but there was no change in emission peak wavelength. This was also reflected in the presence of background signal (due to clusters of Mn) in the ESR spectra. On the other hand, with the presence of increasing amount of CB the sizes and numbers of clusters were increasingly removed. Along with this, the individual $Mn^{2+}$ ions present on the surface also might have been removed. Thus with increasing removal of total $Mn^{2+}$ ions while the intensity of emission decreased, the peak wavelength of emission blue shifted increasingly. This is a consequence of an increase in energy gaps between the two states of $Mn^{2+}$ involved in emission. A plot of the energy gap of $^4T_1$- $^6A_1$ states of

$Mn^{2+}$ present in the Qdots as a function of decreasing percentage of Mn, as shown in Figure 2-2B, revealed a stepwise shift (as mentioned before). A schematic diagram of the energy gap between the $^4T_1$ - $^6A_1$ of $Mn^{2+}$ in the crystals in the presence of increasing amount of CB is shown in Scheme 2-2. The scheme essentially illustrates the presence of band like structures and their gradual removal in the presence of the beads. As a consequence the energy gap increases.

## 2.4. Conclusion

In brief, the results demonstrated a new way of tuning the emission energy of doped quantum dots. This is based on systematic removal of the clusters of dopant ions present on the surface of the crystals using CB. The removal of clusters of ions led to the increase in emission QY especially at lower additions of CB. Results also indicated that initial changes (increase) in the emission QY were without changes in the particle size. On the other hand, further changes in emission (reduction) were due to lowering of concentrations of $Mn^{2+}$. Both $Zn^{2+}$ and $Mn^{2+}$ could be removed in the presence of the beads. Thus a new way of engineering the surface of Qdots could be achieved following their synthesis by systematic removal of surface ions.

The results presented in this chapter point towards significant contribution of surface ions to the overall emission characteristics and newer insights into the origin of photoluminescence especially in doped Qdots.

## References


1) Alivisatos, A. P. *J. Phys. Chem.* **1996**, 100, 13226-13239.
2) Erwin, S. C.; Zu, L.; Haftel, M. I.; Efros, A. L.; Kennedy, T. A.; Norris, D. J. *Nature* **2005**, 436, 91-94.
3) Schwartz, D. A. ; Nor-berg, N. S.; Nguyen, Q. P.; Parker, J. M.; Gamelin, D. R. *J. Am. Chem. Soc.* **2003**, 125, 13205-13218.
4) Norris, D. J.; Efros, A. L.; Erwin, S. C. *Science* **2008**, 319, 1776–1779.
5) Pradhan, N.; Sarma, D. D. *J. Phys. Chem. Lett.* **2011**, 2, 2818–2826.
6) Norris, D. J.; Yao, N.; Charnock, F. T.; Kennedy, T. A. *Nano Lett.* **2001**, 1, 3–7.
7) Srivastava, B. B.; Jana, S.; Karan, N. S.; Paria, S. Jana, N. R.; Sarma, D. D.; Pradhan, N. *J. Phys. Chem. Lett.* **2010**, 1, 1454–1458.
8) Bhargava, R. N.; Gallagher, D.; Hong, X.; Nurmikko, A. *Phys. Rev. Lett.* **1994**, 72, 416-419.
9) Bol, A. A.; Meijerink, A. *J. of Lumin.* **2000**, 315, 87-89.
10) Nag, A.; Cherian, R.; Mahadevan, P.; Gopal, A. V.; Hazarika, A.; Mohan, A.; Vengurlekar, A. S.; Sarma, D. D. *J. Phys. Chem. C* **2010**, 114, 18323–18329.
11) Kennedy, T. A.; Glaser, E. R.; Klein, P. B.; Bhargava, R. N. *Phys. Rev. B* **1995**, 52, R14356.
12) Zhang, W.; Li, Y.; Zhang, H.; Zhou, X.; Zhong, X. *Inorg. Chem.* **2011**, 50, 10432–10438.
13) Chen, D.; Viswanatha, R.; Ong, G. L.; Xie, R.; Balasubramaninan,M.; Peng, X. *J. Am. Chem. Soc.* **2009**, 131, 9333-9339.
14) Zeng, R.; Rutherford, M.; Xie, R.; Zou, B.; Peng, X. *Chem. Mater.* **2010**, 22, 2107-2113.
15) Nag, A.; Chakraborty, S.; Sarma, D. D. *J. Am. Chem. Soc.* **2008**, 130, 10605–10611.
16) Bol, A. A.; Meijerink, A. *J. Phys. Chem. B* **2001**, 105, 10197-10202.
17) Borse, P. H.; Srinivas, D.; Shinde, R. F.; Date, S. K.; Vogel, W.; Kulkarni, S. K. *Phys. Rev. B* **1999**, 60, 8659-8664.
18) Sooklal, K.; Cullum, B. S.; Angel, S. M.; Murphy, C. J. *J. Phys. Chem.* **1996**, 100, 4551-4555.
19) Geszke, M.; Murias, M.; Balan, L.; Medjahdi,G.; Korczynski, J.; Moritz, M.; Lulek,J.; Schneider, R. *Acta Biomater.* **2011**, *7*, 1327-1338.

20) Sohling, U.; Jung, G.; Saenger, D. U.; Lu, S.; Kutsch, B.; Menning, M. *J. Sol-Gel Sci. Techn*. **1998**, *13*, 685.

21) Wang, C.; Gao, X.; Ma,Q.; Su, X. *J. Mater. Chem.* **2009**, 19, 7016–7022.

22) Aboulaich, A.; Balan, L.; Ghanbaja, J.; Medjahdi, G.; Merlin, C.; Schneider, R. *Chem. Mater*. **2011**, 23, 3706–3713.

23) Aboulaich, A.; Geszke,M.; Balan,L.; Ghanbaja, J.; Medjahdi,G.; Schneider, R. *Inorg. Chem*. **2010**, 49, 10940–10948.

24) Shao, P.; Zhang, Q.; Li, Y.; Wang, H. *J. Mater. Chem*. **2011**, 21, 151–156.

25) Beaulac, R.; Archer, P. I.; Gamelin, D. R. *J. Solid State Chem*. **2008**, 181, 1582-1589.

26) Blasse, G.; Grabmaier, B. C. Luminescent Materials; Springer-Verlag: Berlin, **1994**.

27) Mahamuni, S.; Lad, A. D.; Patole, S. *J. Phys. Chem. C* **2008**, 112, 2271–2277.

# Chapter 3

## In situ Reversible Redox Tuning of Photoluminescence in $Mn^{2+}$-doped ZnS Quantum Dots

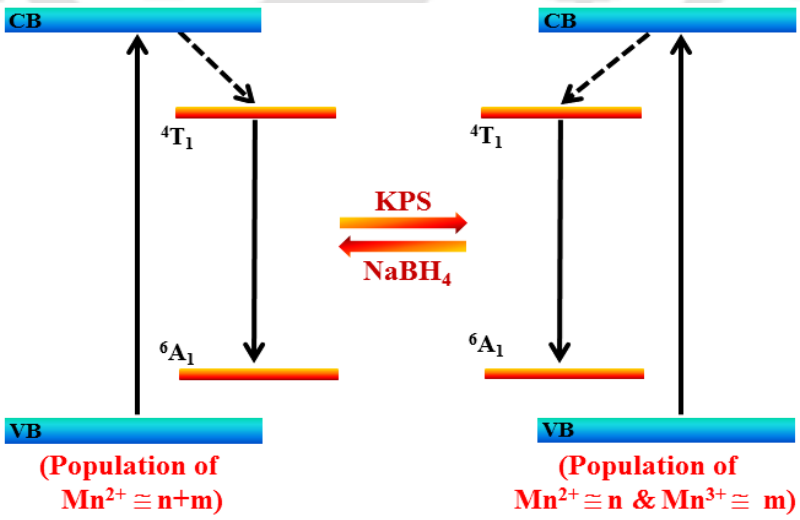

# Chapter 3

**Abstract**: The chapter introduces a new concept and method for in situ reversible tuning of photoluminescence properties of quantum dots (Qdots) by partial oxidation of population of the emitting species and subsequent chemical reduction of their oxidized form. The concept has been demonstrated using $Mn^{2+}$-doped ZnS Qdots stabilized by acetyl acetonate. Treatment of an aqueous solution of the Qdots with potassium peroxodisulfate (KPS) led to reduction of intensity of emission due to $Mn^{2+}$ ($^4T_1$-$^6A_1$). Subsequent treatment of the solution containing KPS-treated Qdots with $NaBH_4$ led to regaining of intensity thus providing reversibility to the tuning. This was possible for more than one cycle. Electron spin resonance (ESR) spectroscopic investigations revealed reduction of population of $Mn^{2+}$ upon treatment with KPS, whereas it went back up upon subsequent treatment with $NaBH_4$.

## 3.1. Introduction

So far, control over size and shape, doping with impurities, surface passivation and functionalization with organic or biological moieties have been the primary strategies for control over optical properties of the Qdots.[1-4] Although chemistry has played a major role in achieving the objectives; many important aspects of it - such as the involvement of redox chemistry – much remain to be explored. For example, the visible fluorescence intensity and peak wavelength of $Mn^{2+}$-doped ZnS Qdots - which have also been synthesized on large-scale with high quantum yield (QY)[5] - are mainly influenced by the extent of doping and the concentration of $Mn^{2+}$ on the surface of the Qdots.[6] However, since different oxidation states of Mn could be stabilized, the emission characteristics should potentially be amenable to oxidation of $Mn^{2+}$ ions. In other words, by partially oxidizing the population of $Mn^{2+}$ ions present in the Qdots, one could potentially control the concentration of $Mn^{2+}$ and thus emission characteristics of the doped Qdots. This is important as one could not only have control over the emission but also the Qdots could potentially be used as probes for redox reactions.

Recently, chemical and electrochemical reduction of Qdots have been a subject of important investigations.[7-8] On the other hand, electron injection into quantum dots as well as their electrochemical reduction has been used to control their emission properties.[9-12] Interestingly, the charged dots so created were not so stable making their potential applications rather limited. On the other hand, different redox states of doped ions in quantum dots could be stabilized due to the inherent stability of the ions in different oxidation states. This would provide an opportunity to have even solid powders of doped Qdots where the dopant ions would be in different oxidation states making the application more versatile. To the best of our knowledge there is no literature on this particular way of reversible tuning of emission of doped Qdots, taking recourse to changing the population of the oxidation states of the dopant.

In this chapter, it has been demonstrated that emission intensity of $Mn^{2+}$-doped ZnS Qdots could be tuned in situ by systematically changing the population of $Mn^{2+}$ ions. In other words, treatment of the Qdots with an oxidizing agent would reduce the intensity of the emission peak due to $Mn^{2+}$; whereas the intensity could be recovered by subsequent addition of a reducing agent. Acetyl acetone was used as the stabilizing agent as acetyl acetonate (AcAc) complexes of $Zn^{2+}$, $Mn^{2+}$ and $Mn^{3+}$ are stable at room temperature, thus could potentially provide stability to the $Mn^{3+}$ ions generated on the surface.

| Redox couple | $E^0$ (in Volt) |
|---|---|
| $Zn^{2+}/Zn$ | -0.76 |
| $S/S^{2-}$ | -0.48 |
| $Mn^{3+}/Mn^{2+}$ | +1.54 |
| $MnO_4^-/Mn^{2+}$ | +1.51 |
| $MnO_4^-/MnO_2$ | +1.68 |
| $S_2O_8^{2-}/HSO_4^{2-}$ | +2.12 |
| $BH_4^-/H_2BO_3^-$ | +1.24 (alkaline) |
| $BH_4^-/B(OH)_3$ | +0.48 (acidic) |

**Table 3-1.** The Table indicates redox potential of important species involved in the redox reactions carried out in the experiments reported herein.[13]

Further, since both $Mn^{2+}$ and $Mn^{3+}$ ions, if present on the surface, could be stabilized by the same ligand i.e. AcAc, possibly through complexation, it is particularly advantageous to oxidize and subsequently reduce Mn ionic species in the presence of the same ligand. It is known that oxidation of $Mn^{2+}$ occurs preferentially in comparison to AcAc especially in the pH range of 5.0 – 6.5, which is the range under which oxidation was carried out in the present experiments.[14] A table with redox potentials of relevant species are shown in Table 3-1.

## 3.2. Experimental section

### 3.2.1. Materials

Zinc acetate dihydrate (98%), manganese acetate tetrahydrate (99%), sodium sulfide (55-58%), acetyl acetone (98%), potassium peroxodisulfate (99%), sodium borohydride (95%) potassium permanganate (98.5%), potassium dichromate (99.5%, Rankem), tri-sodium citrate dihydrate (99%) were used as purchased. All chemicals (except potassium dichromate) were from Merck Limited, Mumbai, India.

### 3.2.2. Synthesis of Qdots

#### 3.2.2.1. Using Mn-acetate as the precursor for Mn

Acetyl acetonate (AcAc) stabilized $Mn^{2+}$-doped ZnS Qdots were synthesized in aqueous medium, as described in the previous chapter. Firstly, 400 µL of acetylacetone was added to 50 mL water and the mixture was heated at 85 $^0$C for 5 min in order to obtain a clear solution. To the solution 5.0 mM each of zinc acetate and sodium sulphide (1:1 ratio) was added, followed by addition of manganese acetate (4.0 mM) and the reaction mixture was allowed to stir for 3 h under refluxing condition. The colloidal solution so obtained was centrifuged at a speed of 22,000 rpm for 20 min and finally redispersed in 50 mL water, following the same procedure as before.

#### 3.2.2.2. Using Potassium permanganate ($KMnO_4$) as the precursor for Mn

The method for the synthesis of the Qdots was the same as above except that potassium permanganate (1.7 mM) was used as the precursor for Mn instead of manganese acetate.

### 3.2.3. Treatment of Qdot solution with potassium peroxodisulfate (KPS)

#### 3.2.3.1. Estimation of KPS

In a stoppered conical flask 20 mL of 0.02 N KPS solution (as prepared) and 20 mL of 0.25 N KI solutions were mixed thoroughly. To that solution 5.0 mL of 0.02 N Mohr's salt was added. The liberated iodine formed a brown color and the color changed with time. After 15 min, liberated iodine was then titrated with 0.1 N sodium thiosulphate. The end point was marked by disappearance of brown color. It was observed that the as-purchased KPS was 47.5 % pure.

#### 3.2.3.2. KPS treatment of Qdots

Three different solutions with concentrations of 17.6 mM, 35.1 mM and 105.5 mM KPS were prepared. 25 µL of each of these solutions were added separately to three different 2.0 mL solutions of Qdots (final concentrations of KPS being 0.22 mM, 0.43 mM and 1.30 mM respectively). Fluorescence spectra of all the solutions were recorded before and after addition of KPS. Each of these solutions was heated again for 10 min at $70^0$C; cooled to room temperature, followed by recording of fluorescence spectrum.

### 3.2.4. Treatment of Qdot solution with sodium borohydride

In a separate experiment, 25 µL of 36.5 mM KPS solution was added to 2.0 mL of as-synthesized Qdots (final concentration of KPS in 2.025 mL solution being 0.45 mM) and fluorescence spectra were recorded before and after addition of KPS. This was followed by heating the solution at $70^0$C for 10 min; then cooling to room temperature and recording of fluorescence spectrum again. Then 20 µL of 1.0 M $NaBH_4$ (final concentration of $NaBH_4$ in 2.045 mL being 9.7 mM) was added to the KPS treated Qdot solution. Fluorescence spectrum of the sample was then recorded after about 15 min till the bubbling of the medium had stopped.

### 3.2.5. Treatment of Qdot solution with tri-sodium citrate

In a way similar as above; however, instead of $NaBH_4$, 50 uL of 0.6 M tri-sodium citrate (final concentration in 2.075 mL being 14.5 mM) was added to (0.22 mM) KPS treated Qdots.

### 3.2.6. Adjustments of pH of the medium

To the as-synthesized Qdots (source of Mn being Mn-acetate) first of all KPS was added and fluorescence spectra were recorded before and after addition. The pH of the solution was measured following addition, which was found to be acidic. This was followed by addition of $NaBH_4$, and then fluorescence spectrum was recorded. It was observed that pH of the solution was alkaline. The solution was further treated with 15.0 μL of dilute hydrochloric acid; pH was measured and then it was treated with KPS again.

### 3.2.7. Treatment to Qdots (synthesized using $KMnO_4$ as the precursor of Mn) with $NaBH_4$ and KPS

To a 2 mL dispersion of Qdots, the fluorescence of which was measured, 25 μL of 1.0 M $NaBH_4$ (final concentration in 2.050 mL being 12.1 mM) was added. This was followed by measurement of fluorescence. The pH of the solution was then adjusted by adding dilute hydrochloric acid. To the dispersion KPS was added so that the final concentration was 0.45 mM followed by recording of fluorescence spectrum. Finally, $NaBH_4$ was added to the dispersion as above, which was followed by recording of fluorescence.

### 3.2.8. Sample preparation for analytical measurements

As described in chapter 2 (section 2.2.5) a large amount of Qdots was prepared, a part of which was treated with KPS, another part was further treated with $NaBH_4$ and powders were obtained as before. About 10.0 mg of powdered sample was used for ESR as well as for FTIR spectroscopic measurements. The rest of the sample for each type (as-synthesized Qdots, KPS-treated Qdots and $NaBH_4$-treated Qdots) which weighed about 120.0 mg for each was used for recording powder XRD. The above steps of preparing samples for XRD and ESR were followed for Qdots, the source of Mn of which was either Mn-acetate or $KMnO_4$.

TEM samples were also prepared for as-synthesized Qdots, KPS-treated Qdots and $NaBH_4$-treated Qdots (source of Mn being Mn-acetate) from the redispersed medium of each type. TEM measurement was also performed for as-synthesized Qdots, the source of Mn of which was $KMnO_4$.

### 3.2.9. Characterization

Characterization of the samples by UV, fluorescence, TEM and XRD measurements were performed by the same model of instruments as mentioned in the chapter 2; section 2.2.6. In addition, here FTIR spectra for as-synthesized Qdots, KPS-treated Qdots and $NaBH_4$-treated Qdots (source of Mn being Mn-acetate) were recorded with a Perkin-Elmer Spectrum One Spectrophotometer.

### 3.2.10. Estimation of $Mn^{2+}$ in the Qdots

Atomic absorption spectroscopic (AAS) measurements were performed to estimate the amount of $Mn^{2+}$ present in the final Qdot dispersion. Four different solutions with 1.0 ppm, 2.0 ppm, 3.0 ppm and 4.0 ppm concentrations of manganese, obtained from Atomic Absorption Standard solution (purity is 999 ppm, SRL, India), were prepared by dilution with water and used as calibration standard. This was followed by measurement with the 10 mL as-synthesized Qdot (the source of Mn being Mn-acetate) dispersion. It was observed that the solution contained 0.338 ppm of Mn. Now, if we assume that all the Zn-acetate in the original solution was converted into ZnS then calculation indicated that a minimum of 0.12 % of Mn was incorporated in the Qdots.

### 3.3. Results and Discussion

It has been established that the emission observed at ca. 593 nm is due to transition from $^4T_1$-$^6A_1$ $Mn^{2+}$ d- states present in the doped ZnS.[15] Thus by following change in emission intensity at 593 nm, one could essentially follow the change in population of $Mn^{2+}$ ions in the Qdots. However, if oxidation or reduction of Mn species were to be carried out using external chemical reagents present in the medium then the surface ions would preferentially get oxidized or reduced, as the ions present in the crystal lattices may not be amenable to redox reactions. For example, when AcAc stabilized as-synthesized $Mn^{2+}$-doped ZnS Qdot samples – the source of Mn during synthesis being $Mn(OAc)_2$- with an absorbance value of 0.04 at 350 nm were treated with 0.22 mM, 0.43 mM and 1.3 mM potassium peroxodisulfate (KPS), the intensity of the emission peak at 593 nm decreased systematically with increasing concentration of KPS, as shown in Figure 3-1A.

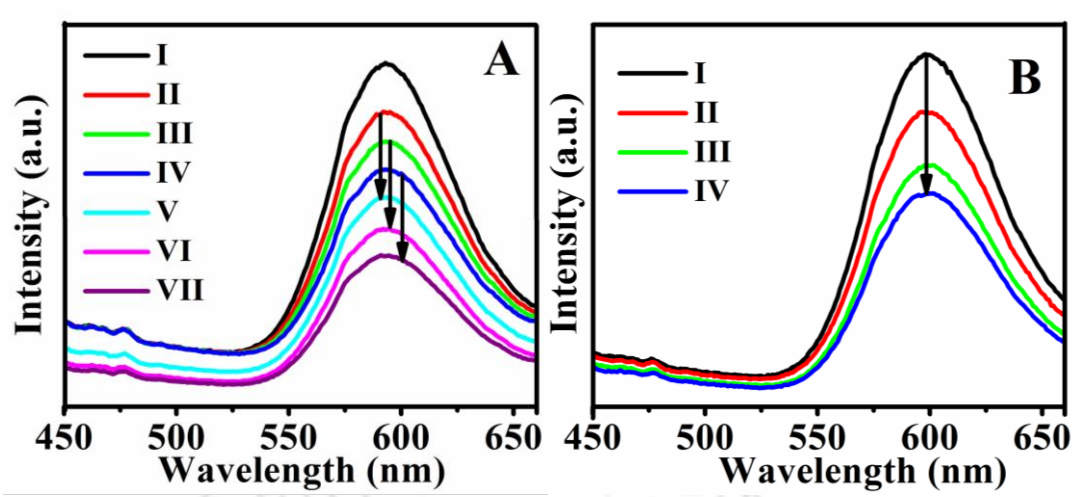


**Figure 3-1.** Fluorescence emission spectra of $Mn^{2+}$-doped ZnS Qdots under different experimental conditions. The excitation wavelength for all the samples was fixed at 350 nm. (**A**) Emission spectra of (**I**) as-synthesized Qdots; and those of Qdots treated with (**II**) 0.22 mM KPS; (**III**) 0.43 mM KPS; (**IV**) 1.3 mM KPS; (**V**) the sample in II upon heating; (**VI**) the sample in III upon heating and (**VII**) the sample in IV upon heating. (**B**) Emission spectra of (**I**) as-synthesized Qdots; (**II**) upon addition of 0.43 mM KPS at room temperature and recorded immediately after addition and (**III**) recorded after 25 min of addition (**IV**) upon addition of 0.43 mM KPS immediately followed by heating and then recorded after it was cooled to room temperature. The source of Mn of the Qdots was Mn-acetate

In addition, upon heating the samples at $70^0$C for 10 min the emission intensities of the samples decreased further. The change in the intensity upon heating followed the trend of that without heating as far as concentration of KPS present in the medium was concerned, with minimum change in the presence of 0.22 mM and the maximum being in the presence of 1.3 mM of KPS (Figure 3-1B). It is to be mentioned here that the reduction of fluorescence intensity occurred slowly at room temperature. On the other hand, at elevated temperatures the emission intensity reduced quickly for a particular concentration of KPS indicating faster reduction of population of $Mn^{2+}$. Interestingly, the concentration of KPS required for changes in the intensity was in excess of the maximum possible concentration of $Mn^{2+}$ present in the Qdots. Thus oxidation of $Mn^{2+}$ (if at all took place to $Mn^{3+}$) required an excess of stoichiometric amount of KPS.

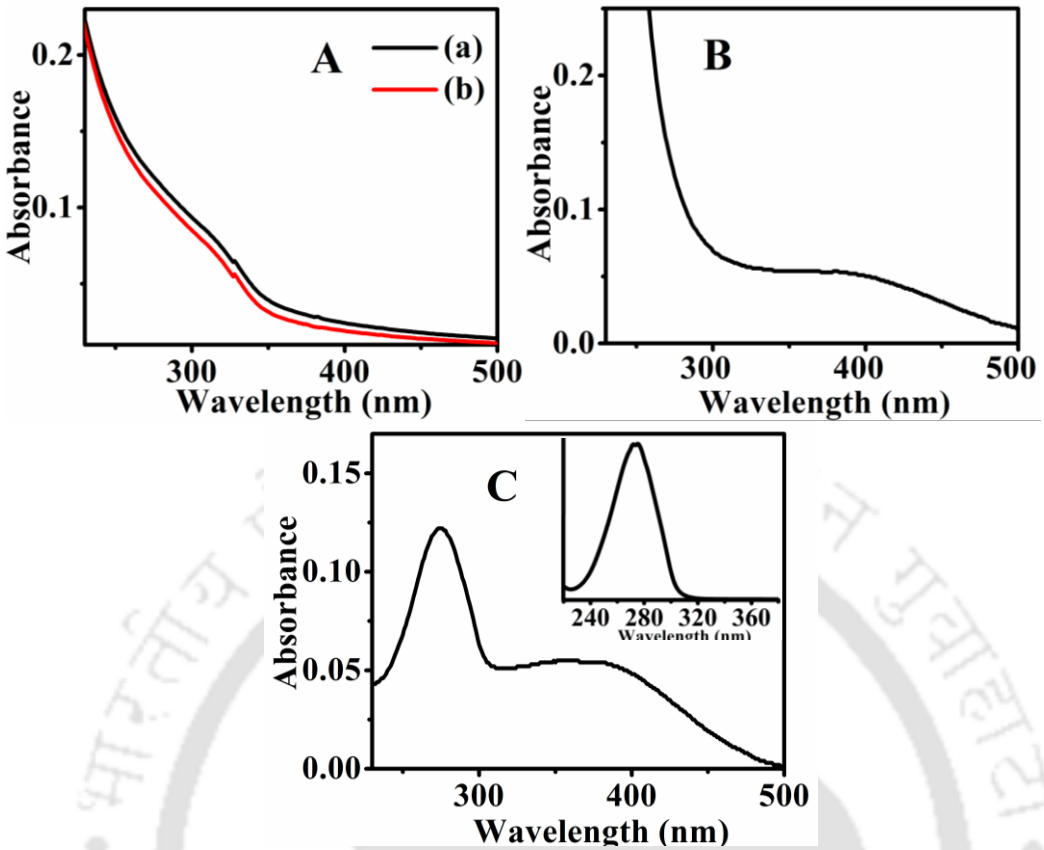


**Figure 3-2.** Optical absorption spectra of (**A**) (**a**) as-synthesized $Mn^{2+}$-doped ZnS Qdots, (**b**) 0.45 mM KPS treated Qdots; (**B**) 7.3 mM KPS treated Qdots; (**C**) Mn $(AcAc)_3$ complex (inset: absorption spectrum of acetyl acetone). The source of Mn of the Qdots was Mn-acetate.

It is important to mention here that near complete loss of fluorescence was observed upon treatment with excess KPS (7.3 mM), followed by heating upon which the solution turned green. The absorption spectrum of the solution consisted of a peak at 400 nm indicating the formation of $Mn(AcAc)_3$ complex (Figure 3-2).

Thus KPS was indeed oxidizing the Qdots which led to the change in fluorescence. It is possible that the presence of excess KPS might have led to the etching of the surface $Mn^{2+}$ ions sufficiently to form the complex in the solution following oxidation, as highly oxidizing species such as benzoyl peroxide are known to etch the surface of Qdots. Further, when Qdots previously treated with 0.45 mM of KPS followed by heating was subsequently treated with 9.7 mM of $NaBH_4$ (at room temperature) the intensity of the peak increased nominally (Figure 3-3A). On the other hand, after 4 h the intensity increased substantially

and interestingly the intensity at 593 nm increased till it reached the original value (i.e. due to as- synthesized Qdots). The QY for the emission due to $Mn^{2+}$ ions, for the as-synthesized Qdots was measured to be 5%, while that of 0.45 mM KPS treated ones was found to be 2.9% and the value of the same for the 9.7 mM $NaBH_4$ treated ones (subsequent to addition of KPS) was observed to be 6%. Thus treatment of an oxidizing agent reduced the QY of the Qdots, while subsequent treatment with a reducing agent increased it back, providing reversibility to the process.

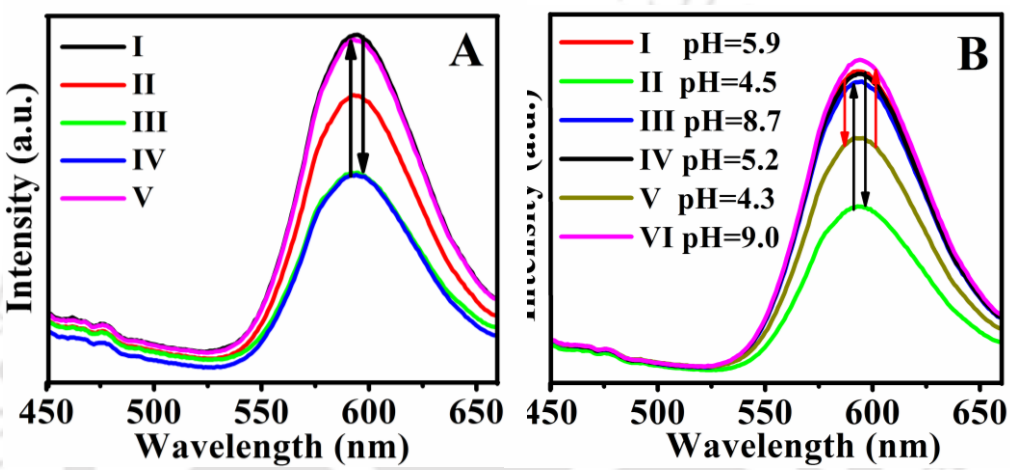


**Figure 3-3.** (**A**) Emission spectra of (**I**) as-synthesized $Mn^{2+}$-doped ZnS Qdots; and those of Qdots treated with (**II**) 0.45 mM KPS; (**III**) the sample in II upon heating; (**IV**) the sample in III upon treatment with 9.7 mM $NaBH_4$ and (**V**) the sample in IV but recorded 4 h after addition of $NaBH_4$. (**B**) Emission spectra of (**I**) as-synthesized Qdots; and those of Qdots treated with (**II**) 0.45 mM KPS; (**III**); the sample in II upon treatment with 9.7 mM $NaBH_4$; (**IV**) the sample in III upon adjustment of pH; (**V**) the sample in IV upon treatment with 0.45 mM KPS and (**VI**) the sample in V upon treatment with 9.7 mM of $NaBH_4$. The source of Mn of the Qdots was Mn-acetate.

It was observed that while treatment of KPS reduced the pH of the medium, addition of $NaBH_4$ turned the solution alkaline. It is rather important to mention here that the changes in pH of the medium had effects on the fluorescence emission which were opposite to the above. In other words, alkaline solution decreased the emission intensity and acidic one increased marginally (refer to Appendix, Figure A3-1).

The process was further pursued to test the reversibility of this phenomenon for additional cycles. To this effect, $NaBH_4$ – treated Qdots (which were previously

treated with KPS) were further treated with KPS but no significant change in fluorescence intensity was noted. It is known that the rate of oxidation of oxalate ion by KPS in alkaline solution is low (as well as in highly acidic medium).[16] Similar mechanisms may be involved here leading to no significant change in the fluorescence intensity upon addition of KPS to alkaline medium. On the other hand, when the pH of the $NaBH_4$ treated solution was adjusted to 5.2 followed by treatment with KPS, the fluorescence intensity decreased significantly as in the case of as-synthesized Qdots (Figure 3-3B). Further, treatment of $NaBH_4$ to the solution resulted in complete recovery of fluorescence thereby indicating reversibility of the process of tuning fluorescence intensity of $Mn^{2+}$-doped ZnS Qdots by treatment with oxidizing and reducing agents in sequence in more than one cycle.

Treatment of as-synthesized Qdots with $K_2Cr_2O_7$ and $KMnO_4$ (Figure 3-4) also decreased the intensity of fluorescence; however, there may be interference from the ions generated in the reaction adding complexity to the process. KPS not only has higher oxidation potential than $K_2Cr_2O_7$ and $KMnO_4$ but also its decomposition does not produce ions which would interfere with the fluorescence of the Qdots.

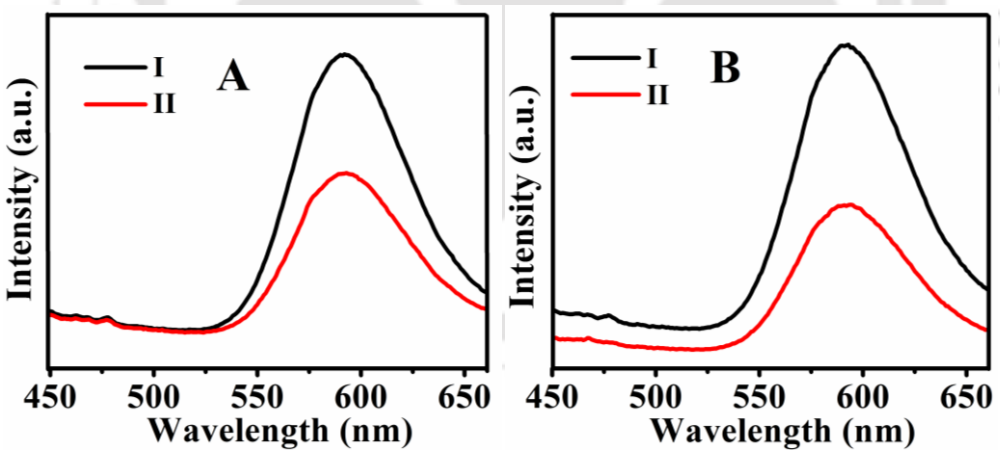


**Figure 3-4.** Fluorescence spectra of different dispersions containing the following (**A**) (**I**) is due to as-synthesized $Mn^{2+}$-doped ZnS Qdots and (**II**) those upon addition of $K_2Cr_2O_7$ solution. (**B**) (**I**) is due to as-synthesized Qdots and (**II**) those upon addition of $KMnO_4$. The spectra were recorded at 10 min after addition of the respective reagents. The source of Mn of the Qdots was Mn-acetate.

Interestingly, addition of sodium citrate to KPS-treated Qdots too led to regaining of the fluorescence back to its original value indicating possible reduction of higher

oxidation states of Mn also by weaker reducing agent (Figure 3-5). It may be mentioned here that addition of sodium citrate to as-synthesized Qdots also increased its fluorescence slightly; however, this increase was less significant in comparison to that with KPS-treated sample, thus supporting the reduction role of citrate (refer to Appendix, Figure A3-2).

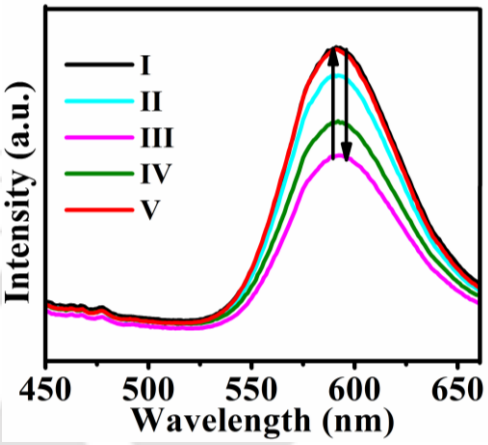


**Figure 3-5.** Fluorescence spectra of (**I**) as-synthesized $Mn^{2+}$-doped ZnS Qdots; (**II**) is that upon addition of 0.22 mM KPS; (**III**) is that of sample in b after heating; while (**IV**) is that due to the sample in c upon addition of 14.5 mM sodium citrate, the spectrum being recorded immediately after addition; (**V**) is due to sample in d recorded 2 h after addition of sodium citrate. The source of Mn of the Qdots was Mn-acetate.

It is known that KPS decomposes in water into radicals which also produces, among others, OH radicals which might be involved here in the oxidation process. The establishment of exact mechanism of oxidation is rather difficult and out of bound for the present work. However, it can be speculated that $Mn^{2+}$ ions present on the surface sites (and possibly in immediate vicinity) would preferentially get oxidized. Also, since the stabilizing molecules (AcAc) are present on the surfaces of the Qdots it is plausible that surface $Mn^{2+}$ would achieve higher oxidation states especially $Mn^{3+}$ ions which would be stabilized by AcAc.

A known method to prepare inorganic complex of $Mn(AcAc)_3$ is by reaction of $KMnO_4$ with acetyl acetone, which also results in the production of $Mn(AcAc)_2$ in the medium.[17] We were interested to prepare Mn-doped ZnS Qdots where not only $Mn^{2+}$ species would be present as the dopant but also $Mn^{3+}$ ions or higher oxidation states of Mn. This was pursued by synthesizing the Qdots with $KMnO_4$ as the source of Mn rather than $Mn(OAc)_2$. Interestingly, if $Mn^{2+}$-doped ZnS Qdots

($Mn(OAc)_2$ as the source of Mn during synthesis) were treated with $NaBH_4$ there was no significant change in fluorescence (refer to Appendix, Figure A3-2).

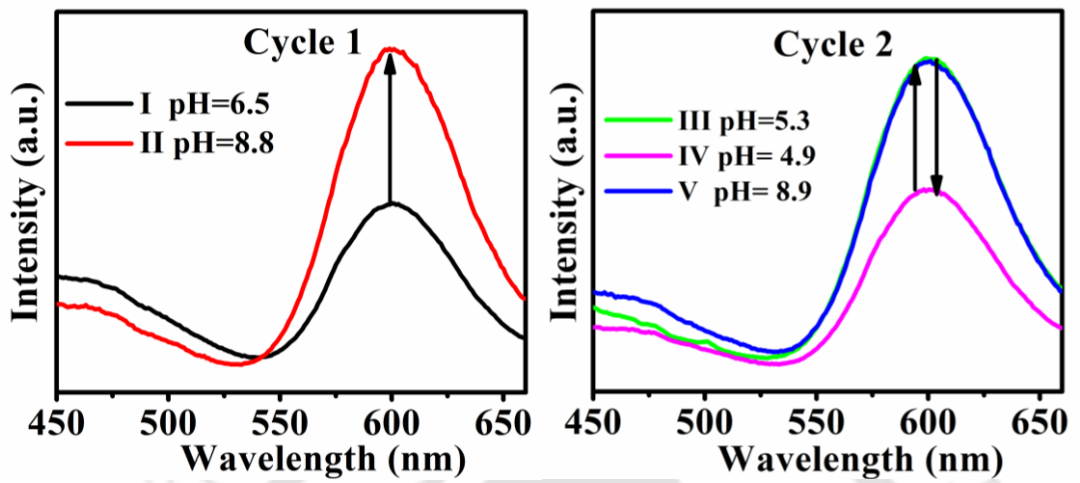


**Figure 3-6.** Emission spectra of (**I**) as-synthesized Qdots (where $KMnO_4$ was used as the source of Mn during synthesis); and those of Qdots treated with (**II**) 12.1 mM $NaBH_4$; (**III**) the sample in II upon adjustment of pH; (**IV**) the sample in III upon treatment with 0.45 mM KPS and (**V**) the sample in IV upon treatment with 12.1 mM $NaBH_4$.

On the other hand, if $Mn^{3+}$ ions (or even higher oxidation states of Mn) were present in the as-synthesized Qdots, in addition to $Mn^{2+}$ ions, then addition of $NaBH_4$ to the as-synthesized Qdots ought to increase the fluorescence via increasing the population of $Mn^{2+}$. When the Qdots were synthesized using $KMnO_4$ as the source of Mn (refer to Appendix, Figure A3-3, 4) and then treated with $NaBH_4$ significant increase in emission intensity (Figure 3-6) was observed. Further treatment of the solution with KPS - following adjustment of pH - reduced the fluorescence, which was regained upon addition of $NaBH_4$. The observations further support that indeed population of $Mn^{2+}$ ions present on the surface of the Qdots could be controlled either during synthesis or by treatment with oxidizing and reducing agents, which would be reflected in the fluorescence emission due to the presence of $Mn^{2+}$ species. That the Qdots could be synthesized with mixed oxidation states of Mn provides additional advantages of tuning fluorescence intensity in situ using redox reaction following synthesis.

ESR spectrum of the powder of as-synthesized AcAc-stabilized $Mn^{2+}$-doped ZnS Qdots (here $Mn(OAc)_2$ was the source of Mn), as shown in Figure 3-7AI, consisted

of four major peaks with two additional peaks not being resolved well. The six peaks are known to be due to $M_S$ = ½ to $M_S$ = -½ transition with splitting due to hyperfine interaction with $Mn^{2+}$ nucleus ($M_I$ = $^5/_2$).[18-21] These peaks typically represent the $Mn^{2+}$ ions occupying the tetrahedral sites inside the crystal corresponding to a hyperfine splitting constant of 64.5 X $10^{-4}$ $cm^{-1}$ (refer to Appendix, Figure A3-5). A strong and broad peak superimposed with the other peaks, being present in the spectrum, indicated $Mn^{2+}$-$Mn^{2+}$ dipolar interactions associated with the presence of cluster of ions, possibly on the surface.[22-23] It may be mentioned here that doping of $Mn^{2+}$ in the as-synthesized Qdots was estimated to have a lower bound of 0.12% (refer to experimental section) and the ESR spectrum was in commensurate with the dopant concentration as is known from the literature.[12-24] On the other hand, the ESR spectrum of KPS-treated Qdots (Figure 3-7AII) clearly showed the presence of six characteristic lines with significantly reduced contribution of the broad peak that was present in Figure 3-7AI, and with a hyperfine splitting constant (64.5 X $10^{-4}$ $cm^{-1}$) corresponding to the $Mn^{2+}$ present in the tetrahedral crystal sites. This possibly means that treatment of the Qdots with KPS led to partial oxidation of population of $Mn^{2+}$ to higher oxidation states (preferably to $Mn^{3+}$ state in the presence of AcAc) thereby reducing the concentration of $Mn^{2+}$ being present on the surface of the Qdots. The weak peaks in between the six intense lines in the spectrum are attributed to the occurrence of forbidden transitions[25-26] at low concentrations of $Mn^{2+}$ ions and they further evidenced the lowering of $Mn^{2+}$ concentration in the Qdots. The peaks occurring at the edges of the spectrum[5] possibly represent the presence of $Mn^{2+}$ occupying the octahedral sites on the surfaces of the Qdots, corresponding to a hyperfine splitting constant of 91.1 X $10^{-4}$ $cm^{-1}$. Thus when the surface $Mn^{2+}$ ions were partially oxidized not only were the dipolar interactions reduced leading to lowering in the background but also the peaks due to surface $Mn^{2+}$ became clear. Interestingly, when the KPS-treated QDots were subsequently treated with $NaBH_4$, the sample resulted in an ESR spectrum (Figure 3-7AIII) consisting again of four major peaks with additional small peaks owing to sextet as was observed in the original sample (although the spectrum appeared to be better resolved).

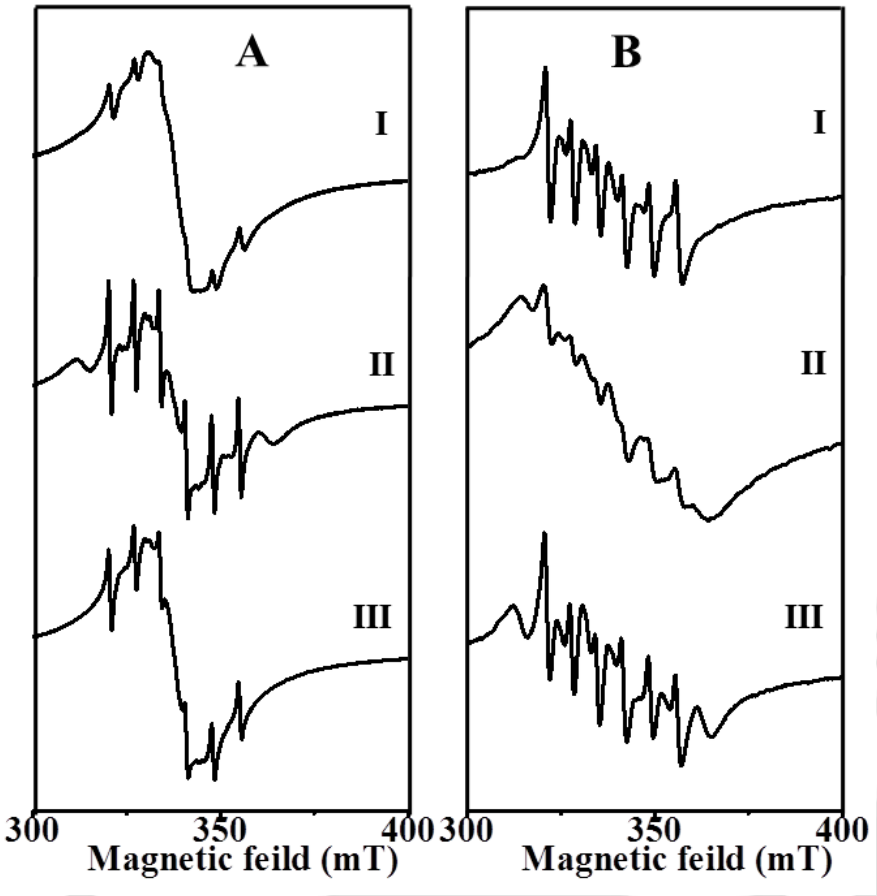


**Figure 3-7.** (**A**) ESR spectra of (**I**) as-synthesized Qdots; (**II**) KPS-treated QDots and (**III**) $NaBH_4$ treated Qdots. (**B**) ESR spectra of (**I**) as-synthesized Qdots; (**II**) $NaBH_4$ treated Qdots and (**III**) KPS-treated QDots. In (**A**), the source of Mn for the Qdots used was Mn-acetate, while in (**B**) it was $KMnO_4$.

Smaller additional peaks which were present in KPS-treated sample nearly disappeared. In addition, the broad signal reappeared indicating the recurrence of clusters of $Mn^{2+}$ ions on the surface. Thus $NaBH_4$ reduced the higher oxidation states of Mn to increase the population of $Mn^{2+}$ ions on the surface of the Qdots as was reflected in the ESR spectrum.

Interestingly, ESR spectrum of Qdots which were synthesized using $KMnO_4$ as the source of Mn (Figure 3-7BI) consisted of six sharp lines (corresponding to a hyperfine splitting constant of 64.5 X $10^{-4}$ $cm^{-1}$) with additional smaller peaks and the broad background being nearly absent, which is indicative of low population of $Mn^{2+}$ on the surface of the Qdots. However, when the as-synthesized Qdots were treated with $NaBH_4$ the broad background appeared with diminished sharpness of

the peaks (Figure 3-7BII), indicating the presence of $Mn^{3+}$ ions (or ions in higher oxidation states of Mn) on the surface of the as-synthesized Qdots, which were reduced to $Mn^{2+}$ upon treatment with $NaBH_4$. Additionally, when $NaBH_4$ treated Qdots were further reacted with KPS sharp peaks appeared again (Figure 3-7BIII) evidencing the reduction of population of $Mn^{2+}$. The presence of peaks at the edges with hyperfine splitting constant of 91.1 X $10^{-4}$ $cm^{-1}$ further supported the occurrence of $Mn^{2+}$ on the surface of the crystals. Further, here also the weak peaks due to forbidden transitions could be observed. Essentially, the ESR studies indicated that $Mn^{2+}$ were present both in the tetrahedral and octahedral sites of the crystals; however, the treatment with oxidizing species reduced the population of $Mn^{2+}$ on the surface, with accompanying lowering of $Mn^{2+}$-$Mn^{2+}$ dipolar interactions. The presence of the reducing species increased the dipolar interaction pointing towards the presence of clusters on the Qdot surface.

The X-ray diffraction patterns of the as-synthesized Qdot powder (with Mn-acetate being the source of Mn here), shown in Figure 3-8AI, consisted of three broad peaks occurring at 2θ values of $28.6^0$, $47.8^0$ and $56.6^0$ corresponding to diffractions from (111), (220) and (311) planes of ZnS. The average particle size as calculated using Scherrer's formula was found to be 3.8 nm. The XRD patterns corresponding to the KPS-treated sample (Figure 3-8AII) consisted of the same three peaks. However, the particle size here was calculated to be 4.5 nm, indicating possible agglomeration of some of the particles due to centrifugation and other processing during solidification. The XRD patterns of the $NaBH_4$ treated sample (Figure 3-8AIII) consisted of three main peaks as those of the other two samples and average particle size was calculated to be 4.6 nm, indicating the presence of some agglomerated particles. However, similar particles sizes for all three samples indicted that the particles were largely intact. XRD patterns of the Qdots with the source of Mn being $KMnO_4$ indicated formation of smaller particles (average size being 2.4 nm), the size of which did not change significantly upon treatment with $NaBH_4$ and subsequently with KPS (Figure 3-8B).

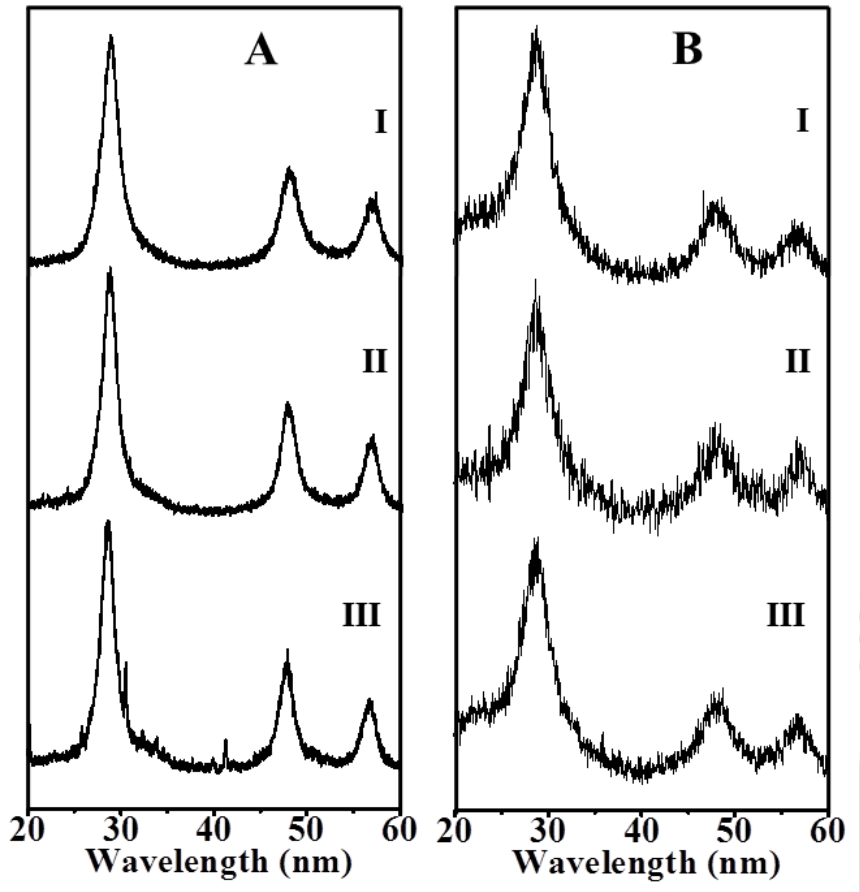


**Figure 3-8.** X-ray diffraction patterns of powders of (**A**) (**I**) as-synthesized Qdots; (**II**) KPS-treated Qdots and (**III**) $NaBH_4$ treated Qdots; (**B**) (**I**) is the pattern for as-synthesized Qdots; (**II**) is for $NaBH_4$ treated Qdots and (**III**) is KPS-treated Qdots, where KPS was added subsequent to $NaBH_4$ treatment. In (**A**), the source of Mn for the Qdots used was Mn-acetate, while in (**B**) it was $KMnO_4$.

Further, X-ray photoelectron spectroscopy (XPS) measurements indicated the formation of $Mn^{3+}$ species (accompanied by an increase in binding energy) upon treatment with the oxidizing agent (KPS), although the spectrum was noisy. On the other hand, the as-synthesized sample or $NaBH_4$ treated sample consisted of $Mn^{2+}$ species only (Figure 3-9). Thus the results indicated that the treatment of the Qdots with KPS was indeed reducing the concentration of $Mn^{2+}$ and at the same time increasing the concentration of the $Mn^{3+}$ ions.

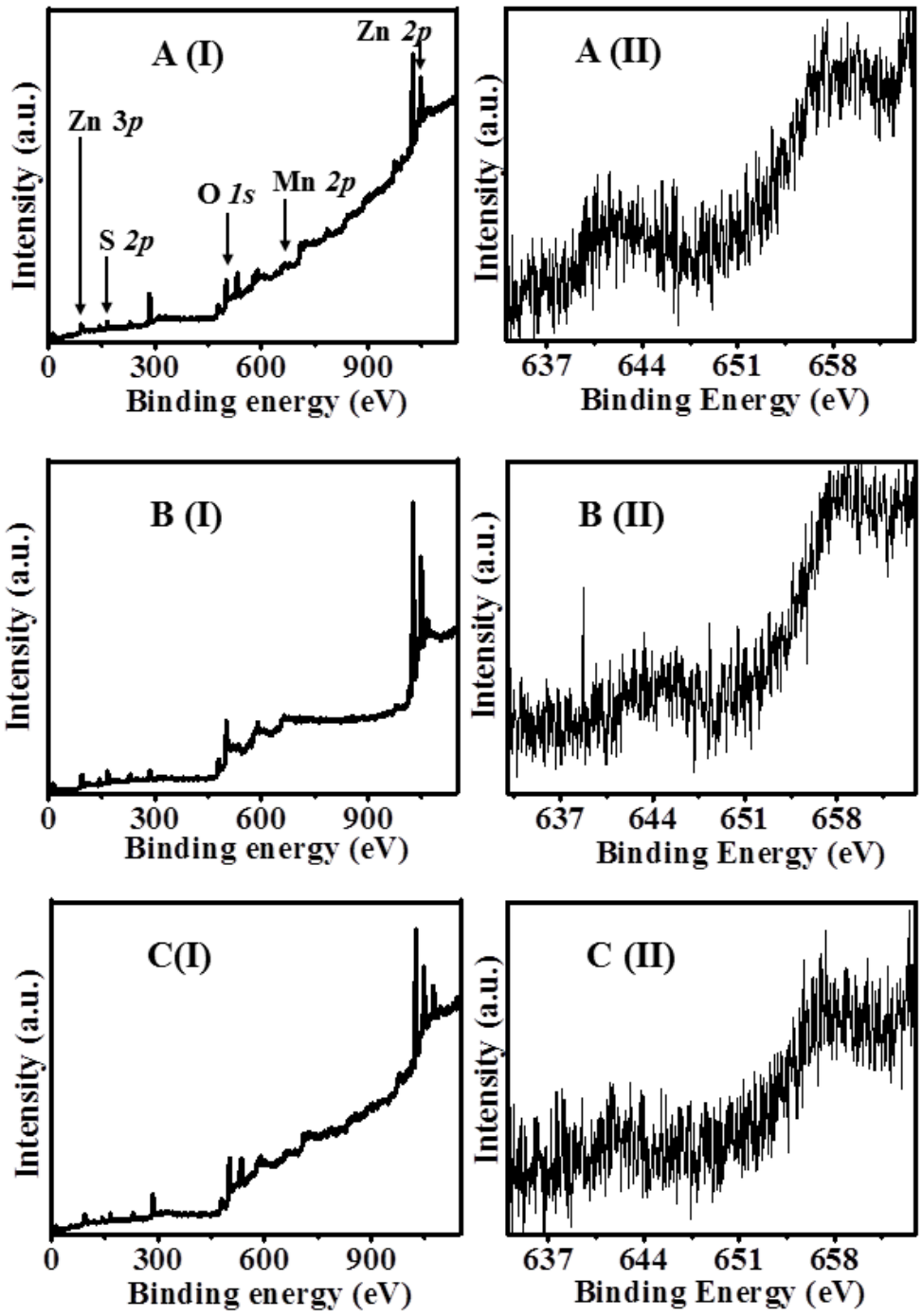


**Figure 3-9. A (I), B (I)** and **C (I)** are X-ray photoelectron spectra (XPS) of as -synthesized $Mn^{2+}$-doped ZnS Qdots; KPS treated Qdots and subsequent $NaBH_4$ treated Qdots respectively. A (**II**), B (**II**) and C (**II**) are expanded views corresponding to manganese (2P) peaks. The source of Mn of the Qdots was Mn-acetate.

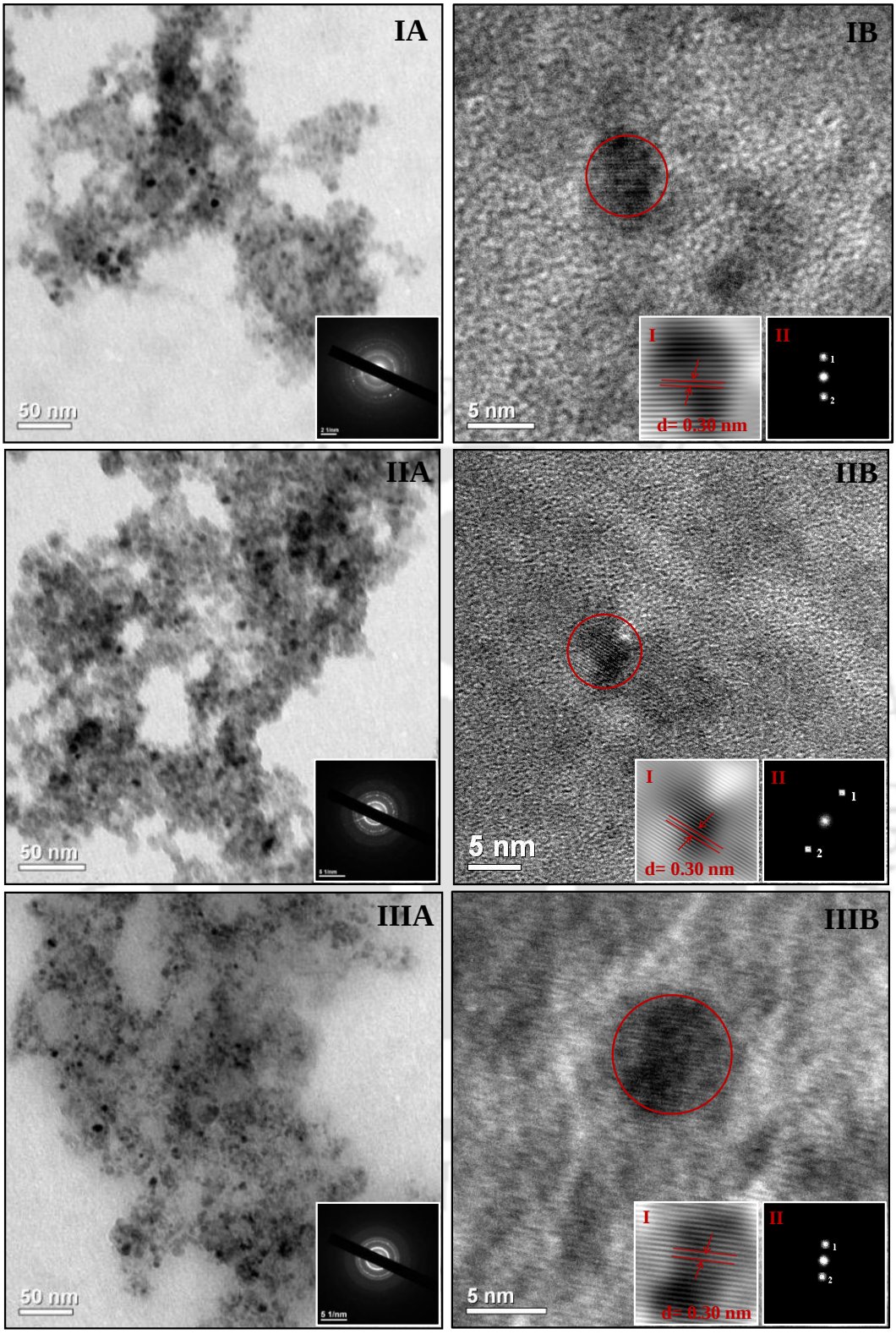


**Figure 3-10.** Transmission electron microscopic (TEM) images with selected area electron diffraction (SAED) in the inset are shown in (**A**), while high resolution TEM images with (**I**) Inverse Fast Fourier Transform (IFFT) image of the selected region and (**II**) the corresponding FFT image in the inset of (B) of (**I**) as-synthesized $Mn^{2+}$-doped ZnS Qdots; (**II**) KPS treated QDots and (**III**) reduced Qdots respectively. The source of Mn of the Qdots was Mn-acetate.

TEM measurements (Figure 3-10) of the as-synthesized Qdots, KPS-treated and $NaBH_4$ treated Qdots (TEM samples being prepared from the solutions) indicated that particle sizes remained largely intact following oxidation and reduction in solution, further suggesting that the processes did not etch off the Qdots substantially. It may further be mentioned here that the samples for XRD and ESR studies were prepared after solidification through centrifugation from a larger collection of independently synthesized Qdot samples. This was required as the amount of Qdots generated from each synthesis was small.

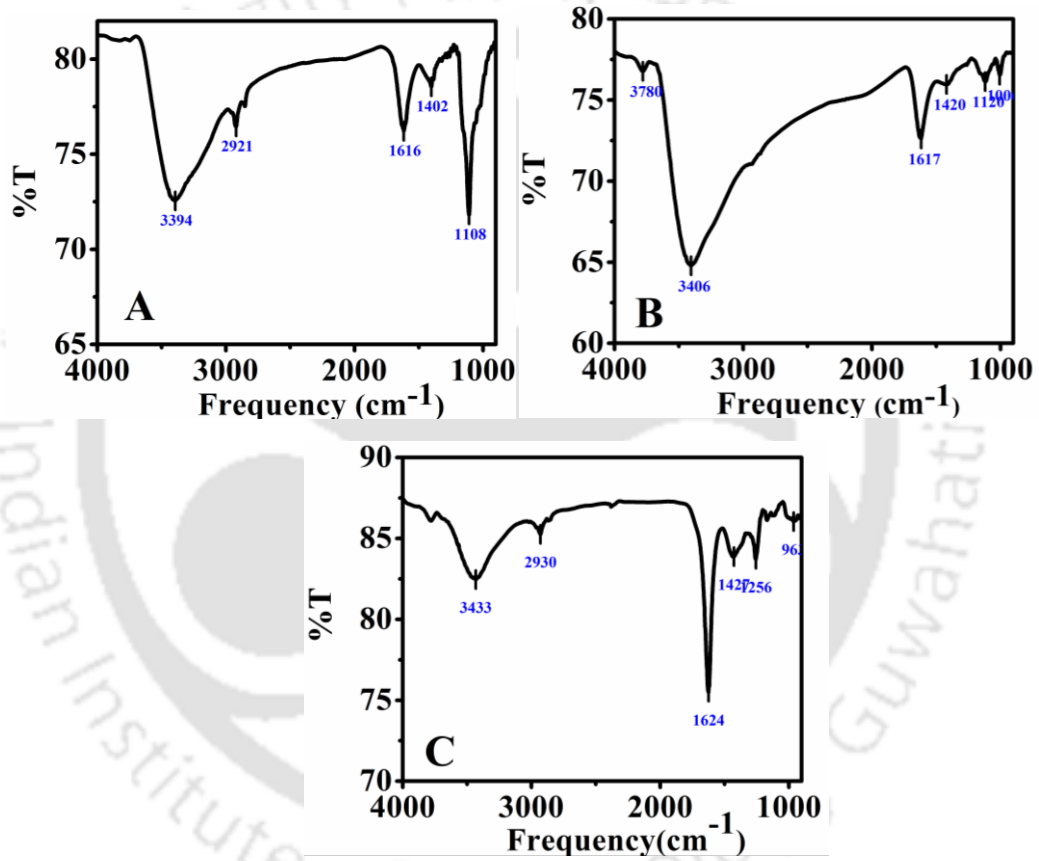


**Figure 3-11.** FTIR spectra of (**A**) as-synthesized Qdots, (**B**) KPS treated Qdots and of (**C**) acetyl acetone. The source of Mn of the Qdots was Mn-acetate.

On the other hand, the TEM (as-synthesized, oxidized and then reduced) samples were from the same stock obtained from a single synthesis. The TEM results exhibited that in the medium there was no agglomeration of the Qdots in solution even after going through the cycle of oxidation and reduction. However, some of the samples for XRD obtained from a larger collection might have agglomerated

during solidification. FTIR spectroscopic measurements of the as-synthesized Qdots and KPS-treated ones showed the presence of AcAc, as the spectra were similar to each other and also with that of acetyl acetone (Figure 3-11).

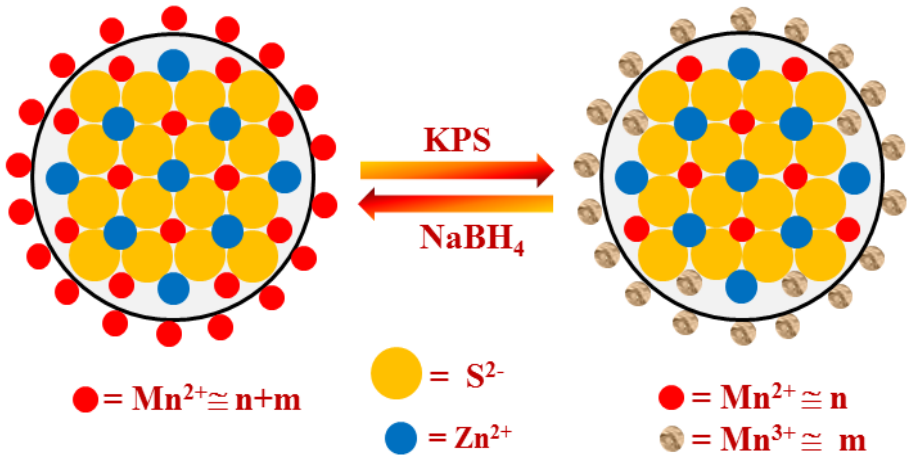


**Scheme 3-1.** Schematic representation of $Mn^{2+}$-doped ZnS Qdots and the reversible mechanism involved whereby the redox reagents reacted with the $Mn^{2+}$ dopant ions present on the surface and the immediate vicinity of the Qdots. As shown, out of '(n+m)' number of total $Mn^{2+}$ ions, 'm' number of $Mn^{2+}$ ions reacted.

### 3.4. Conclusion

In brief, the chapter demonstrated that the emission characteristics of doped Qdots could be modified by controlling the concentration of the dopant through partial oxidation of the population following Qdot preparation (as demonstrated in scheme 3-1). In addition, when the as-synthesized Qdots consisted of emitting species in mixed oxidation states with the lowest state being the emitting state, the reduction of higher oxidation states also increased the fluorescence intensity.

This is fundamentally different from the traditional approach of synthesizing Qdots with specific concentration of the dopant, where the exact and systematic control might not be as precise. The advantage lies not only in the simplicity of the process but also the possibility of tuning the properties in situ and the reversibility of the process. In the present system, fluorescent active $Mn^{2+}$ (when doped in Qdots such as ZnS) and silent $Mn^{3+}$ or higher oxidation states were chosen for ease of probe of convertibility using easy to access reaction conditions at ordinary temperatures.

This idea has been extended to other doped Qdots with the ability to tune optical and magnetic properties by resorting to redox chemistry in rest of the chapters. The idea will not only help gauge emission of the Qdots but also the intensity of emission and provide vital clues about local oxidation/reduction process, so ubiquitous in biological entities and systems such as mammalian cells and microbes. That the mixed oxidation states of the emitting species (dopant) – while prepared in solution - could also be obtained in solid state as stable species, will further provide an eminent opportunity for achieving versatility in their applications.

## References


1) Jun Y. W.; Jung Y.; Cheon J. *J. Am. Chem. Soc*. **2002**, 124, 615-619.
2) Aldeek F.; Balan, L.; Lambert, J.; Schneider, R. *Nanotechnol*. **2008**, 19, 475401-475409.
3) Pradhan N.; Peng, X. *J. Am. Chem. Soc.* **2007**, 129, 3339-3347.
4) Yuan, C.T.; Chou, W. C.; Chuu D. S.; Chang, W. H.; Lin H. S.; Ruaan, R. C. *J. Med. Bio. Eng*. **2006**, 26, 131-135.
5) Srivastava, B.B.; Jana, S.; Karan, N. S.; Paria, S.; Jana, N. R.; Sarma, D.D.; Pradhan, N. *J. Phys. Chem. Lett.* **2010**, 1, 1454–1458.
6) Bol, A. A.; Meijerink, A. *J. Phys. Chem. B* **2001**, 105, 10197-10202.
7) Becker, W.G.; Bard, A. J. J. of Phys. Chem. **1983**, 87, 4888-4893.
8) Brus, L.E. *J. Chem. Phys*. **1983**, 79, 5566-5571.
9) Wang, C.; Chim, M.; Sionnest, P. G. *Science*, **2001**, 291, 2390-2392.
10) Chim, M.; Sionnest, P. G. *Nature* **2000**, 407,981-983.
11) Gooding, A. K.; Gómez, D. E.; Mulvaney, P.; *ACS Nano* **2008**, 2, 669-676.
12) Wehrenberg B. L.; Sionnest P. G. *J. Am. Chem. Soc*. **2003**, 125, 7806-7807
13) CRC Handbook of Chemistry and Physics, 91st ed.; Hayness, W. M., Ed.; CRC Press: Boca Raton, NY, **2010**; p 8-20.
14) Cartledge, G. H. (Cornell Aeronautical Laboratory, Inc., USA). Method of preparing a manganese Chelated compound. US 2, 556, 316, June 12, **1951**.
15) Bhargava, R. N.; Gallagher, D.; Hong, X.; Nurmikko, A. *Phys. Rev. Lett.* **1994**, 72, 416-419.
16) Po, H. N.; Allen, T. L. *J. Am. Chem. Soc.* **1968**, 1127-1131.
17) Chaudhuri, M. K.; Dehury, S. K.; Dhar, S. S. ; Bora, U.; Chaudary, M.; Mannepalli, L. K. (CSIR, India). Process of making metal acetylacetonates. US 7, 282, 573 B2 October 16, **2007**.
18) Borse, P. H.; Srinivas, D.; Shinde, R. F.; Date, S. K.; Vogel, W.; Kulkarni, S. K. *Phys. rev.* **1999**, 60, 8659-8664.
19) Stoji´c, B. B.; Comor, D M.; Vodnik, V. *Phys. Condens. Mat*. **2004**, 16, 4625-4633.
20) Murase, N.; Jagannathan, R.; Kanematsu, Y.; Watanabe, M.; Kurita, A.; Hirata, K.; Yazawa, T.; Kushida, T. *J. Phys. Chem. B* **1999**, 103, 754-760.

21) Norman, T. J.; Magana, J.D.; Wilson, T.; Burns, C.; Zhang, J. Z.; Cao, D.; Bridges, F. *J. Phys. Chem. B* **2003**, 107, 6309-6317.

22) Kennedy, T. A.; Glaser, E. R.; Klein, P. B.; Bhargava, R. N. *Phys. rev*. *B* **1995**, 52, 356-359

23) Biswas, S.; Kar, S.; Chaudhuri, S. *J. Phys. Chem. B* **2005**, 109, 17526-17530.

24) Nag, A.; Sapra, S.; Nagamani, C.; Sharma, A.; Pradhan, N; Bhat, S. V.; Sarma, D.D. *Chem. Mat.* **2007**, 19, 3252-3259.

25) Beermann, P.A. G.; Mc Garvey, B. R.; Muralidharan, S.; Sung, R. C. W. *Chem. Mat*. **2004**, 16, 915–918;

26) Beermann, P. A. G.; Mc Garvey, B. R.; Skadtchenko, B. O.; Muralidharan, S.; Sung, R. C. W. *J. of Nanopart. Res*. **2006**, 8, 235-241.

# Chapter 4

## Recovering Hidden Emission from $Cu^{2+}$ -doped ZnS Quantum Dots in Reductive Environment

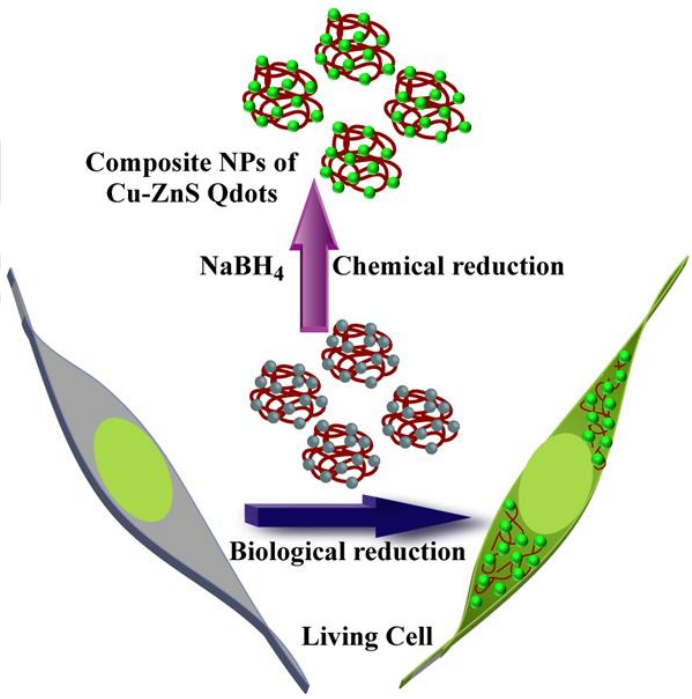

# Chapter 4

**Abstract:** The chapter deals with experiments involving plausible recovery of the photoluminescence of doped quantum dots (Qdots) in presence of a chemical or cellular reducing environment, otherwise lost in the oxidized form of the dopant. For example, as-synthesized $Cu^{2+}$-doped ZnS Qdots in water medium showed weak emission with a peak at 420 nm following excitation with UV light (320 nm). However, addition of a reducing agent led to the appearance of green emission with peak at 540 nm and with quantum yield as high as 10%, in addition to the weak peak now appearing as a shoulder. The emission disappeared in the presence of an oxidizing agent or with time under ambient conditions. Nanoparticulate forms of the Qdots and chitosan (a biopolymer) composite exhibited similar emission characteristics. Interestingly, when mammalian cancer cells or non-cancerous cells were treated with the composite nanoparticles (NPs), characteristic green fluorescence was observed. Further, the intensity of the fluorescence diminished when the cells were treated later with pyrogallol. Overall, the results indicated a new way of probing reducing nature of mammalian cells using the emission properties of the Qdot based on the redox state of its dopant.

## 4.1. Introduction

The pre-eminence of Qdots over conventional organic dyes in biological cell labelling, in their use as markers for cellular events and in therapy, based on their electron and energy transfer properties, has clearly been established.[1-6] That the interactions between the functional groups, present on the surface of a Qdot and an analyte or Qdot itself, causes observable change in the emission characteristics of the Qdot forms the basis of sensing in vitro as well as in vivo,[7-12] including intracellular sensing of pH and changes in redox potential.[13-14] On the other hand, imaging primarily has been demonstrated to involve specific interactions between the stabilizing and the target molecules, with or without necessary consequent changes in the emission characteristics of the Qdot.[15-16] These have been used as the principles behind probing intracellular events, serving as markers for health or otherwise.[17-18] Although, these non-invasive probes have been used for cellular

events and presence or absence of target species, the inherent nature of emission from the Qdots does not preclude spurious signal as it is not necessarily dependent on binding between the Qdot and the target molecules. In other words, mere presence of the fluorescent Qdots inside the cells may also give rise to their detection and thus signal, even in absence of interactions with the target.

On the other hand, the scope of functionalized-molecule-independent use of Qdots as probes can have certain advantages, which may otherwise not be available using specific functional groups. For example, the repertoire of drug delivery vehicles, available for use in passive as well as targeted delivery, may not be easily compatible with the surface stabilizers of Qdots, owing to specificity of interactions. In such a situation, further tweaking of the stabilizing molecules is required, which may involve extensive chemistry or which may not be easy to attend keeping all other functions intact. Thus there is an opportunity for new applications, where properties of Qdots would depend on the nature or event of its immediate environment, which would act as a marker of the specificity of event or the environment. For example, one could foresee the changes in redox balance of a cell or presence of excess of an oxidizing or reducing species inside the cell, leading to either turning on or off the emission of Qdots. This may not be dependent on the nature of stabilizing molecules present on the surface of the Qdots. Conversely, this would depend on the sensitivity of the emission to the oxidation state of the dopants present in the Qdots.

The present study demonstrated that as-synthesized and weakly-emissive $Cu^{2+}$-doped ZnS Qdots gave rise to a new green emission (450-650 nm) in the presence of UV light, following treatment with a reducing agent. On the other hand, the emission disappeared when the Qdots were further treated with an oxidizing agent. The emission characteristics were retained in the nanoparticulate form of a composite of the Qdots and chitosan. The composite NPs were used as probe for the reducing nature of mammalian cancer as well as non-cancerous cells. The choice of the Qdots has been based on several advantages. First of all, the $Cu^{2+}$-doped ZnS Qdot and its constituent elements are not known to be cytotoxic, unlike $Cd^{2+}$- based Qdots.[19-20] Secondly, they can be synthesized in aqueous medium at relatively lower temperatures. More importantly, the emission characteristics of the doped Qdots depend on the oxidation state of Cu.

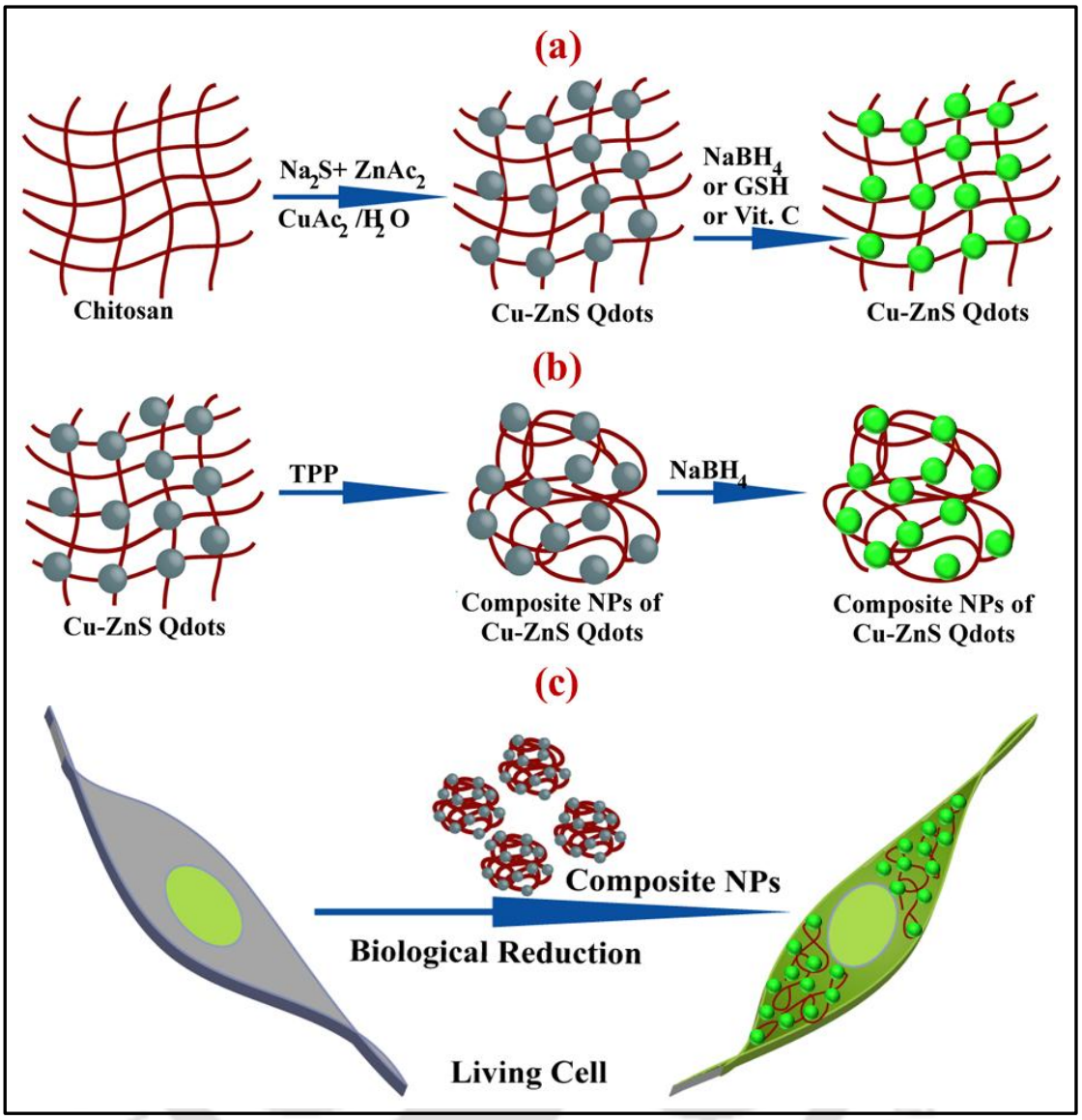


**Scheme 4-1.** A new method of preparing copper-doped ZnS Qdots, the emission of which is sensitive to the redox environment, is reported. (**a**) The doped Qdots could be prepared in aqueous medium in the presence of chitosan. The Cu-doped Qdots in chitosan were weakly emissive as such. However, in the presence of a chemical reducing agent ($NaBH_4$, glutathione or vitamin C) the characteristic (green) fluorescence of the doped Qdots could be observed. (**b**) Nanoparticle of the composite of the polymer and Qdots could be prepared using tripolyphosphate (TPP). The as-prepared composite nanoparticles were weakly fluorescent. However, in the presence of a reducing agent the fluorescence (green) could be observed. (**c**) When mammalian cells were treated with the composite nanoparticles, cells were observed to be fluorescent (green).

It was observed that in the aqueous based method of synthesis newly developed by us - the Qdots were generally weakly emissive, when $Cu^{2+}$ ions were incorporated as such. On the other hand, in the presence of chemical reducing

agents like sodium borohydride, glutathione and ascorbic acid green emission could be observed. In addition, when the as-synthesized weakly-emissive composite nanoparticles (NPs) were treated with mammalian cells, green fluorescence, illuminating the cells, was observed. Interestingly, when the cells were treated with a reactive oxygen species generator (pyrogallol), the intensity of the emission was diminished. Further, ZnS Qdots emitted in the blue region as-synthesized (as reported in the literature [21-23]) or while in the cell. Overall, the results indicated that, as the emission was observed in the presence of a reducing environment, the emitting species might have been $Cu^{+}$ rather than $Cu^{2+}$. Scheme 4-1 represents the general method of synthesis of chitosan-stabilized weakly fluorescent Qdots and their reductions to strongly fluorescent Qdots in the presence of chemical reducing agents or mammalian cells.

## 4.2. Experimental Section

### 4.2.1. Reagents

Zinc acetate dihydrate (98%), copper acetate monohydrate (99%), sodium sulfide (55-58%), potassium peroxodisulfate (99%), sodium borohydride (95%), chitosan (Sigma- Aldrich; medium molecular weight), trisodium citrate dihydrate (99%) and ammonium thiocyanate (98%), ascorbic acid (99%), L-glutathione (GSH, Sigma- Aldrich; 98%) were used as purchased. For performing biological experiments, 2, 3-bis-(2-methoxy-4-nitro-5-sulfophenyl)-2H-tetrazolium-5 carboxanilide (XTT; Sigma-Aldrich), and 2, 7-dichlorofluoresceindiacetate (DCFH-DA; Sigma-Aldrich, USA) were used. Source of all chemicals - not mentioned above – was from Merck Limited, Mumbai, India.

### 4.2.2. Synthesis of Qdots

For the *de novo* synthesis of copper doped ZnS Qdots, a simple aqueous colloidal precipitation method was employed in our laboratory, using zinc acetate dihydrate, copper acetate monohydrate, sodium sulphide as the starting materials and Milli-Q/Elix grade water as the solvent. First, 50 mL of water was heated to boiling, followed by addition of the capping agent. Three different capping agents were used for synthesis of three different types of Qdots; chitosan (medium molecular weight; 0.05 mg/mL), trisodium citrate dihydrate (5 mM) and

ammonium thiocyanate (5 mM). To the solution 5.0 mM each of zinc acetate and sodium sulphide was added, followed by addition of copper acetate (0.25 mM) and the reaction mixture was allowed to stir for 3 h under refluxing condition. Finally, the colloidal solution so obtained was centrifuged twice at a speed of 22,000 rpm for 20 min each; the pellet was washed with water, redispersed in 200 mL water and sonicated for 20 min.

### 4.2.3. Treatment to Qdot dispersion with redox reagents

Solid $NaBH_4$ was weighed and added to 3 mL of Qdot sample taken in a vial. Fluorescence spectra were recorded for the sample from time to time. When maximum shift and intensity were achieved, 25 uL of 50 mM KPS (KPS is 47.5% pure; final concentration in the medium being 0.2 mM) was added. It may be mentioned here that whenever pH adjustment was required (prior to addition of KPS), dil. HCl was added to the medium to bring down the pH to desired value.

### 4.2.4. Synthesis of Qdot-Chitosan Composite Nanoparticles

Ionic gelation method was employed to synthesize Qdot-chitosan composite NPs. 100 uL from a stock solution of tripolyphosphate - TPP (4 mg/mL) - was added to 3 mL dispersion of Qdots, which was further diluted to 10 mL by addition of 7 mL water. The dispersion was then kept under stirring condition at room temperature for 15 min, which was followed by centrifugation at 22000 rpm for 15 min. The pellet so obtained was redispersed in either water or phosphate buffered saline (PBS; 0.01 M, pH 7.4) depending on the experiments to be performed and was further sonicated for 5 min. Average hydrodynamic diameter was measured by dynamic light scattering (DLS) based particle size analysis of the dispersion and also from TEM images recorded for drop-cast sample.

### 4.2.5. Treatment of Qdot-Chitosan Composite Nanoparticles with GSH and $NaBH_4$

The composite NPs obtained as above were dispersed in water using sonication. They were then treated separately with GSH and $NaBH_4$ and each was incubated for 1 h. Emission spectra were then recorded. Further, 100 uL of each of the dispersions was drop-cast over a clean microscope glass slide and air-dried.

Fluorescent microscopic images were recorded thereafter using a fluorescence microscope (Nikon ECLIPSE, TS100, Tokyo). UV-excitation filters with band pass 340-380 nm and corresponding emission band pass filters of blue (435-485 nm) and green (515-555 nm) were used for imaging.

### 4.2.6. Quantum Yield (QY) Calculation:

QY has been calculated with respect to quinine sulphate ($Q_S$) in 0.1 M $H_2SO_4$, using the formula:

$Q_S = Q_R \times (I_S/I_R) \times (A_R/A_S) \times (\eta^2_S/\eta^2_R)$

Where,

$Q_S$ = QY of sample; $Q_R$ = QY of reference; $I_S$ = area under emission spectrum of sample; $I_R$ = area under emission spectrum of reference; $A_R$ = absorbance of the reference; $A_S$ = absorbance of the sample; $\eta_S$ = refractive index of sample; $\eta_R$ = refractive index of reference.

Quinine sulphate in 0.1 M $H_2SO_4$ absorbs in the UV region with $\lambda_{max}$ at 347 nm; however, emission spectra were recorded using an excitation wavelength of 320 nm (near the $\lambda_{max}$ corresponding to the Qdots). Absorbance values at 320 nm were therefore considered for $Q_S$ as well as for the Qdots for the determination of QY. $Q_S$ (literature QY=0.54) was dissolved in 0.1M $H_2SO_4$ (refractive index ($\eta_s$) of 1.33) and the Qdots were dispersed in distilled water ($\eta_R$=1.33).

### 4.2.7. Characterization

Absorption spectra were recorded on a Hitachi U-2900 spectrophotometer and emission spectra in Horiba Jobin Yvon Fluorolog-3 spectrofluorometer. The XRD patterns for the powder samples were recorded by a Bruker D2 Phaser X-ray diffractometer having Cu Kα irradiation (λ= 1.5418 Å) and fluorescent microscopic images were recorded in a Nikon eclipse Ti machine.

On the other hand, ESR and TEM measurements, and elemental analysis were carried out using the same instruments as mentioned in the previous chapters.

### 4.2.8. Cell Culture

HeLa (human cervical carcinoma) and HEK 293 cells were propagated in Dulbecco's modified Eagle's Medium (DMEM), supplemented with L-glutamine (4

mM), penicillin (50 units $mL^{-1}$) and streptomycin (50 µg/mL), by maintaining at $37^0$C and 5% $CO_2$. Above cells were obtained from National Center for Cell Sciences (NCCS); Pune, India.

### 4.2.9. Microscopic Imaging

For imaging, 1× $10^4$ HeLa and HEK 293 cells were seeded into 6-well plates and incubated for 24 h before treating them with composite NPs, containing doped Qdots (0.234 mg/mL) and pyrogallol (12.6 µg/mL) for 3 h at the same physiological condition and medium. Then, media was removed, cells were washed with 10 mM PBS and imaging was performed using a fluorescent microscope (Nikon ECLIPSE, TS100, Tokyo).

### 4.2.10. Cell Viability Assay

To measure the cell viability, XTT assay was performed. For this, 1×$10^4$ HeLa cells/well were seeded in 96-well microtiter plate and incubated overnight. Then, cells were treated with different concentrations of composite NPs, containing doped Qdots, ranging from 0.066 mg/mL to 0.5 mg/mL and incubated for 24 h, following which XTT assay was performed. Respiring mitochondria in viable cells convert tetrazolium compound, XTT [2, 3-bis-(2-methoxy-4-nitro-5-sulfophenyl)-2H-tetrazolium-5 carboxanilide] to water soluble orange colour formazan product in the presence of phenazinemethosulfate (PMS). Thus, absorbance at 450 nm, due to the formation of formazan product is directly proportionate to the number of live cells, after subtracting the media absorbance at 690 nm. The percentage (%) of cell viability was determined by using this relationship, stated below.

$$\%\,Viable\ Cells = \frac{(A_{450} - A_{690})_{sample}}{(A_{450} - A_{690})_{control}} \times 100$$

### 4.2.11. ROS Measurements by FACS

Reactive oxygen species (ROS) generation was measured by using 2, 7-dichlorofluoresceindiacetate (DCFH-DA) staining. This was pursued using the popular flow cytometry, based on the principle of fluorescence activated cell sorter (FACS).[24] Briefly, the nonpolar DCFH-DA can enter into the cells, where the cellular esterases hydrolyse its ester bond to generate a non-fluorescent polar

compound DCFH, which upon oxidation by intracellular ROS gets easily converted in to a highly fluorescent DCF (dichlorofluorescein, emission at 530 nm). Thus, the quantitative measurement of fluorescent intensity of DCF using flow-cytometry directly correlates the amount of ROS generation inside cells.

Experimentally, $5\times 10^4$ HeLa cells were seeded into 6 -well plate and incubated for 24 h by using same condition and medium mentioned as above. Cells were treated with 0.234 mg/mL of composite NPs containing doped Qdots, 100 μM of pyrogallol (final concentration was 12.6 μg/mL) and both (composite NPs and pyrogallol at those individual concentrations) and incubated for another 2 h. After that, the medium was removed from the cells, washed with PBS and suspended in 1 mL of DMEM with 7 μM DCFH-DA and was kept for 12 min at $37^0$C, for the formation of DCF in the presence of ROS. Finally, cells were collected by trypsinization followed by centrifugation at 650 RCF for 6 min and analysed in a flow cytometer (FacsCalibur, BD Biosciences, NJ) at an excitation wavelength of 488 nm and emission wavelength of 530 nm, which corresponds to FL1-H, by probing the fluorescence of DCF. The fluorescence data were recorded with the CellQuest program (BD Biosciences) for 15, 000 cells in each sample.

To probe the production of intracellular ROS, flow cytometer analysis was performed subsequently, by treatment with pyrogallol, Qdots and both, by using DCFH-DA staining method.

### 4.3. Results and Discussion

Majority of the experiments presented herein have been carried out using chitosan-stabilized $Cu^{2+}$-doped ZnS Qdots or ZnS Qdots. Use of chitosan provided the additional advantage of facile fabrication of nanocarrier for cellular delivery of the Qdots, as explained in the subsequent sections.[25] Additionally, experiments were carried out with Qdots where ammonium thiocyanate or trisodium citrate (TSC) was used as the stabilizer. The newly developed syntheses and reactions and other experiments were performed in aqueous medium.

The absorption spectrum of as-synthesized chitosan-stabilized $Cu^{2+}$ doped ZnS Qdots was essentially similar to that of ZnS Qdots (refer to Appendix, Figure A4-1), with both exhibiting an excitonic peak at 320 nm, being equivalent to known bandgap energy of 3.87 eV. The emission spectrum of chitosan-stabilized ZnS Qdots consisted of a single peak at 440 nm, when excited by 320 nm UV light.

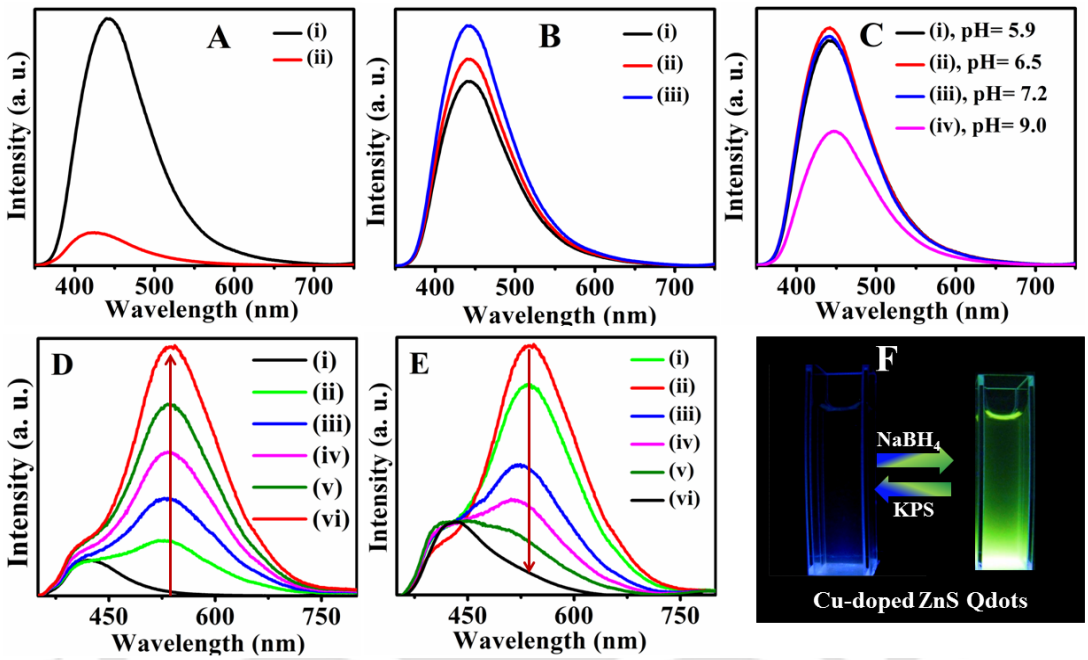


**Figure 4-1.** Emission spectra of chitosan-stabilized ZnS Qdots (**A**) (**i**) as-synthesized ZnS Qdots and (**ii**) the same Qdots treated with 50 uL of 0.5 mM copper acetate solution. (**B**) (**i**) as-synthesized ZnS Qdots (**ii**) those treated with 12 mM $NaBH_4$ and incubated for 10 min and (**iii**) the same after 20 min. (**C**) (**i**) as-synthesized ZnS Qdots at pH 5.9; those of (**ii**) sample treated with 10 uL, (**iii**) 25 uL and (**iv**) 50 uL of dilute NaOH solutions and incubated for 1 h, respectively. Emission spectra of chitosan-stabilized $Cu^{2+}$-ZnS Qdots (**D**) Time-evolution of emission spectra of the Qdots treated with 12 mM of $NaBH_4$. The time sequence is as follows- (**i**) as-synthesized Qdots, and incubation for (**ii**) 10 min (**iii**) 20 min (**iv**) 30 min (**v**) 40 min (**vi**) 60 min. (**E**) (**i**) the same Qdots solution treated with $NaBH_4$, (**ii**) following pH adjustment by adding dilute HCl acid, and then treated with KPS recorded (**iii**) immediately and after (**iv**) 5 min, (**v**) 10 min and (**vi**) 15 min. (**F**) Digital images of as synthesized $Cu^{2+}$-doped ZnS Qdots (left) and those of treated with $NaBH_4$ (right); the images were recorded using UV light as the excitation source.

The QY was measured to be 2.5%. Interestingly, when 50 uL of 0.5 mM copper acetate solution was added to a 2.5 mL dispersion (with an absorbance value of 0.09) of ZnS Qdots, the emission at 440 nm was quenched, (Figure 4-1A). On the other hand, the emission spectrum of $Cu^{2+}$- doped ZnS consisted of a weak peak at

420 nm (Figure 4-1D). However, when 3 mL dispersion of as-synthesized $Cu^{2+}$-doped ZnS Qdots (with an absorbance value of 0.05) was treated with solid $NaBH_4$ (with a final solution concentration of 12 mM), the weak peak was accompanied by the a new and stronger peak at 540 nm (Figure 4-1D).

It was further observed that the intensity of the peak increased gradually following addition of $NaBH_4$, with a maximum value corresponding to QY of 10% being reached in 1 h. Further, when the sample was kept as such in open air, the intensity of the peak started to diminish in another 30 min. Thus, by 1½ h, since the addition of $NaBH_4$, the intensity of the peak at 540 nm vanished completely and emission spectrum in the end appeared to be the same as the as-synthesized one. On the other hand, upon addition of potassium peroxodisulfate (KPS, with a final solution concentration of 0.2 mM) to the $NaBH_4$ - treated Qdots (added at the time when the maximum intensity at 540 nm was achieved), the intensity went down immediately and within 15 min of KPS addition, the emission spectrum was the same as that of the as-synthesized Qdots (shown in Figure 4-1E). Photographs of dispersion of as-synthesized Qdots and that treated with $NaBH_4$ are shown in Figure 4-1F. Control experiment involving addition of $NaBH_4$ to ZnS Qdots led to moderate increase in intensity (Figure 4-1B), possibly due to either surface passivation of the Qdots or increase in pH of the medium. This was followed by addition of KPS. The pH of the as-synthesized Qdot medium was measured to be 5.9, which increased to 8.5 after addition 12 mM of $NaBH_4$. We observed that there was no change in emission intensity of Qdots when pH increased from 5.9 to 7.2. However, beyond this pH, emission intensity decreased discernibly (Figure 4-1C). Thus, the appearance of a new peak at 540 nm had to be due to the presence of the dopant element, as addition of $NaBH_4$ to ZnS Qdots did not lead to any such peak. Changes in emission intensity with change in pH for Cu doped ZnS Qdots are also shown in Appendix, Figure A4-2. It may be mentioned here that the redox tuning of photoluminescence of the Qdots could be achieved for more than one cycle. The results are shown in Figure 4-2. Overall, the spectra revealed reversibility of redox induced fluorescence emission changes for two consecutive cycles.

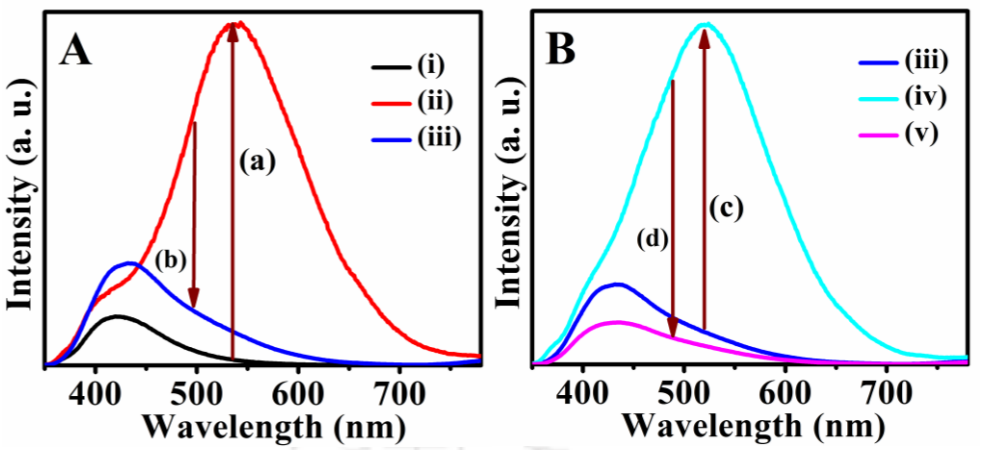


**Figure 4-2.** Emission spectra of (**A**) (**i**) as-synthesized Qdots, (**ii**) the Qdots following treatment with $NaBH_4$ and pH adjustment, and (**iii**) that following KPS addition (**B**) The emission spectra of (**iii**) the same Qdot dispersion as in (**A-iii**), (**iv**) Qdots following treatment with $NaBH_4$ and pH adjustment, and (**v**) that when was again treated with KPS.

An important point that needs to be mentioned here is that in all the above experiments there was no significant change in the absorption spectrum indicating that the particle sizes of the Qdots might not have changed during the course of chemical treatments. This was further substantiated by TEM measurements (Figure 4-3) that showed an average particle size of 3.3 $\pm$ 0.3 nm for the doped Qdots (particle size distribution plot shown in Figure 4-4A), while that for the undoped one was found to be 3.5 $\pm$ 0.2 nm (refer to Appendix, Figure A4-3).

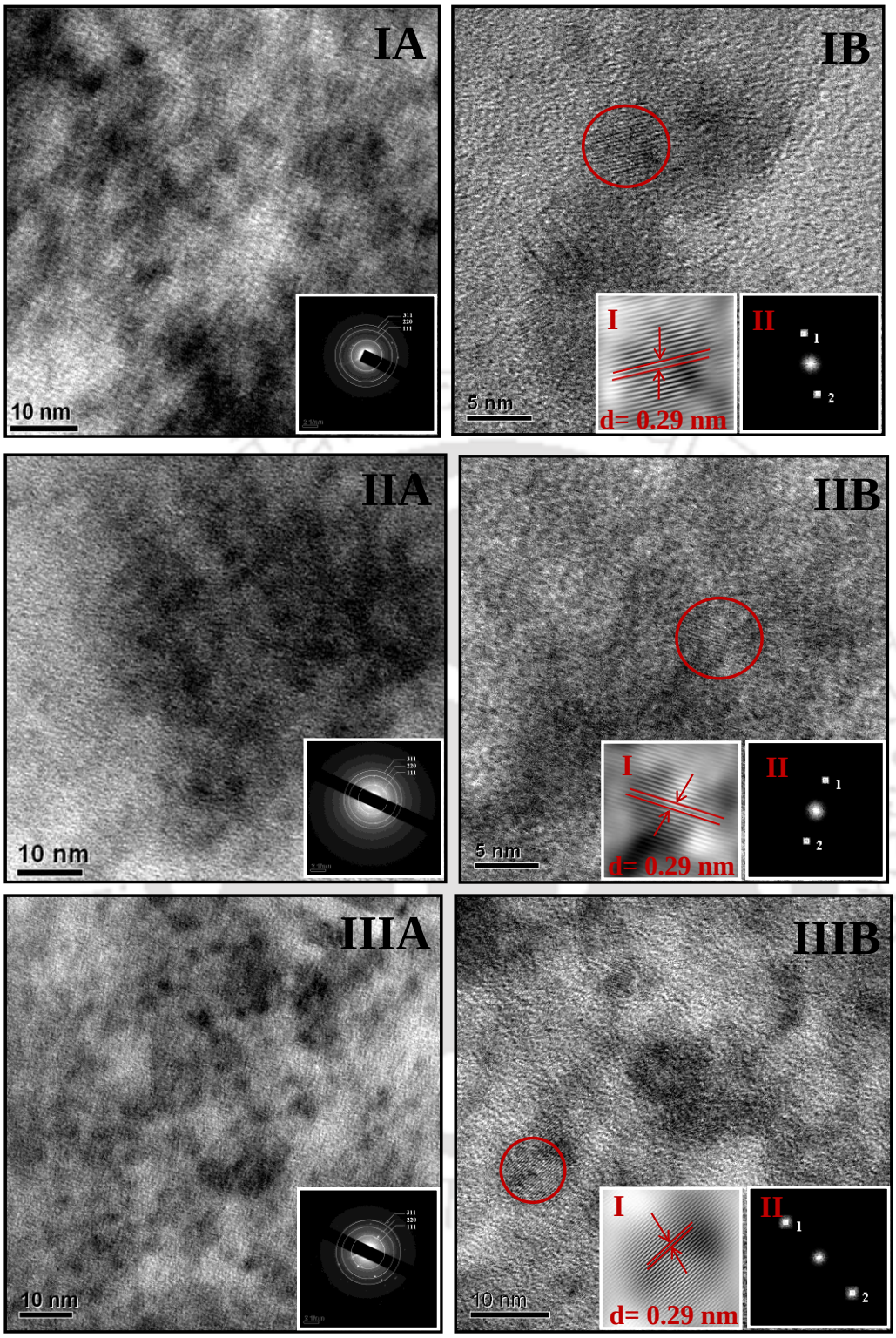


**Figure 4-3.** (**A**) TEM image with selected area electron diffraction (SAED) pattern in the inset, (**B**) high resolution TEM (HRTEM) image with (**I**) Inverse Fast Fourier Transform (IFFT) image of the selected region and (**II**) corresponding FFT image in the inset. Here, (**I**) represents image due to as-synthesized chitosan-stabilized Cu doped ZnS Qdots (**II**) the same Qdots treated with $NaBH_4$ and (**III**) subsequent treatment with KPS.

Powder X-ray diffraction patterns for as-synthesized chitosan-stabilized Cu-doped ZnS Qdots is shown in Figure 4-4B, which consisted of three peaks at 2θ values of $28.8^0$, $48.3^0$ and $56.8^0$, corresponding to diffractions from (111), (220), and (311) planes of ZnS nancrystals, respectively, and no peak corresponding to copper sulphide was observed. Further, the average size calculated from the peaks was determined to be 2.9 nm, which is close to the observed value from TEM analysis.

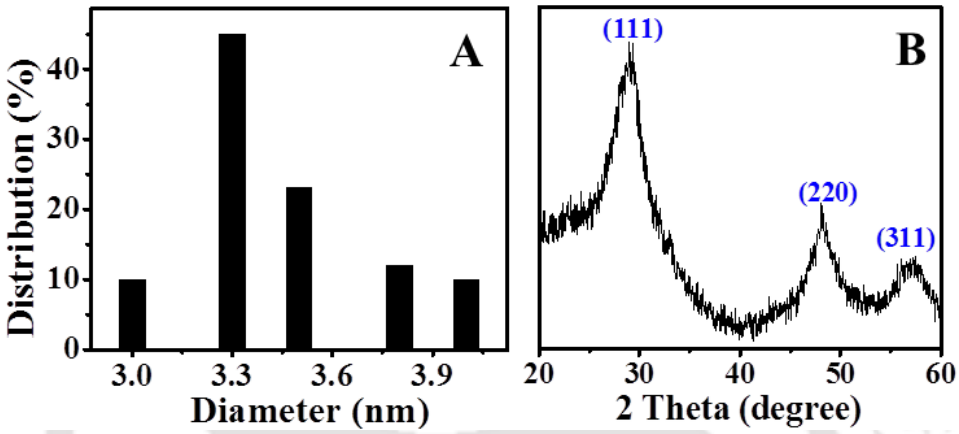


**Figure 4-4.** (**A**) Particle size distribution plot calculated from TEM images (**B**) Powder X-ray diffraction pattern of as-synthesized chitosan-stabilized $Cu^{2+}$- doped ZnS Qdots.

The green emission band of Cu-doped ZnS Qdots has been attributed to the presence of either of $Cu^+$ or $Cu^{2+}$ luminescent centres in the fluorescent crystals.[28-32] It has been proposed that when the dopant is present as $Cu^+$ i.e. in $3d^{10}$ configuration following optical excitation, a hole from the valence band of the Qdot is captured by the t-level of Cu. This is followed by radiative transfer of an electron from the conduction band of the Qdot to Cu, leading to green emission.[33-36] On the other hand, when the dopant is present as $Cu^{2+}$ i.e. in $3d^9$ configuration, radiative transfer of an electron from the conduction band of the Qdot to the t-level of the dopant leads to the observed fluorescence. Further, the presence of Cu in the Qdots was confirmed by X-ray photoelectron spectroscopy, shown in Figure 4-5. The Cu $2p_{3/2}$ and Cu $2p_{1/2}$ peaks at 932.02 eV and 952.2 eV, respectively, correspond to presence of $Cu^{2+}$.[37] The present results indicated that the as-synthesized Qdots consisted of $Cu^{2+}$ ions as dopant which upon reaction with a

chemically reducing agent resulted in the formation of $Cu^{+}$. The $Cu^{+}$ species, the luminescent centres, were thus generated in the doped Qdots.

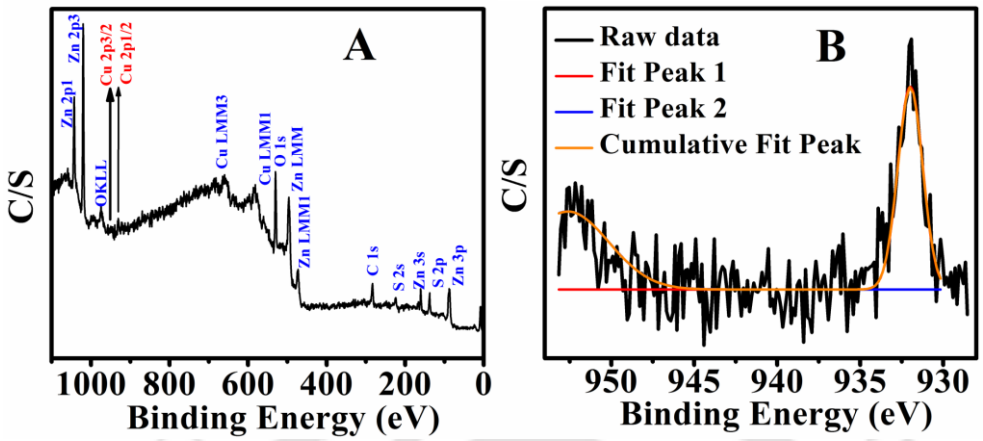


**Figure 4-5.** (**A**) X-ray photoelectron spectrum of as-synthesized Cu-doped ZnS Qdots. (**B**) Expanded view of the same depicting Cu- peaks. The peaks in (**B**) were fitted with Gaussian curves.

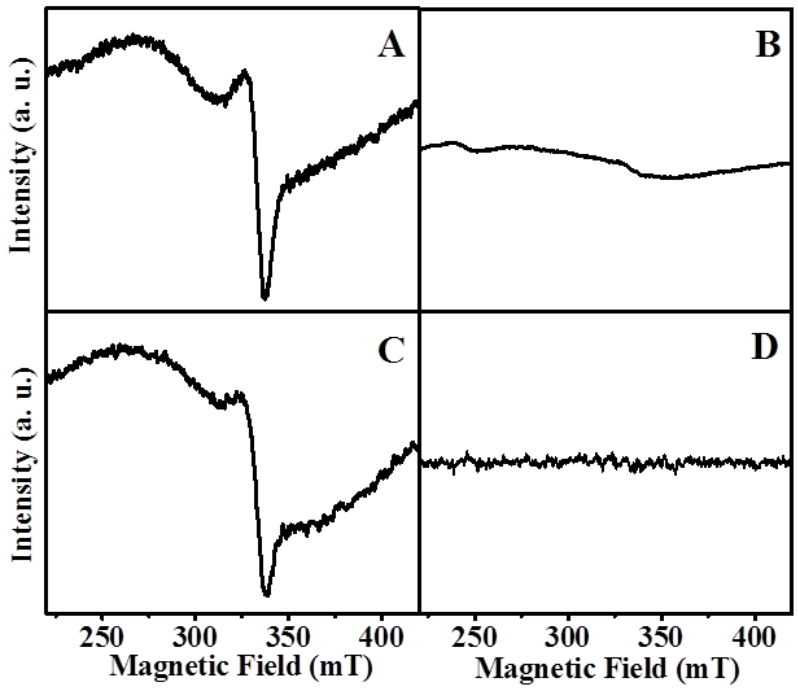


**Figure 4-6.** ESR spectra of (**A**) as-synthesized chitosan-stabilized $Cu^{2+}$-doped Qdots, (**B**) those of treated with $NaBH_4$, (**C**) recorded following subsequent addition of KPS and (**D**) as-synthesized chitosan-stabilized ZnS Qdots.

Electron spin resonance (ESR) experiments with the doped Qdots indicated the presence of $Cu^{2+}$ ions (Figure 4-6A) in the as-synthesized Qdots - as was evidenced by the observed peak at 340 mT. On the other hand, treatment of the Qdots with $NaBH_4$ led to the disappearance of the peak indicating the reduction of $Cu^{2+}$ to $Cu^{+}$ (Figure 4-6B). The presence of a broad background in the spectrum indicated partial oxidation of the ions during the course of sample handling and measurements under ambient conditions. Additionally, treatment of the $NaBH_4$ treated Qdots with KPS led to the reappearance of the peak (Figure 4-6C), suggesting conversion of $Cu^{+}$ back to $Cu^{2+}$. ESR spectrum for ZnS Qdots (shown in Figure 4-6D) indicated absence of any such peak.

That the emitting species in the doped Qdots was $Cu^{+}$ was further evidenced by the observed green emission from as-synthesized Qdots generated in different reducing environment. For example, 3.5 $\pm$ 0.3 nm (Figure A4-4, Appendix) Cu-doped ZnS Qdots synthesized in the presence of $NH_4SCN$ or trisodium citrate (TSC) exhibited similar green emission. Interestingly, the as-synthesized Qdot emission at 505 nm disappeared in 2 h (for $NH_4SCN$ stabilized one) or 8 h (for TSC stabilized one) following synthesis. The typical QY for the as-synthesized Qdots was 3%, which upon addition of $NaBH_4$ increased to as much as 7%. Further, treatment of the Qdots with KPS led to the disappearance of the peak. The results are shown in Figure 4-7A, for $NH_4SCN$ stabilized Qdots and in Figure 4-7B for TSC stabilized Qdots. Additionally, ascorbic acid could be used as the reducing agent and the results were similar to the above. Further, all of the emission spectra with their peak in the green region of wavelength could be fitted with Gaussian function. Emission spectra, corresponding to Figure 4-1D, have been fitted with two Gaussian peaks – with one having a peak in the green (540 nm) -; the results are shown in Figure 4-8. This indicated that the emission in the green by the doped Qdots was from a single emitting species, which could well be $Cu^{+}$. The above results generally indicated that in the presence of reducing environment the doped Qdots could be synthesized, where $Cu^{+}$ species was predominant. Also, $NH_4SCN$ form stable complex with $Cu^{+}$.[38] It is plausible that generation of Qdots in its presence led to enhanced stability through surface functionalization of the ions, in contrast to that in the presence of chitosan.

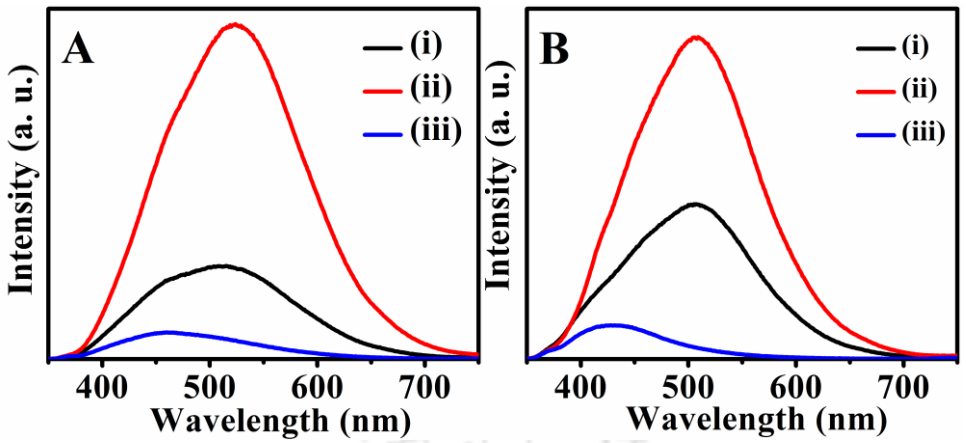


**Figure 4-7.** Emission spectra of (**A**) (**i**) as-synthesized $NH_4SCN$ stabilized Cu-doped ZnS Qdots, (**ii**) those treated with 12 mM of $NaBH_4$ and (**iii**) those following 0.2 mM of KPS addition, subsequent to $NaBH_4$ treatment. (**B**) Emission spectra of trisodium citrate-stabilized $Cu^{2+}$-doped ZnS Qdots (**i**), followed by treatment with ascorbic acid (**ii**), and then following addition of KPS.

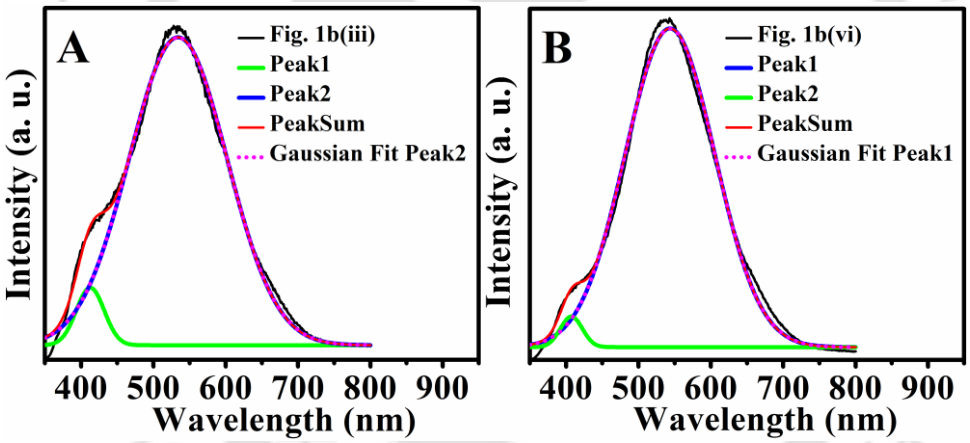


**Figure 4-8.** Fitting of emission spectra in Figure 4-1D by two Gaussian peaks. The left panel spectrum (in black) corresponds to Figure 4-1D (**iii**), while that in the right panel (in black) corresponds to Figure 4-1D (**vi**).

Atomic absorption spectroscopic (AAS) measurements indicated the presence of 3.2 % of Cu in the Qdots, irrespective of the stabilizing agent. Further, excitation spectra of the doped Qdots upon treatment with $NaBH_4$ became more prominent with minimum shift in its peak (Figure A4-5, Appendix). This was in commensurate with the increase in emission intensity of the Qdots indicating minimal change in the structure of the Qdots in the presence of the reducing

species. Also, no changes were observed in the excitation spectra of the Qdots in the presence of $NaBH_4$, indicating the stability of the dots.

We were further interested in using the $Cu^{2+}$-doped ZnS Qdots in probing the reductive/oxidative nature of cellular environment. This is based on the above observations that the Qdots exhibited discernible green fluorescence in the presence of even moderately reducing species. Biological cells consist of delicate balance between oxidizing and reducing species and processes. The presence of species like glutathione (GSH) contributes to the reducing environment, while the production of peroxides under stress makes the cellular environment oxidative. In order to pursue this, chitosan-stabilized doped Qdots were first made into composite NPs by treatment with tripolyphosphate (TPP), based on a reported method. [39] The mean particle size calculated from TEM images was 91 $\pm$ 10 nm (Figure 4-9A). On the other hand, the mean hydrodynamic diameter measured using dynamic light scattering (DLS) based experiments indicated the particles to be 122 $\pm$ 15 nm (Figure 4-9B). It may be emphasized here that DLS measurements revealed the particle size of the overall composite NP containing chitosan and the Qdot. On the other hand, TEM measurements revealed the particle sizes of both the Qdot and the composite NP. Thus the larger particle size of the composite NP obtained from TEM matched closely with the size obtained from DLS measurement. The difference in sizes could arise from the drying of the dispersion for TEM sample preparation. It is likely that composite NPs of chitosan and Qdots redispersed in solution were surrounded by a hydration shell. During TEM sample preparation, it could be expected that the process of air-drying removed the water from the Qdots as well as from the composite NPs as a whole, including the hydration shell. Thus a size difference was observed between the two measurements i.e. TEM and DLS based particle size analysis. Powder SAED and XRD patterns for composite NPs of Cu doped ZnS Qdots and chitosan, substantiating the presence of ZnS, are shown in Figure 4-9C and 4-9D.

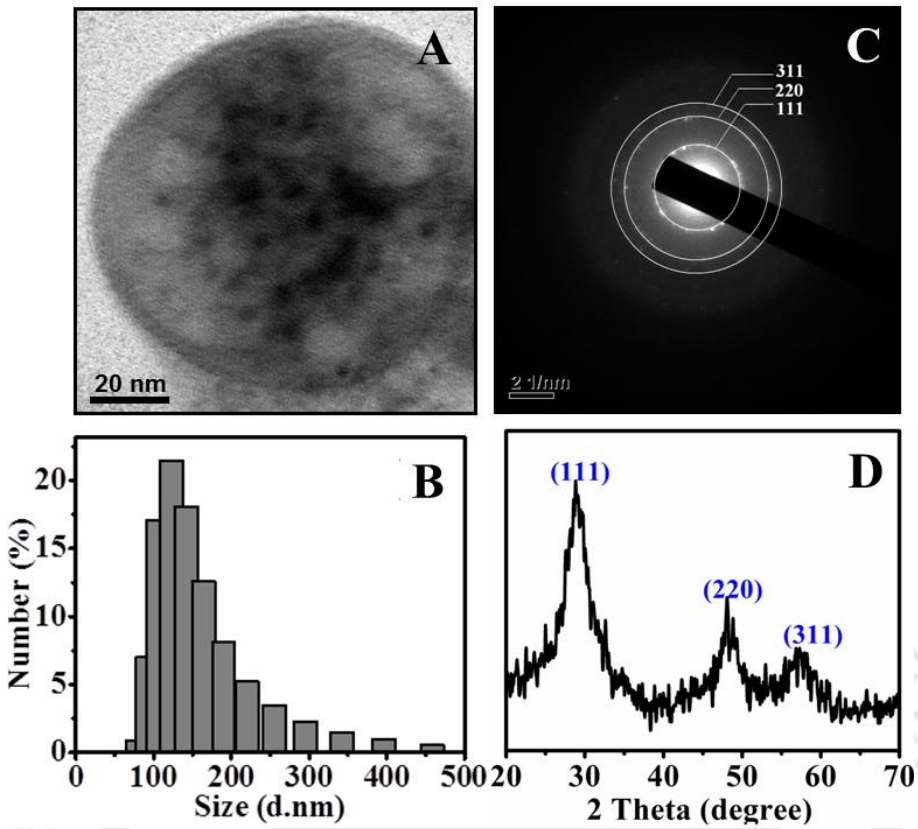


**Figure 4-9.** (**A**) Transmission electron microscopy (TEM) image of a typical composite NP of chitosan-stabilized $Cu^{2+}$-doped ZnS Qdots (**B**) Dynamic light scattering (DLS)-based Particle size distribution of the composite NPs (**C**) SAED patterns corresponding to the sample in A with the diffraction corresponding to lattice planes being identified (**D**) Powder XRD patterns of the composite NPs.

The average size of the composite NPs in the dispersion is ideal for accumulation of the NPs into human embryonic kidney (HEK 293) cells as well as human cervical carcinoma (HeLa) cells by endocytosis.[40-43] The composite NPs upon treatment with $NaBH_4$ and GSH showed characteristic green fluorescence of the doped Qdots. The emission spectrum for $NaBH_4$ and GSH treated composite NPs is shown in Figure 4-10. Fluorescence microscopy measurements with the evaporated NPs (generated by drop-cast) indicated the presence of individual particles which were green when previously treated with $NaBH_4$ (Figure 4-11A) or GSH (Figure 4-11B). Also, the green fluorescence disappeared in the presence of KPS; further images captured using blue emission filter (435-485 nm), are shown in Appendix, Figure A4-6.

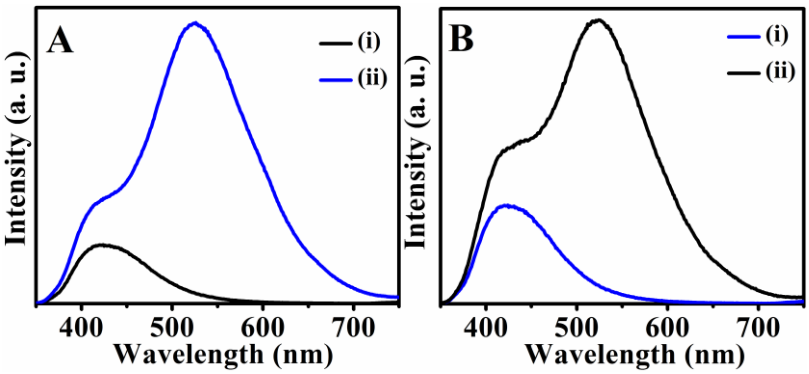


**Figure 4-10.** Emission spectra of (**i**) composite NPs of chitosan stabilized Cu-doped ZnS (**ii**) the same treated with equivalent amount of (**A**) $NaBH_4$ (**B**) GSH; spectra recorded after addition and incubation for 1 h.

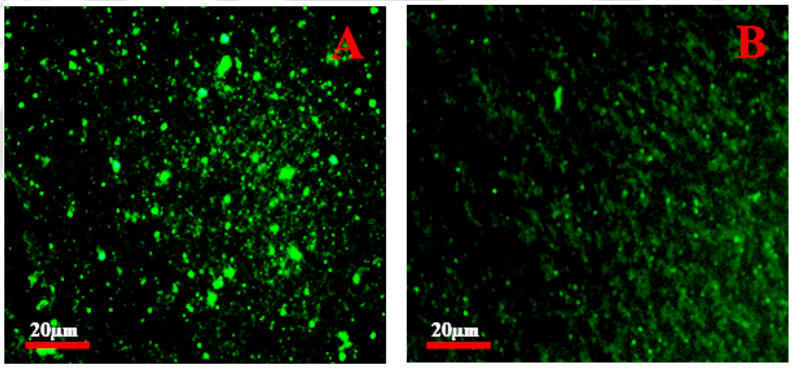


**Figure 4-11.** Epifluorescence microscopic images of the composite NPs following treatment with (**A**) $NaBH_4$ and (**B**) GSH. The images were captured using green emission filter (515-555 nm); Scale bar: 20 μm.

Control experiments with ZnS and $NaBH_4$ treated ZnS Qdots containing composite NPs did not yield any fluorescence in the green when the images were captured using green emission filter (515-555 nm), shown in Appendix, Figure A4-7, while characteristic blue fluorescence of the same was observed when blue emission filter (435-485 nm) was used, shown in Figure 4-12.

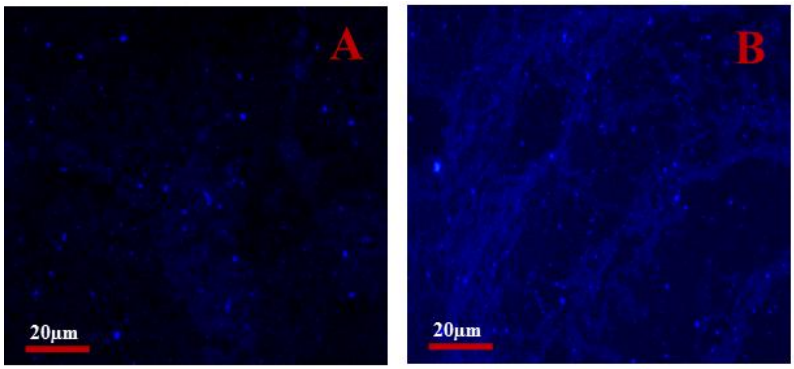


**Figure 4-12.** Epifluorescence microscopic images of the composite NPs of (**A**) ZnS Qdots and (**B**) those following treatment with $NaBH_4$. The images were captured using blue emission filter (435-485 nm); Scale bar: 20 µm.

Further, XTT based cytotoxicity studies indicated that the composite NPs were not cytotoxic to mammalian cells (Figure 4-13). For example, viability was observed for HeLa cells and HEK 293 cells, 24 h after treatment with the composite NPs.

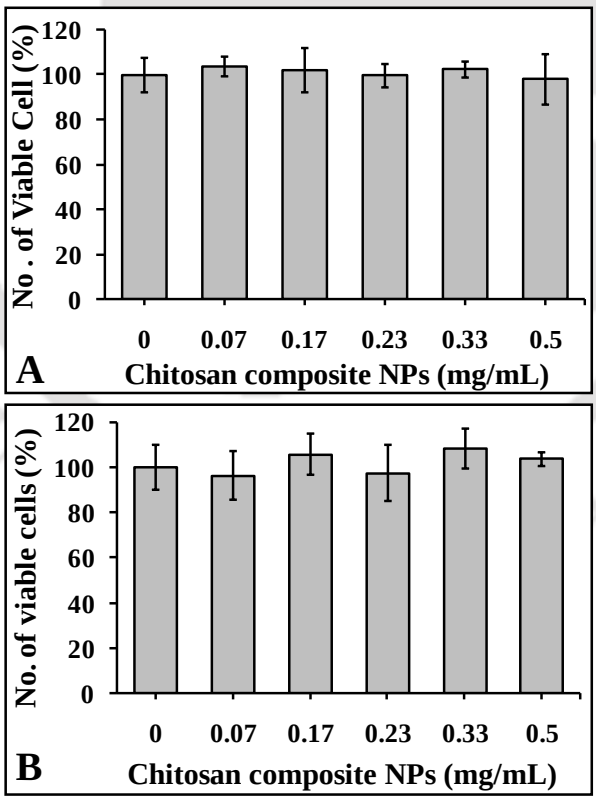


**Figure 4-13.** XTT based cell viability assay for (**A**) HeLa cells (**B**) HEK 293 cells at different concentrations of chitosan composite NPs. Data are presented as the mean ± SD of three individual experiments.

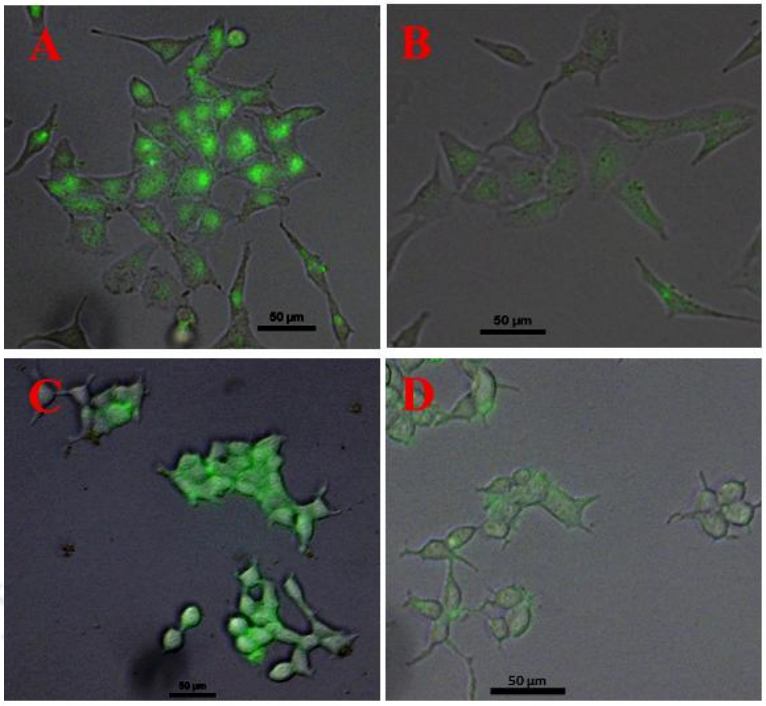


**Figure 4-14.** Epifluorescent microscopic image of (**A**) HeLa cells treated with the composite NPs and (**B**) of those treated with pyrogallol; (**C**) HEK 293 cells and (**D**) those treated with pyrogallol.

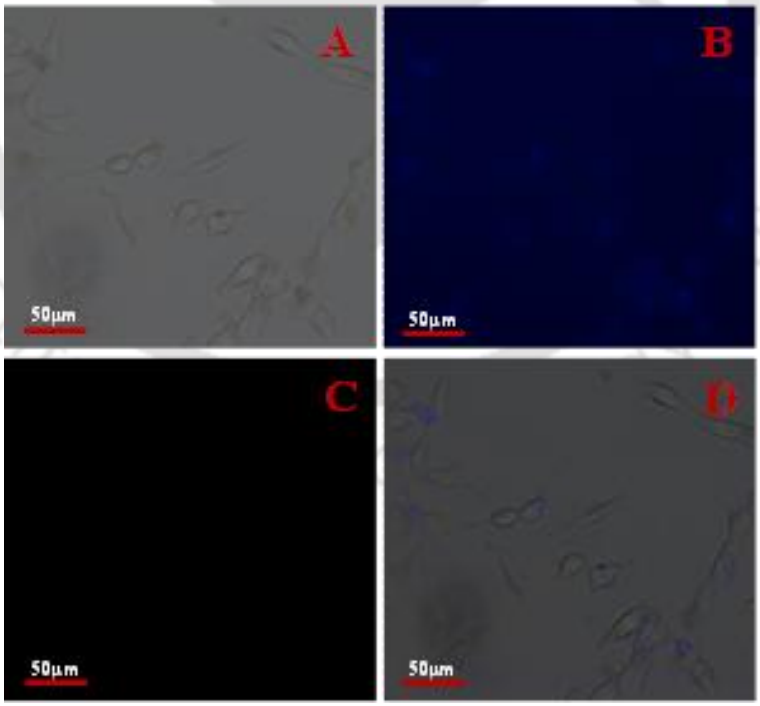


**Figure 4-15.** Epifluorescent microscopic image of HeLa cells treated with composite NPs of ZnS Qdots; captured under irradiation of (**A**) White light, (**B**) blue emission filter (435-485 nm), (**C**) using green emission filter (515-555 nm) (**D**) Merged image of (**A**) and (**B**); Scale bar: 50 µm

Interestingly, when the mammalian cancer (HeLa) cells as well as HEK 293 were treated with the composite NPs, containing doped Qdots, green fluorescent coloration of the cells could be observed, when followed using epifluorescence microscope (Figure 4-14, A and C, respectively). Further, treatment of the cells with pyrogallol, following addition of the composite, led to loss of fluorescence of the cells (Figure 4-14, B and D). Pyrogallol, a polyphenolic compound, generally acts as a reducing agent and ideally ought not to reduce the intensity of the emission from the doped Qdots.

However, previous studies demonstrated that pyrogallol increases intracellular superoxide anions ($O^{2\bullet-}$), which are potent reactive oxygen species (ROS), and subsequently reduces GSH level in various type of cells including HeLa and HEK 293.[44-48] Thus, the decrease in intensity of emission from the Qdots present in the cells, following addition of pyrogallol, suggested that the generation of reactive oxygen species (ROS) in the cells by pyrogallol overwhelmed the reducing effect of pyrogallol. Control experiments involving treatment of HeLa cells with composite NPs containing ZnS Qdots did not indicate any change in the fluorescence properties of the NPs; i.e. the emission remained blue (Figure 4-15).

The formation of ROS was confirmed by flow cytometric analysis, as probed by using 2', 7'-dichlorfluorescein-diacetate (DCFH-DA) staining in a fluorescent activated cell sorter (FACS) machine, which showed a prominent shift of fluorescence intensity in FL1-H channel (Figure 4-16). The results indicated the generation of intracellular oxidative stress in case of cells treated with pyrogallol as compared to cells treated with only composite NPs and control (cells only). As mentioned in the experimental section, DCFH-DA is a non-fluorescent molecule, which readily diffuses into the cell through the plasma membrane where it gets hydrolysed to fluorescent DCF (green) by intracellular oxidation and gets trapped inside the cells. Hence, the amount of fluorescence intensity is directly correlated with the amount of ROS production inside the cells. Thus, ROS possibly oxidized the doped Qdots, thereby reducing their green emission intensity. Overall, the results suggested the presence of reducing environment in both the cells, which also indicated the induction of oxidative stress, in the presence of pyrogallol, by way of loss of fluorescence. They clearly substantiated the ability of the doped Qdots to indicate the nature of redox environment in a cell.

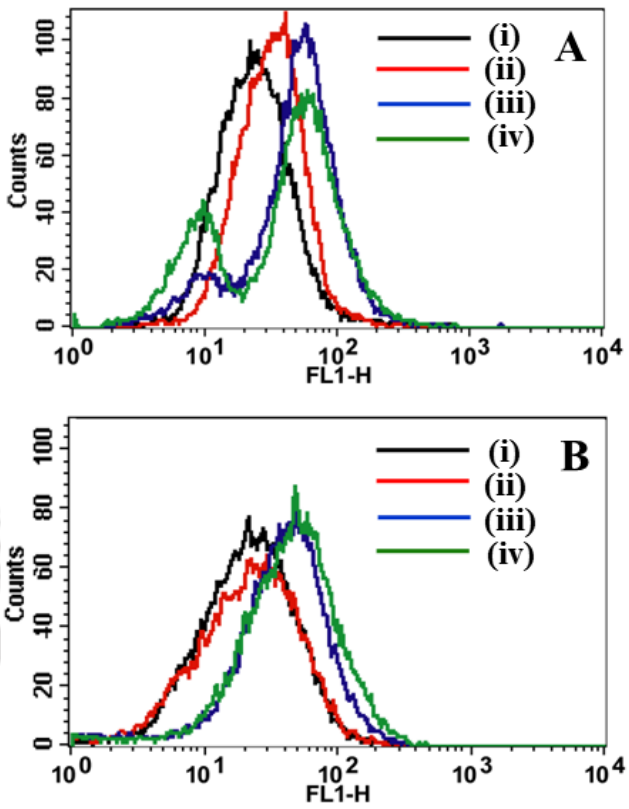


**Figure 4-16.** ROS measurements by FACS experiments with (**A**) HeLa cells (**B**) HEK 293 cells. Histogram for (**i**) control (cells only), (**ii**) cells treated with composite NPs consisting of $Cu^{2+}$-ZnS Qdots, (**iii**) cells treated with pyrogallol and (**iv**)Cells treated with pyrogallol and composite NPs consisting of $Cu^{2+}$-ZnS Qdots.

### 4.4. Conclusion

The observations presented here indicated a new chemistry involving reaction of doped Qdot, with the ability to turn on and off its emission reversibly. Thus the emission of a Qdot, which could be 'hidden' by way of incorporation of a dopant, could be recovered at a longer wavelength following the change in the oxidation state of the same. The $Cu^{2+}$-doped ZnS Qdots which otherwise emit weakly, give rise to prominent green emission (at 540 nm) upon treatment with reducing agents and also, when incorporated in the reductive environment of a cell. While there are several methods available for probing cellular phenomena using organic chemical reactions,[49] this is a new approach using highly emissive and stable Qdots. It is hoped that this work would propel further interests in generating newer Qdots and use of their emission characteristics and chemistry in probing cells at the molecular levels, which may not otherwise be attainable using organic dyes or even simple emissions of Qdots. That the Qdots are compatible with NPs of

chitosan indicates possible versatile applications using drug delivery vehicle, which are commercially available for use. Finally, the emissivity tuning of the Qdots based on redox reactions may provide new ways in healthcare diagnostics as well as in therapeutics.

**References**


1) Green, M. *Angew. Chem. Int. Ed*. **2004**, 43, 4129 –4131.

2) Samia, A. C. S.; Chen X.; Burda, C. *J. Am. Chem. Soc.* **2003**, 125, 15736–15737.

3) Willard, D. M.; Carillo, L. L.; Jung, J.; Orden, A. V. *Nano Lett.* **2001**, 1, 469–474.

4) Weng, K. C.; Noble, C. O.; Papahadjopoulos-Sternberg, B.; Chen, F. F.; Drummond, D. C.; Kirpotin, D. B.; Wang, D.; Hom, Y. K.; Hann, B.; Park, J. W. *Nano Lett.* **2008**, 8, 2851-2857.

5) Medintz, I. L.; Mattoussi, H. *Phys. Chem. Chem. Phys*. **2009**, 11, 17–45.

6) Bruchez, M.; Moronne, M. Jr.; Gin, P.; Weiss, S.; Alivisatos, A. P. *Science* **1998**, 281, 2013–2016.

7) Mattoussi, H.; Mauro, J. M.; Goldman, E. R.; Anderson, G. P.; Sundar, V. C.; Mikulec, F. V.; Bawendi, M. G. *J. Am. Chem. Soc.*, **2000**, 122, 12142–12150.

8) Santra, S.; Yang, H.; Holloway, P. H.; Stanley, J. T.; Mericle, R. A. *J. Am. Chem. Soc*. **2005**, 127, 1656-1657.

9) W. Liu, M. Howarth, A. B. Greytak, Y. Zheng, D. G. Nocera, Ting, A. Y.; Bawendi, M. G. *J. Am. Chem. Soc.* **2008**, 130, 1274-1284.

10) Yong, K. T.; Ding, H.; Roy, I.; Law, W. C.; Bergey, E. J.; Maitra, A.; Prasad, P. N. *ACS Nano* **2009**, 3, 502-510.

11) Hohng, S.; Ha, T. *J. Am. Chem. Soc.* **2004**, 126, 1324-1325.

12) Jeong, S.; Achermann, M.; Nanda, J.; Ivanov, S.; Klimov, V. I.; Hollingsworth, J. A. *J. Am. Chem. Soc.* **2005**, 127, 10126-10127.

13) Clarke, S. J.; Hollmann, C. A.; Zhang, Z.; Suffern, D.; Bradforth, S. E.; Dimitrijevic, N. M.; Minarik, W. G.; Nadeau, J. L. *Nat. Mater.* **2006**, 5, 409–417.

14) Medintz, I. L.; Stewart, M. H.; Trammell, S. A.; Susumu, K.; Delehanty, J. B.; Mei, B. C.; Melinger, J. S.; Blanco-Canosa, J. B.; Dawson, P. E.; Mattoussi, H. *Nat. Mater.* **2010**, 9, 676–684.

15) Chan, W. C. W.; Nie, S. *Science* **1998**, 281, 2016–2018.

16) Michalet, X.; Pinaud, F. F.; Bentolila, L. A.; Tsay, J. M.; Doose, S.; Li, J. J.; Sundaresan, G.; Wu, A. M.; Gambhir, S. S.; Weiss, S. *Science* **2005**, 307, 538-544.

17) Alivisatos, A. P. *Angew.Chem. Int. Ed*. **2004**, 43, 4129-4131.

18) Medintz, I. L.; Uyeda, H. T.; Goldman, E. R.; Mattoussi, H. *Nat. Mater.* **2005**, 4, 435–446.

19) Derfus, A. M.; Chan, W. C. W.; Bhatia, S. N. *Nano Lett*. **2004**, *4*, 11-18.

20) Kirchner, C.; Liedl, T.; Kudera, S.; Pellegrino, T.; Javier, A. M.; Gaub, H. E.; Sto1lzle, S.; Fertig, N.; Parak, W. J. *Nano Lett*. **2005**, 5, 331–338.

21) Sooklal, K.; Cullum, B. S.; Angel, S. M.; Murphy, C. J. *J. Phys. Chem*. **1996**, 100, 4551-4555.

22) Becker, W. G.; Bard, A. *J. Phys. Chem*. **1983**, 87, 4888- 4893.

23) Zhou, W.; Baneyx, F. *ACS Nano* **2011**, 5, 8013–8018.

24) Wang, Q.; Bao, Y.; Zhang, X.; Coxon, P. R.; Jayasooriya, U. A.; Chao, Y. *Adv. Healthcare Mater.* **2012**, 1, 189–198.

25) Sanpui, P.; Chattopadhyay, A.; Ghosh, S. S. *ACS Appl. Mater. Interfac.* **2011**, 3, 218–228.

26) Begum, R.; Chattopadhyay, A. *Langmuir* **2011**, 27, 6433–6439.

27) Po, H. N.; Allen, T. L. *J. Am. Chem. Soc*. **1968**, 1127–1131.

28) Meulenberg, R. W.; Buuren, T. V.; Hanif, K. M.; Willey, T. M.; Strouse, G. F.; Terminello, L. J. *Nano Lett.* **2004**, 4, 2277–2285.

29) Corrado, C.; Hawker, M.; Livingston, G.; Medling, S.; Bridgesb, F.; Zhang, J. Z. *Nanoscale* **2010**, 2, 1213–1221.

30) Corrado, C.; Jiang, Y.; Oba, F.; Kozina, M.; Bridges, F.; Zhang, J. Z. *J. Phys. Chem. A* **2009**, 113, 3830–3839.

31) Sun, L.; Liu, C.; Liao, C.; Yan, C. *J. Mater. Chem*. **1999**, 9, 1655–1657.

32) Ehlert, O.; Osvet, A.; Batentschuk, M.; Winnacker, A.; Nann, T. *J. Phys. Chem. B* **2006**, 110, 23175-23178.

33) Peka, P.; Schulz, H. J. *Phys. B* **1994**, 193, 57-65.

34) Peka, P.; Schulz, H. J. *Solid State Commun*. **1994**, 89, 225-228.

35) Bol, A. A.; Ferwerda, J.; Bergwerff, J. A.; Meijerink, A. *J. of Lumin.* **2002**, 99, 325–334.

36) Khosravi, A. A.; Kundu, M.; Jatwa, L.; Deshpande, S. K.; Bhagwat, U. A; Sastry, M.; Kulkarni, S. K. *Appl. Phys. Lett*. **1995**, 67, 2702–2704.

37) Liu, Y.; Liang, H.; Xu, L.; Zhao, J.; Bian, J.; Luo, Y.; Liu, Y.; Li, W.; Wu, G.; Du, G. *J. App*. *Phys.* **2010**, 108, 113507-1-113507-4.

38) P. Yanga, C. Songa, M. Lüa, G. Zhoub, Z. Yangc, D. Xua and D. Yuana, *J. of Phys. Chem. of Solids* 2002, 63, 639–643.

39) Calvo, P.; Remunan-Lopez, C.; Vila-Jato, J. L.; Alonso, M. J. *J. Appl. Polym. Sci.* **1997**, 63, 125-132.

40) T. D. Santos, J. Varela, I. Lynch, A. Salvati and K. A. Dawson, *PLoS One* **2011**, 6(9), 1-10, e24438.

41) Peer, D.; Karp, J. M.; Hong, S.; Farokhzad, O. C.; Margalit, R.; Langer, R. *Nat. Nanotechnol.* **2007**, 2, 751.

42) Lee, D. W.; Yun, K. S.; Ban, H. -S.; Choe, W.; Lee, S. K.; Lee, K. Y. *J. of Control Release* **2009**, 139, 146–152.

43) Gratton, S. E. A.; Ropp, P. A.; Pohlhaus, P. D.; Luft, J. C.; Madden, V. J.; Napier, M. E.; DeSimone, J. M. *Pnas*, **2008**, 105, 11613–11618.

44) Kim, S. W.; Han, Y. W.; Lee, S. T.; Jeong, H. J.; Kim, S. H.; Kim, I. H.; Lee, S. O.; Kim, D. G.; Kim, S. H.; Kim, S. Z.; Park, W. H. *Mol. Carcinog*., **2008**, 47, 114-125.

45) Han, Y. H.; Kim, S. Z.; Kim, S. H.; Park, W. H. *Int. J. Mol. Med*. **2008**, 21, 721-730.

46) Mitsuhashi, S.; Saito, A.; Nakajima, N.; Shima, H.; Ubukata, M. *Molecules* **2008**, 13, 2998-3006.

47) Meena, R.; Pal, R.; Pradhan, S. N.; Rani, M.; Paulraj, R. *Adv. Mat. Lett*. **2012**, 3, 459-465.

48) Park, W. H.; Han, Y. H.; Kim, S. H.; Kim, S. Z. *Toxicology* **2007**, 235, 130–139.

49) Chan, J.; Dodani, S. C.; Chang, C. J. *Nat. Chem.* **2012**, 4, 973-984.

# Chapter 5

## Redox Tuned Three-color Emission in Double Doped ZnS Quantum Dots

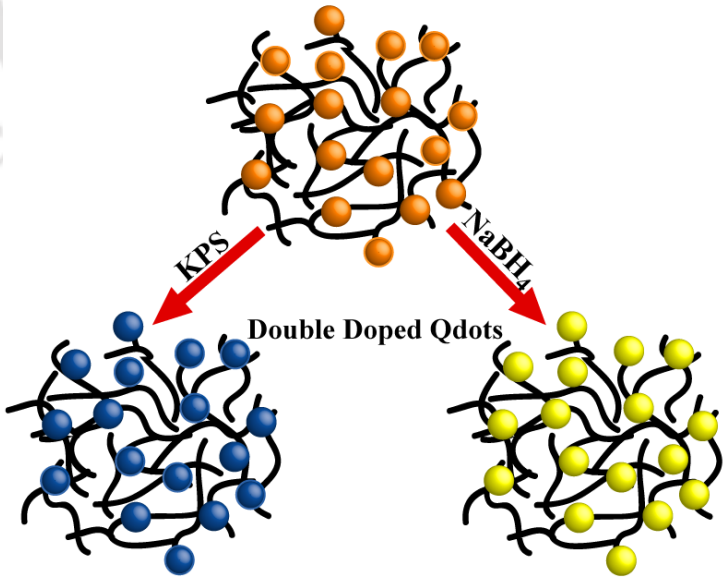

# Chapter 5

**Abstract:** The photoluminescence characteristics of colloidal $Mn^{2+}$ and $Cu^{2+}$ (double) doped ZnS quantum dots (Qdots) could be drastically influenced by reactions with redox reagents. Importantly, experiments revealed $Cu^{+}$ in ZnS nanocrystals rather than $Cu^{2+}$, in conjunction with $Mn^{2+}$, as the emitting dopant. Thus, as-synthesized aqueous Qdots emitted orange (with peaks at 460 nm and 592 nm) due to the host and $Mn^{2+}$ dopant emissions. However, upon treatment with reducing agent the color changed to yellow with dual peaks positioned at 520 nm and 590 nm, due to $Cu^{+}$ and $Mn^{2+}$ dopant emissions. The characteristics could be changed reversibly with appropriate redox reagents. Further, treatment with excess of an oxidizing agent led to blue emission with single peak at 450 nm.

## 5.1. Introduction

The primary challenge involving synthesis of colloidal Qdots with high photoluminescence (PL) quantum yield (QY), wavelength-selected emission, and with photo and chemical stabilities appears to have been significantly addressed.[1-2] However, large-scale practical use also necessitates understanding their reactions with chemical species. This is deemed important, given plenty of chemically reactive moieties which are present in biological and environmental milieu.[3] This could involve redox reaction,[4-5] ion exchange,[6-7] surface ion removal,[8] exchange of stabilizing species present on the surface of the Qdots[9-10] and electrochemical charge injection.[11-12] Recent reports suggest reactions of Qdots with chemical species lead to increase in luminescence QY, recovery of hidden quanta,[13] and formation of heterodimer and other Qdots which are otherwise difficult to synthesize using established procedures.[14-15]

As discussed in previous chapters, not only is the concentration of dopant in a doped Qdot important but also oxidation state plays important role in determining its emission, as observed in case of $Mn^{2+}$-doped ZnS Qdots[16] and $Cu^{2+}$-doped ZnS[13] Qdots. In fact, observations from another laboratory also suggested photochemical redox reactions greatly influencing the luminescence QY of Qdots.[17]

A more interesting case could be the Qdots doped with two different impurity transition metal ions, where emission could occur over a wide wavelength range. Initial reports by Yang et al. apparently indicated no special characteristics other than difference in emission wavelength and intensity for crystals doped with different combinations of two transition metal ions.[18] Recently, Panda et al. reported the emission of Cu and Mn doped ZnSe to be occurring at 485 nm and 585 nm.[19] This was followed by the report of Jana et al. that in Cu and Mn doped ZnS the emission is due to $Mn^{2+}$ and that in ZnSe host is due to $Cu^{2+}$ ions.[20] It is thus necessary to understand the origin of emission in double doped Qdots from the standpoint of chemistry and their applications.

The chapter demonstrates that as-synthesized $Cu^{2+}$ and $Mn^{2+}$ (double) doped ZnS nanocrystals (NCs) emit due to $Mn^{2+}$ impurity, in addition to that due to the host. However, upon treatment with a reducing agent additional emission at 520 nm – which could be assigned to $Cu^{+}$ species – appeared. This also led to significant increase in the overall luminescence QY. The emission could be turned off reversibly in the presence of an oxidizing agent. Further, the presence of an excess oxidizing agent led to disappearance of emission due to both dopants; however, emission due to host could still be observed. Emission of three colors under different redox conditions and their origin are depicted in Scheme 1.

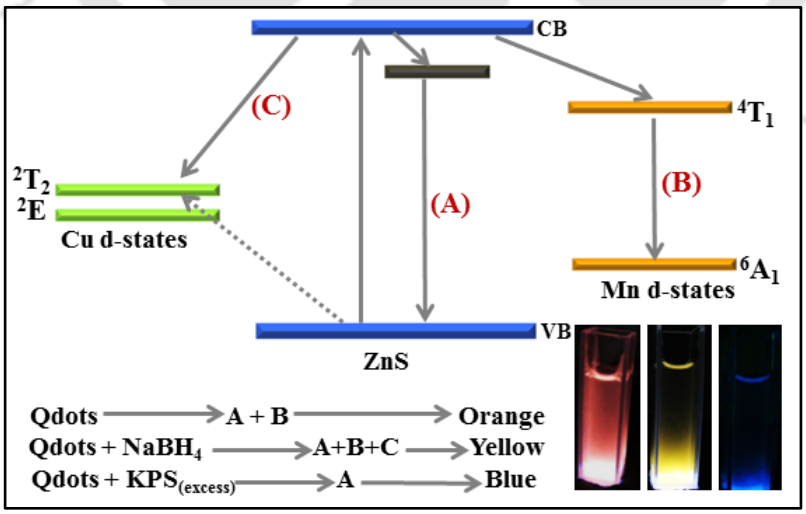


**Scheme 5-1.** Energy level diagram of $Mn^{2+}$ and $Cu^{2+}$ (double) doped ZnS Qdots; the as-synthesized Qdots emit orange, while depending on the redox nature of the medium, the Qdots emits - blue in an oxidizing medium, while yellow in reducing medium. The nature of emitting species is also delineated.

## 5.2. Experimental Section

### 5.2.1. Materials

Zinc acetate dihydrate (98%), manganese acetate tetrahydrate (99%), copper acetate monohydrate (99%), sodium sulphide (55-58%), potassium peroxodisulfate (99%), sodium borohydride (95%), chitosan (Sigma- Aldrich; medium molecular weight) were used as procured. All chemicals other than chitosan were from Merck Limited, Mumbai, India.

### 5.2.2. Synthesis and characterization of double doped Qdots

$Mn^{2+}$ and $Cu^{2+}$ (double) doped ZnS Qdots were prepared as follows: To 50 mL of Elix quality water, which was first heated to boiling, chitosan (medium molecular weight; 0.05 mg/mL) was added. To the solution, 5.0 mM each of zinc acetate and sodium sulphide was added, followed by addition of manganese acetate (0.08 mM) and then copper acetate (0.25 mM). The aqueous colloidal solution was refluxed for 3 h under continuous stirring condition; it was then cooled to room temperature. Finally, the medium was centrifuged at a speed of 22,000 rpm for 20 min; this was followed by addition of water and centrifugation again. The pellet so obtained was rinsed with water, redispersed in 200 mL water and sonicated for 20 min.

### 5.2.3. Treatment to Qdot dispersion with redox reagents

Solid $NaBH_4$ was weighed and added to 3 mL of $Mn^{2+}$ and $Cu^{2+}$ (double) doped ZnS Qdot sample taken in a vial, final concentration being 12 mM. Fluorescence spectra were recorded for the sample from time to time. Then, 25 uL of 50 mM and 0.45 M KPS (KPS is 47.5% pure; final concentration in the medium being 0.2 mM and 1.8 mM, respectively) were added.

### 5.2.3. Characterization

All characterizations were made similar to chapter 4 and same model of instruments have been used herein.

## 5.3. Results and Discussion

The experiments were based on the development of a new method of synthesis of the doped Qdots embedded in chitosan biopolymer in the form of composite. This was done keeping in view that chitosan with embedded Qdots could chemically be converted into nanoparticle (NP), which can be used for cellular delivery of drugs or probes. The absorption spectrum of the Qdots exhibited excitonic peak of ZnS at 320 nm, which was similar to singly doped $Mn^{2+}$-doped ZnS Qdots and $Cu^{2+}$-doped ZnS Qdots (refer to Appendix, Figure A5-1, 2). Further, the tail observed in the absorption spectrum of the double doped Qdots, which is similar to Urbach tail, could be due to mixing of the surface trap states and Qdot states. Such tailing of absorption spectrum, based on the mixing of surface states and Qdot states, has been reported previously.[21-22] Similar tailing could also be observed in the singly-doped Qdots

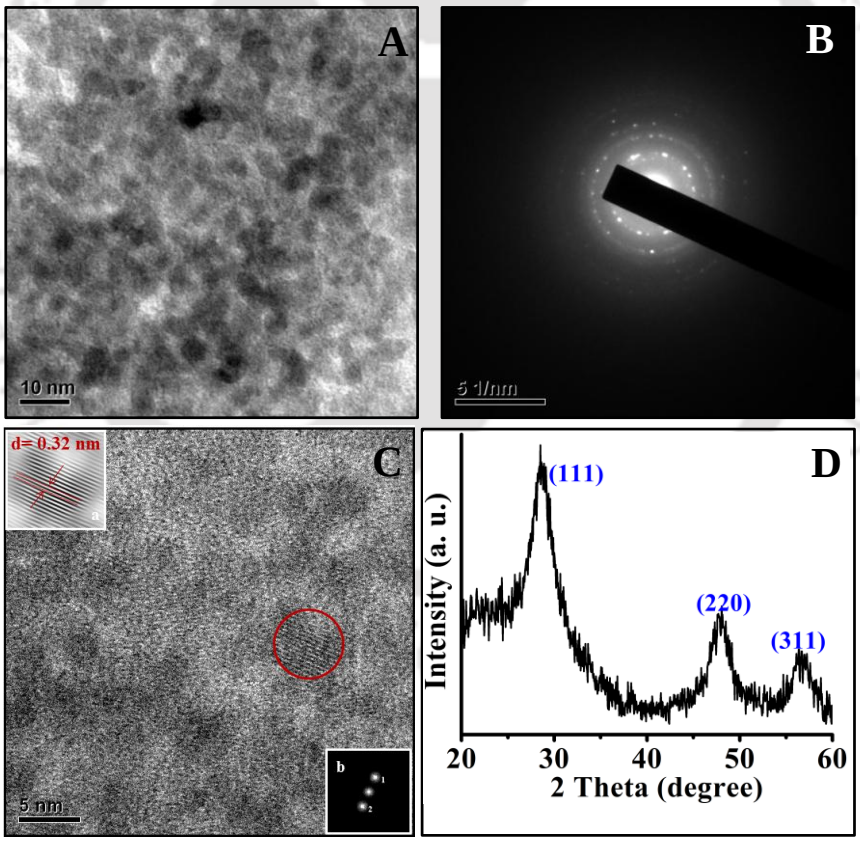


**Figure 5-1.** (**A**) TEM image, (**B**) SAED patterns, (**C**) High Resolution TEM image with inset (**a**) inverse FFT image of the selected region marked by red circle and inset (**b**) is the corresponding FFT image and (**D**) Powder X-ray diffraction of the as-synthesized $Mn^{2+}$ and $Cu^{2+}$ (double)-doped ZnS Qdots.

TEM and powder XRD measurements confirmed the formation of ZnS NCs with d-spacing of 0.32 nm and average particle size of 3.5±0.5 nm (Figure 5-1). AAS study indicated the metal composition of zinc (95.6%), manganese (0.6%) and copper (3.8%) in the crystals.

The emission spectrum of the as-synthesized double-doped ZnS Qdots consisted of peaks at 592 nm and 460 nm, (Figure 5-2A (i)) with a QY of 3%.

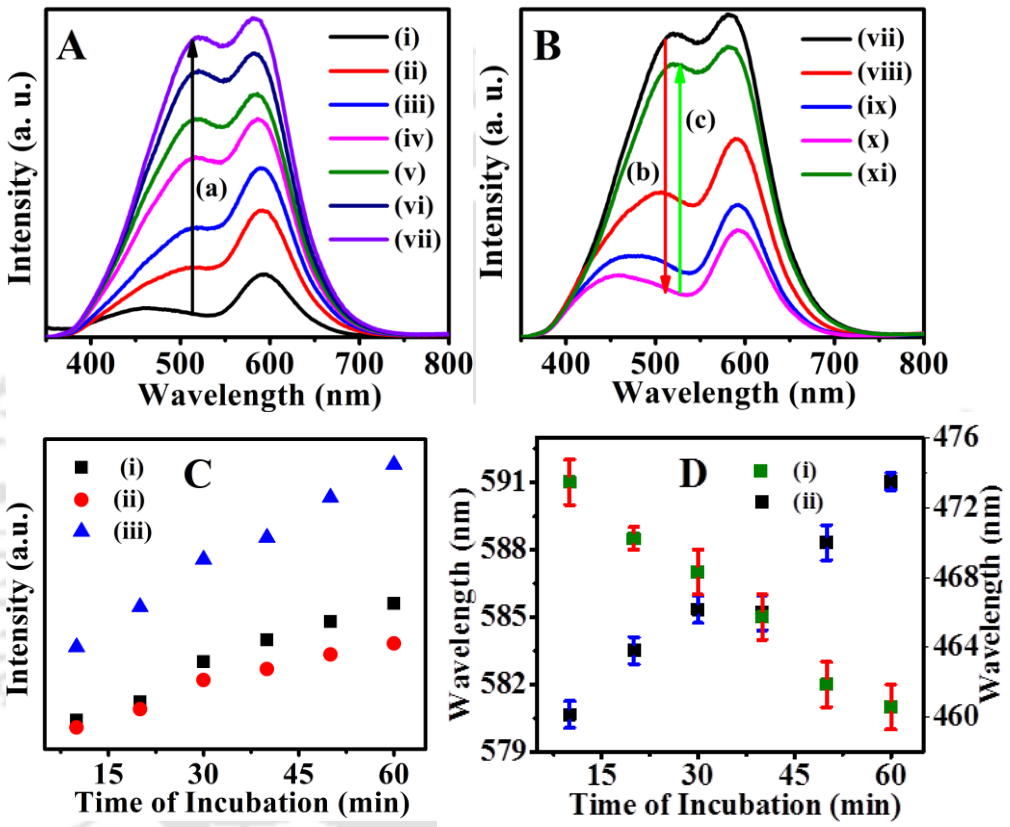


**Figure 5-2.** Time evolution of emission spectrum of 3.0 mL of $Mn^{2+}$ and $Cu^{2+}$ (double) doped ZnS Qdots having optical absorbance 0.04: (**A**) (**i**) as-synthesized Qdots and at (**ii**) 5 min, (**iii**) 10 min, (**iv**) 20 min, (**v**) 30 min, (**vi**) 40 min and (**vii**) 60 min, following addition of 12 mM of $NaBH_4$. Time evolution of emission spectrum when (**B**) 0.2 mM of potassium peroxodisulphate (KPS) was added 60 min after addition of $NaBH_4$ (subsequent to pH adjustment) and again incubated for (**viii**) 0 min, (**ix**) 5 min and (**x**) 10 min; (**xi**) 12 mM of $NaBH_4$ was added finally to check reversibility. Arrows labeled with (a), (b) and (c) indicate the direction of changes in emission spectra following addition of appropriate redox reagents. (**C**) Change in emission intensity of (**i**) host emission, (**ii**) atomic emission corresponding to Cu and (**iii**) atomic emission due to Mn with time. (**D**) Change in wavelength corresponding to maximum intensity for host emission and atomic emission of Mn; of the double doped Qdots sample treated with 12 mM of $NaBH_4$ versus time of incubation up-to 1 h. (**C**) and (**D**) were plotted from deconvoluted peaks of spectra in (**A**).

The spectrum is similar to $Mn^{2+}$-doped ZnS Qdots corresponding to Mn atomic emission ($^4T_1$ to $^6A_1$) at 593 nm and host emission at 454 nm. The emission spectrum of as-synthesized $Cu^{2+}$-doped ZnS Qdots has a weak peak at 420 nm (refer to Appendix, Figure A5-3). The excitation wavelength was set at 320 nm for all the measurements.

On the other hand, when aqueous dispersion of as-synthesized double-doped Qdot sample was treated with 12 mM of $NaBH_4$, a new peak appeared at 520 nm – with emission color changing from orange to yellow; emission intensity continuously increased with time till it reached a constant value in 1 h (Figure 5-2A). It was further observed that upon addition of $NaBH_4$, the intensity of the peak at 592 nm, as well as peak at 460 nm also increased with concomitant shift in the wavelengths. While there was a red shift of the host emission, the Mn atomic emission was blue-shifted with rapid increase in intensity. The results are shown in Figure 5-2C and D. Further, the spectra in Figure 1A were deconvoluted into three peaks, as shown in the Figure 5-3. Here also results indicated the appearance of a new peak at 520 nm with increase in intensity of all the peaks.

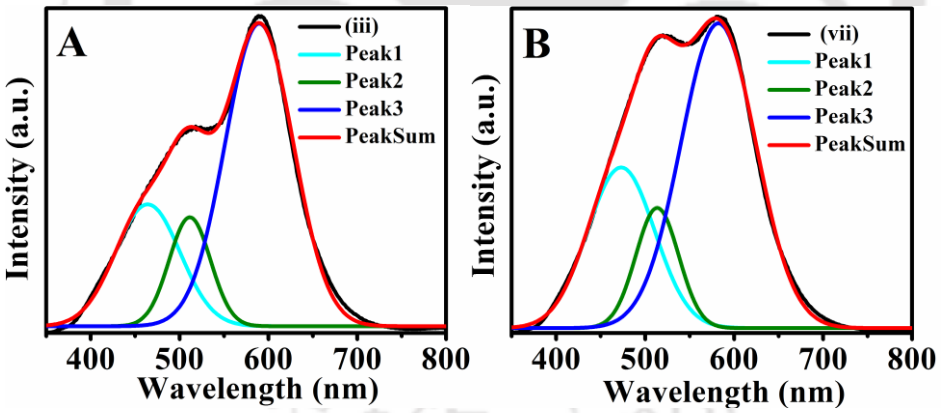


**Figure 5-3.** Fitting of emission spectra in Figure 5-2A by three Gaussian peaks. The spectra (in black) correspond in (**A**) is Figure 5-2A (iii) and (**B**) is Figure 5-2A (vii).

The appearance of the new peak at 520 nm could be due to the change in the oxidation state of $Cu^{2+}$ upon treatment with $NaBH_4$. It is likely that during synthesis, both the transitional metal ions were doped in their 2+ oxidation state and both the dopants interacted with each other. $Cu^{2+}$ ions are known as effective quencher of Qdot fluorescence, which could have reduced the overall quantum

efficiency. A control experiment with addition of $Cu^{2+}$ to $Mn^{2+}$-doped ZnS Qdots led to significant reduction in fluorescence intensity (Figure 5-4A). However, upon addition of $NaBH_4$ to the double doped Qdots, $Cu^{+}$ might have been formed which did not quench the emission in case of double doped Qdots.[12] This resulted in not only increase in QY due to $Mn^{2+}$ impurity and host emissions for the double-doped Qdots but also appearance of emission due to $Cu^{+}$ impurities. The change in wavelength of emission due to $Mn^{2+}$ could be due to presence of clusters on the surface the nature of which changed following addition of the reducing agent.

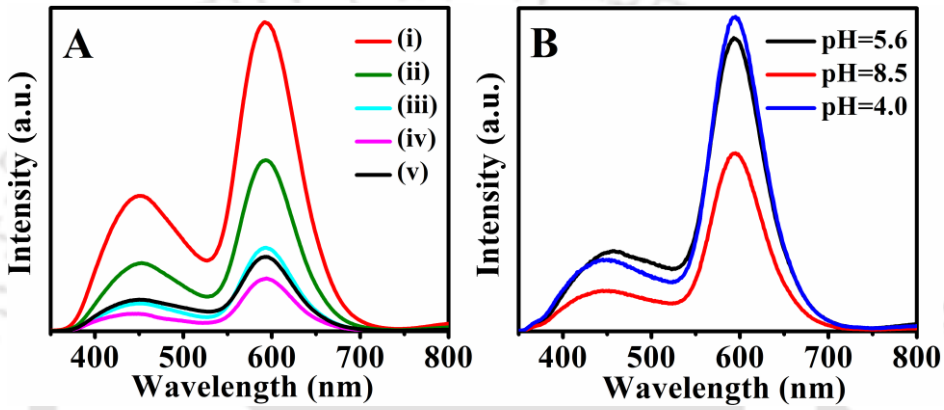


**Figure 5-4.** (**A**) Emission spectra of the (**i**) as-synthesized $Mn^{2+}$-doped ZnS Qdots and those treated with (**ii**) 50 uL and (**iii**) 100 uL of 0.5 mM of copper acetate, followed by treatment with 12 mM of $NaBH_4$ and incubated for (**iv**) 10 min and (**v**) 30 min. (**B**) Emission spectra of the as-synthesized $Mn^{2+}$ and $Cu^{2+}$ (double) doped ZnS Qdots at different pH.

The QY of the $NaBH_4$ treated sample reached its maximum of 17% within 1 h, after which the intensity started to decrease. It normally took about 6 h for reverting back to the original spectrum. The peak due to $Mn^{2+}$ decreased simultaneously. On the other hand, if the $NaBH_4$ treated sample was subsequently treated with KPS; the original spectrum was obtained in 10 min (Figure 5-2B). The reversibility of emission could easily be observed for two cycles; however, adjustment of pH of the medium was necessary for reaction to occur. Emission spectra of the double doped Qdots at different pH are shown in Figure 5-4B. Similar reversibility has also been observed for double doped Qdots treated first with KPS and then with $NaBH_4$ (Figure 5-5A). Interestingly, upon addition of excess (1.8 mM) KPS to the QDots the peak due to $Mn^{2+}$ disappeared completely

and only the peak corresponding to the host ZnS remained (Figure 5-5B). Further, addition of $NaBH_4$ did not result in the reversal of intensity. It could be that upon addition of higher concentration of KPS, surface ions responsible for emission were etched out irreversibly.

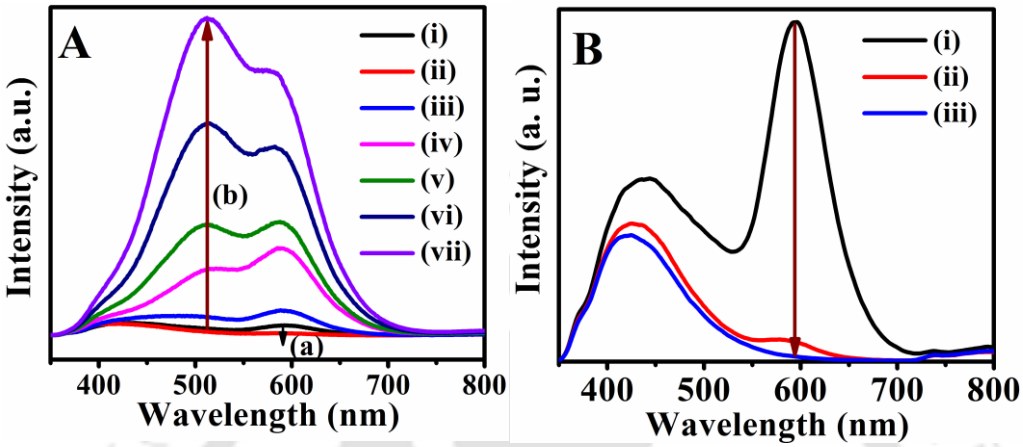


**Figure 5-5.** Time evolution of emission spectrum of (**i**) 3.0 mL of as-synthesized $Mn^{2+}$ and $Cu^{2+}$ (double) doped ZnS Qdots when treated with (**A**) 0.2 mM of KPS (**ii**), which was followed by 12 mM $NaBH_4$ addition at different time interval up to 1 h (iii-vii); Arrows labeled with (a) and (b) indicate the direction of changes in emission spectra following addition of appropriate redox reagents. (**B**) Emission spectra of the Qdots in the presence of 1.8 mM of KPS incubated for (**ii**) 5 min and (**iii**) 10 min.

Overall, orange (as-synthesized Qdots), yellow ($NaBH_4$ treated Qdots) and blue (excess KPS treated Qdots) coloured emission could thus be achieved. It may be added here that the increase in intensity of emission of as-synthesized double doped Qdots could also be observed in the presence of a milder reducing agent (glutathione) confirming the role of a reducing agent in increasing the QY (Figure 5-6).

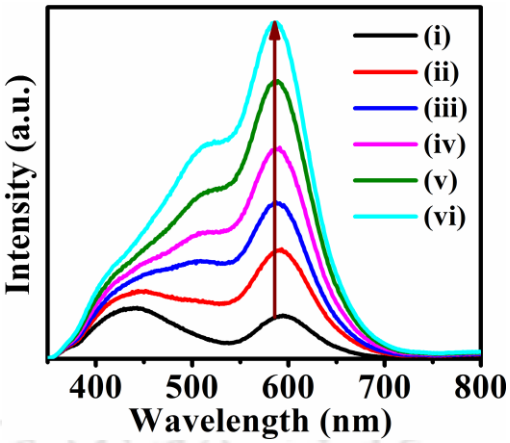


**Figure 5-6.** Time evolution emission spectra of (**i**) as-synthesized $Mn^{2+}$ and $Cu^{2+}$ (double) doped ZnS Qdots upon addition of glutathione and incubation for (**ii**) 10 min, (**iii**) 20 min, (**iv**) 30 min, (**v**) 40 min and (**vi**) 60 min.

Additionally, experiments were performed to compare the fluorescence properties of a mixture of singly doped Qdots vis-à-vis those of double doped Qdots. Dispersions of mixtures of different fractions of the $Cu^{2+}$-doped ZnS and $Mn^{2+}$-doped ZnS Qdots were prepared and their fluorescence behaviour under reducing condition was pursued. The results indicated that when $NaBH_4$ was added to mixture of Qdots, the fluorescent intensity increased less significantly in comparison to that in the case of double doped Qdots. This was true for different fractional mixtures of singly doped Qdots. Interestingly, when the spectra of the as-synthesized mixtures were subtracted from the spectra obtained following addition of $NaBH_4$ only the peak due to Cu could be observed (Figure 5-7). There was no clear peak due to Mn emission. Similar results were observed when Cu-doped ZnS Qdots were first treated with $NaBH_4$ and then Mn-doped ZnS Qdots were added to it, shown in Figure 5-8. On the other hand, similar analysis for the double doped Qdots indicated the presence of peaks due to both Cu and Mn species (Figure 5-7D). This means that emissions from the dopants in double doped Qdots were correlated and thus addition of $NaBH_4$ changed the intensities of emission due to both the species. On the other hand, emissions from the mixture were not correlated and thus they were independent of each other.

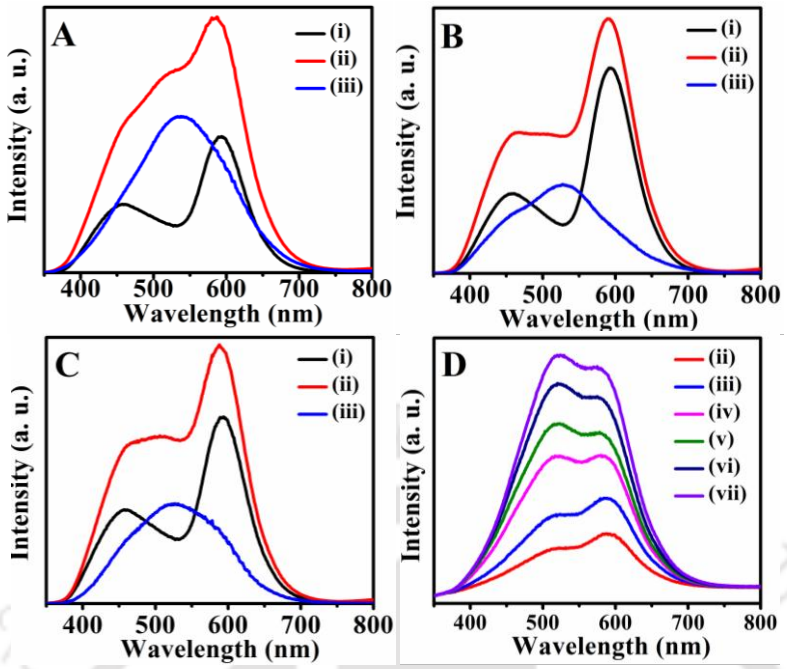


**Figure 5-7.** Fluorescence emission spectra of mixtures of $Cu^{2+}$-doped ZnS and $Mn^{2+}$-doped ZnS Qdots. Spectra in (**A**) are due to a mixture of 1.5 mL of $Cu^{2+}$-doped ZnS and 0.5 mL of $Mn^{2+}$-doped ZnS, (**B**) are due to a mixture of 0.5 mL of $Cu^{2+}$-doped and 1.5 mL of $Mn^{2+}$-doped ZnS, while in (**C**) are due to a mixture of 1.0 mL of $Cu^{2+}$-doped and 1.0 mL of $Mn^{2+}$-doped ZnS Qdots. Also, for all the panels' spectra labelled as (**i**) are due to as-synthesized Qdot mixture, (**ii**) are due to the same dispersion when treated with $NaBH_4$ and incubated for 1.0 h and (**iii**) represent spectra obtained following subtraction of (**i**) from (**ii**). (**D**) Fluorescence emission spectra of $Cu^{2+}$ and $Mn^{2+}$ double doped ZnS Qdots (in the presence of $NaBH_4$) obtained following subtraction of spectrum 5-2A(i) from the rest of the spectra in Figure 5-2A. The resultant spectra in (D) are very different from those obtained following same procedure from the spectra of a simple mixture of singly doped Qdots.

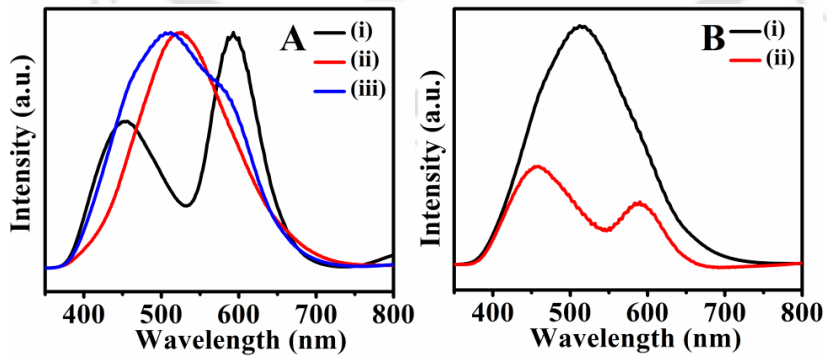


**Figure 5-8.** (**A**) Fluorescence emission spectra of (**i**) 2 mL of Mn-doped ZnS Qdots, (**ii**) 2 mL of Cu-doped ZnS Qdots treated with $NaBH_4$ and **(iii)** mixture of Qdots containing- 2 mL of dispersion in (**ii**) to which 0.5 mL of (**i**) had been added. (**B**) (**iv**) The emission spectra obtained following subtraction of spectrum in (**A**) (**iii**) by (**A**)(**i**) and that following subtraction of spectrum in (**A**) (**iii**) by (**A**) (**ii**). The volume dilution due to mixing was factored in the calculation.

In other words, in a mixture, singly doped Qdots do not affect emission of each other and emission of one could easily be separated from the other. However, in double doped Qdots emissions from two species were correlated and thus simple subtraction would not result in separation of emissions from both the species. Further, we would like to mention here that the current results do not exclude the possibility of presence of individual singly doped Qdots in the medium. This can possibly be concluded using fluorescence microscopic or spectroscopic studies of individual crystals of Qdots. In addition, time-resolved fluorescence emission studies may also provide additional information about the level of double doping in the crystals.

It is important to mention here that UV-vis spectrum of the Qdots was not affected by the presence of reducing or oxidizing agent indicating their stability. This was further supported by the excitation spectrum which remained unaffected in the presence of the redox agents. Excitation spectra were also recorded corresponding to Cu and Mn emission at 520 nm and 590 nm, respectively (Figure 5-9). The results indicated that both ions were doped in the same crystals as the resultant spectra were nearly identical. Additionally, the Qdots were excited - following addition of $NaBH_4$ and incubation for 1 h - at wavelengths beyond the band gap of ZnS NCs (Figure A5-5, Appendix). Weak emission intensity was observed for excitation at energy lower than the band edge energy of the crystals (i.e. at 380 nm), indicating emission originating from the tail region of the absorption spectrum.

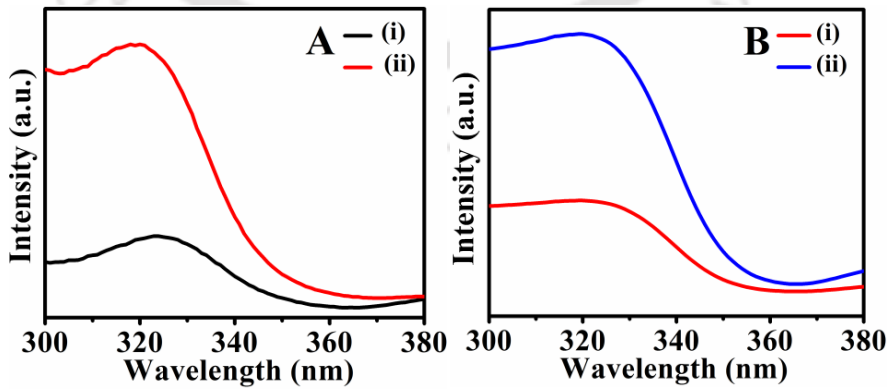


**Figure 5-9.** Excitation spectra of (**i**) as-synthesized $Mn^{2+}$ and $Cu^{2+}$ (double) doped ZnS Qdots and (**ii**) the same Qdots treated with 12 mM of $NaBH_4$ and incubated for 15 min. Emission wavelength was set at 590 nm in (**A**) and 520 nm in (**B**).

Additionally, powder XRD (Figure 5-10) and TEM (Figure 5-11) measurements of the double doped Qdots indicated no change in the size following treatment with the redox agents.

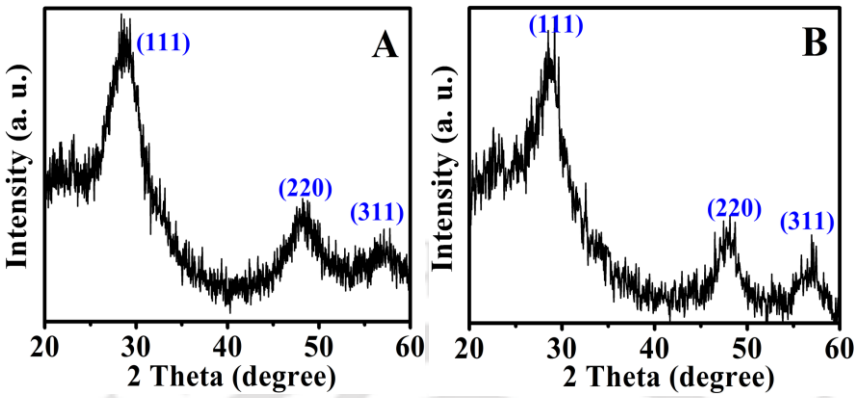


**Figure 5-10.** Powder XRD patterns recorded for $Mn^{2+}$ and $Cu^{2+}$ (double) doped ZnS Qdots treated with (a) 12 mM of $NaBH_4$ and (b) 0.2 mM of KPS.

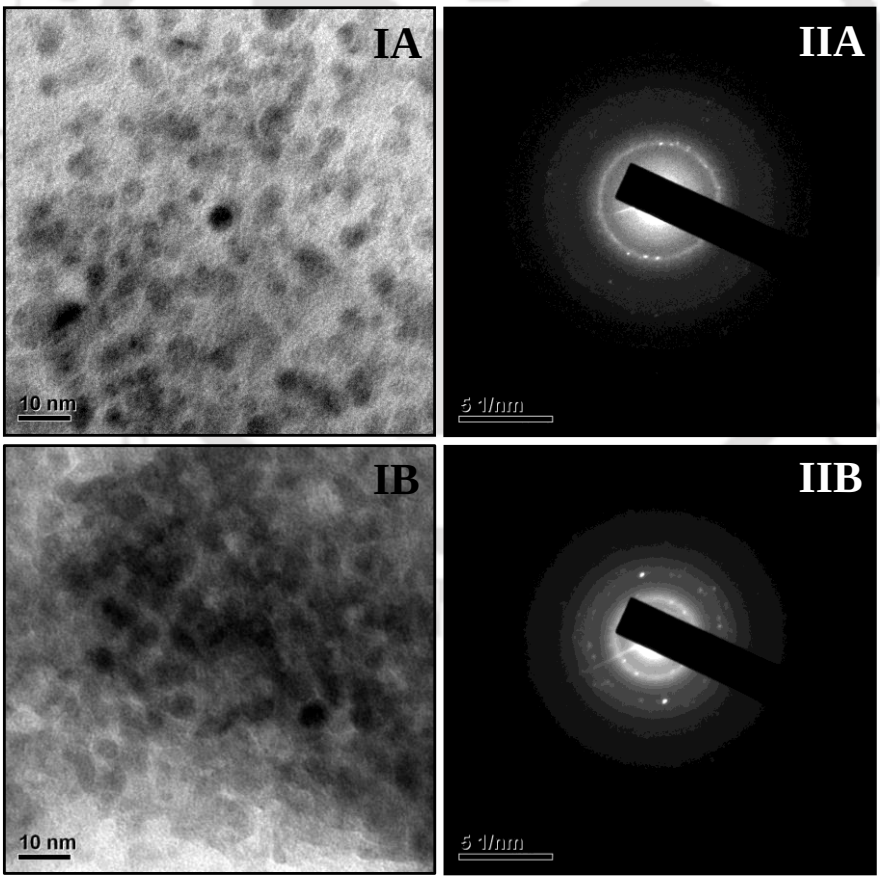


**Figure 5-11.** (**I**) TEM image and (**II**) SAED patterns recorded for $Mn^{2+}$ and $Cu^{2+}$ (double) -doped ZnS Qdots treated with (**A**) $NaBH_4$ (**B**) KPS.

Electron spin resonance (ESR) spectrum of as-synthesized Qdots suggested the presence of both $Cu^{2+}$ and $Mn^{2+}$ ions. Four allowed transition lines corresponding to quadruple interaction with the $Cu^{2+}$ nucleus ($M_I=^3/_2$) and six hyperfine splitting corresponding to $Mn^{2+}$ nucleus ($M_I=^5/_2$) are expected to occur. However, it was observed that broadening of peaks in the ESR spectrum of as-synthesized Qdots (Figure 5-12A) and thus the spectrum could not be resolved. This broadening could be attributed to magnetic dipole- dipole interaction between the nuclei present on the surface as clusters.[23-24] Further, that the spectra of the two ions partially overlapped complicated the matter (Figure 5-12A), along with weak signal due to $Cu^{2+}$. When the sample was treated with $NaBH_4$ the spectrum due to $Mn^{2+}$ ions appeared more prominently (Figure 5-12B), as because $Cu^{+}$ does not exhibit ESR signal.[25] On the other hand, treatment with KPS led to appearance of prominent $Cu^{2+}$ signal, along with weaker $Mn^{2+}$ signal (Figure 5-12C). Further, when Qdots treated with KPS were subsequently treated with $NaBH_4$, the peaks corresponding to $Cu^{2+}$ did not disappear completely; however spectrum corresponding to Mn reappeared (Figure 5-12D). Overall, the quality of signal was poorer for the double doped Qdots in comparison to singly doped Qdots for the same ions (Figure 5-12E, F). Still, the presence of Cu and Mn peaks could be differentiated from the difference in the signal pattern corresponding to both the ions. Additionally, the shifts in the peak positions due to both Cu and Mn in comparison to singly doped Qdots indicated dipolar interactions between the (hetero) ions, in addition to cluster formation of the same ions. However, such dipolar interactions are found to be absent in the mixture of two singly doped Qdots (Mn-doped ZnS and Cu-doped ZnS), where peaks corresponding to $Cu^{2+}$ and $Mn^{2+}$ were simply superimposed at 333 mT for g value equal to 2.024 (Figure 5-12G, H).

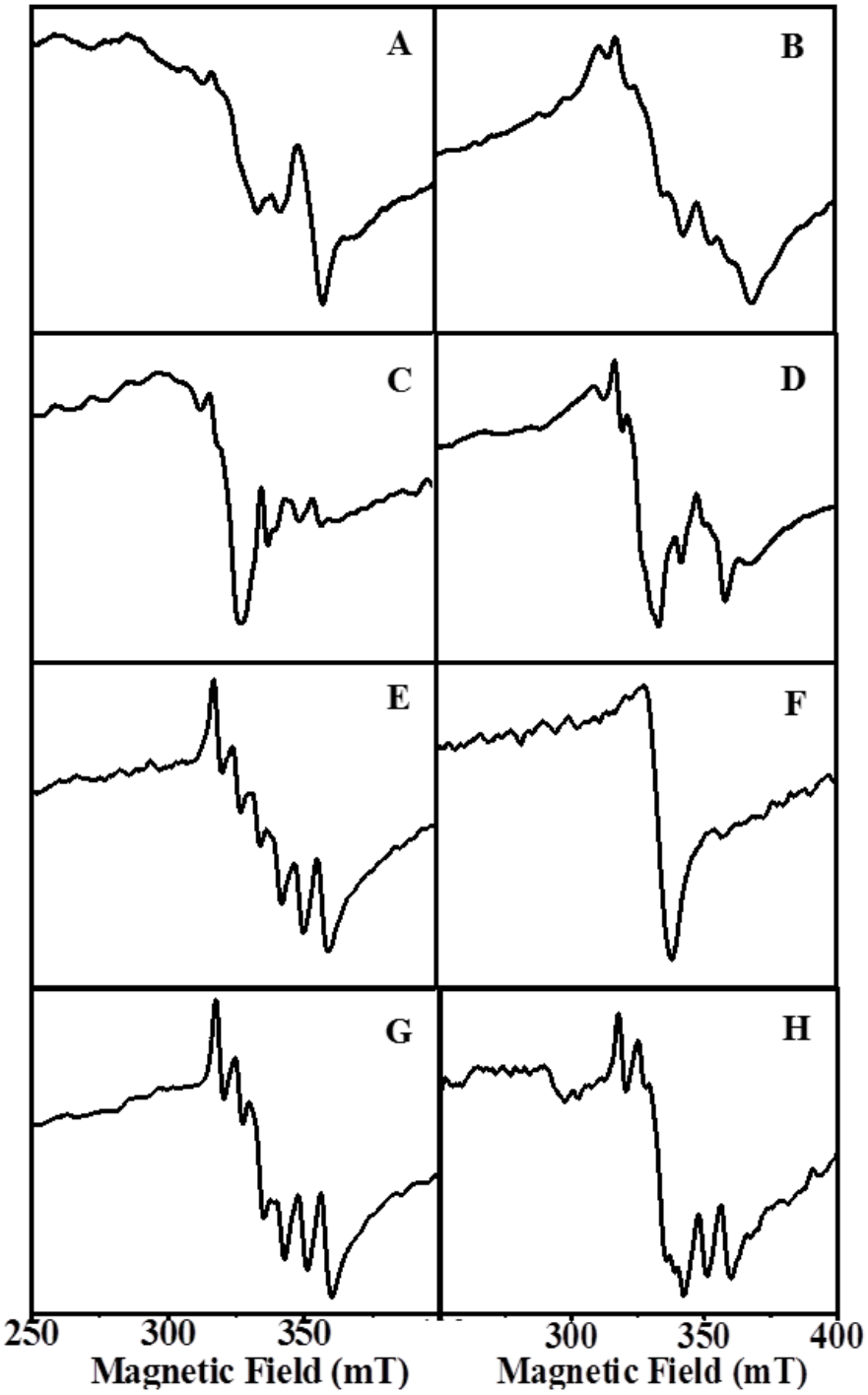


**Figure 5-12.** ESR spectra of $Mn^{2+}$ and $Cu^{2+}$ (double) doped ZnS Qdots; (**A**) as-synthesized; (**B**) those treated with $NaBH_4$; (**C**) those treated with KPS and (**D**) $NaBH_4$ added to KPS treated Qdots (sample in C); ESR spectra of as-synthesized (**E**) $Cu^{2+}$-doped ZnS, (**F**) $Mn^{2+}$-doped ZnS Qdots, (**G**) and (**H**) are due to mixtures of different ratio of sample in (E) and (F).

The results further corroborated the fluorescence measurements with mixture of singly doped Qdots. In other words, the double doped Qdots indeed consisted of both $Cu^{2+}$ and $Mn^{2+}$ ions in the same Qdot and their behaviour could not be explained based on those of a simple stoichiometric mixture of singly doped Qdots.

## 5.4. Conclusion

In conclusion, the chapter describes development of a new and simple method of aqueous synthesis of $Mn^{2+}$ and $Cu^{2+}$ (double) doped ZnS Qdots in the presence of chitosan biopolymer. The results presented above indicated that $Cu^{2+}$ ions in the as-synthesized Qdots were non-emissive, although fluorescence due to host lattice and $Mn^{2+}$ impurities could be observed. Following chemical reduction, additional emission due to $Cu^{+}$ could be observed, accompanied by increase in overall QY. The emission due to Cu could be turned off again in the presence of an oxidizing species. That the redox reactions changed the emission characteristic of a double doped Qdots not only indicated the prominent role of chemical reaction in switching the emission but also pointed to the importance of oxidation state of the emitting dopant. Further, one could envision the application of redox tuned emissive Qdots in electroluminescent devices and in chemical and biological sensing. Finally, that the chemical reaction could decide the fate of emission of Qdots provides a new paradigm in their applications in diverse chemical and biological environment.

## References


1) Reiss, P.; Protie`re M.; Li, L. *Small* **2009**, 5, 154–168.
2) Dabbousi, B. O.; Rodriguez-Viejo, J.; Mikulec, F. V.; Heine, J. R.; Mattoussi, H.; Ober, R.; Jensen, K. F.; Bawendi, M. G. *J. Phys. Chem. B* **1997**, 101, 9463-9475.
3) Derfus, A. M.; Chan, W. C. W.; Bhatia, S. N. *Nano Lett.* **2004**, 4, 11-18.
4) Rinehart, J. D.; Weaver, A. L.; Gamelin, D. R. *J. Am. Chem. Soc.* **2012**, 134, 16175–16177.
5) Han, J.; Zhang, H.; Tang, Y.; Liu, Y.; Yao, X.; Yang, B. *J. Phys. Chem. C* **2009**, 113, 7503–7510.
6) Son, D. H.; Hughes, S. M.; Yin, Y.; Alivisatos, A. P. *Science* **2004**, 306, 1009-1012.
7) Li, H.; Brescia, R.; Krahne, R.; Bertoni, G.; Alcocer, M. J. P.; Andrea, C. D.; Scotognella , F.; Tassone, F.; Zanella, M.; Giorgi, M. D.; Manna, L. *ACS Nano* **2012**, 6, 1637–1647.
8) Begum, R.; Bhandari, S.; Chattopadhyay, A. *Langmuir* **2012**, 28, 9722–9728.
9) Wang, X. S.; Dykstra, T. E.; Salvador, M. R.; Manners, I.; Scholes, G. D.; Winnik, M. A. *J. Am. Chem. Soc.* **2004**, 126, 7784-7785.
10) Lingley, Z.; Lu, S.; Madhukar, A. *Nano Lett.* **2011**, 11, 2887–2891.
11) Wang, C.; Shim, M.; Sionnest P. G. *Science* **2001**, 291, 2390-2392.
12) Weaver, A. L.; Gamelin, D. R. *J. Am. Chem. Soc.* **2012**, 134, 6819–6825.
13) Begum, R.; Sahoo, A. K.; Ghosh, S. S.; Chattopadhyay, A. *Nanoscale* **2014**, DOI:10.1039/C3NR05280J
14) Robinson, R. D.; Sadtler, B.; Demchenko, D. O.; Erdonmez, C. K.; Wang, L. W.; Alivisatos, A. P. *Science* **2007**, 317, 355-358.
15) Jain, P. K.; Amirav, L.; Aloni, S.; Alivisatos, A. P. *J. Am. Chem. Soc.* **2010**, 132, 9997–9999.
16) Begum, R.; Chattopadhyay, A. *Langmuir* **2011**, 27, 6433-6439.
17) Duncan, T. V.; Polanco, M. A. M.; Kim, Y. J.; Park, S. J. *J. Phys. Chem. C* **2009**, 113, 7561–7566.
18) Yang, P.; Lü, M.; Xü, D.; Yuan, D.; Zhou, G. *Appl. Phys. A* **2001**, 73, 455–458.
19) Panda, S. K.; Hickey, S. G.; Demir, H. V.; Eychmüller, A. *Angew. Chem.* **2011**, 123, 4432–4436.

20) Jana, S.; Srivastava, B. B.; Pradhan, N. *J. Phys. Chem. Lett.* **2011**, 2, 1747–1752.

21) Mocatta, D.; Cohen, G.; Schattner, J.; Millo, O.; Rabani, E.; Banin U. *Science* **2011**, 332, 77-81.

22) Sionnest, P. G.; Lhuillier, E.; Liu, H. *J. Chem. Phys*. **2012,** 137, 154704-1-6.

23) Kennedy, T. A.; Glaser, E. R.; Klein, P. B.; Bhargava, R. N. *Phys. Rev. B* **1995**, 52, 356–359.

24) Biswas, S.; Kar, S.; Chaudhuri, S. *J. Phys. Chem. B* **2005**, 109, 17526–17530.

25) Isarov, A. V.; Chrysochoos, J. *Langmuir* **1997**, 13, 3142-3149.

# Chapter 6

## Thesis Overview and Future Prospects

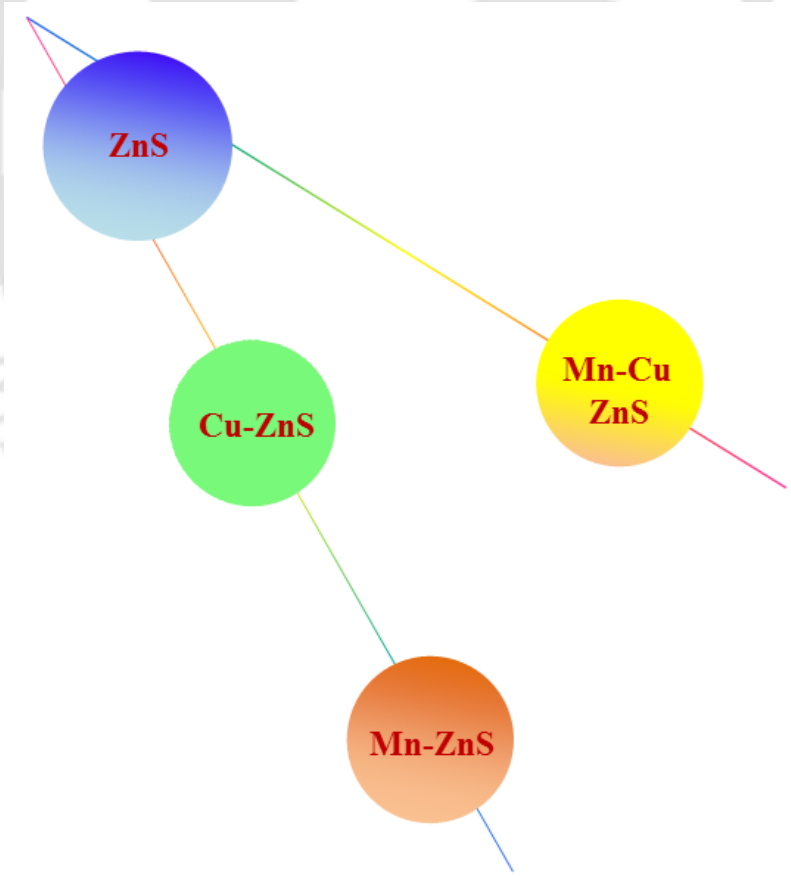

# Chapter 6

## 6.1. Overview of the work done

Quantum dots (Qdots) have the potential to revolutionize, among others, display technologies, solar power harvesting and bioimaging because of their unique optical properties, which could be engineered either by varying their size, shape, composition or through impurity doping. Although substantial research progress has been made with respect to origin of the photoluminescence, there are still scopes for addition to the repertoire of knowledge. A question can be asked about the nature and contribution of the emissive states present on the surface and sub-surface of the Qdots. In this regard, the work undertaken in the current thesis focuses on understanding the chemical reactivity of doped Qdots via surface states which affect their optical properties.

The first study describes surface ion engineering of $Mn^{2+}$-doped ZnS Qdots. When aqueous dispersion of the Qdots was treated with cation exchange resin beads, the quantum yield (QY) increased at lower concentration of beads, which upon treatment with higher amount of beads led to a net decrease. Further, it was observed that at the higher amount of bead treatment, not only there was reduction in QY but also there was a blue shift in the emission peak. This has been interpreted as systematic removal of $Mn^{2+}$ ions as well as clusters of them in the presence of the beads. Thus while the reduction in the number of ions contributed to the decrease in intensity, the reduction in the number of clusters increased the intensity and contributed to the blue shift of the emission. The chapter reports a new approach to tune the optical properties of Qdots following their synthesis, which has not been addressed so far.

Further, reversibly tuned emission in $Mn^{2+}$-doped ZnS Qdots was demonstrated by chemical reaction of dopant ions with redox reagents (Chapter 3). When acetyl acetonate stabilized $Mn^{2+}$-doped ZnS Qdots were treated with potassium peroxodisulfate (KPS), the intensity of emission at 598

nm due to $^4T_1$-$^6A_1$ transition of $Mn^{2+}$ reduced systematically with increasing concentration of KPS and reaction temperature. On the other hand, the emission could be recovered by subsequent treatment of the solution containing KPS-treated Qdots with $NaBH_4$, thus providing reversibility to the tuning, which was possible for more than one cycle. The results have been interpreted as reversible change in the population of the emitting $Mn^{2+}$ ions (via formation of non-emitting $Mn^{3+}$ species). Finally, it has been established that emission due to the dopant element is not only dependent on its concentration but also on its electronic state. Thus, simply by following the emission of the doped Qdots one can possibly probe redox changes in biological cells.

The next work involved development of an intracellular redox sensitive Qdots, which is a chitosan stabilized $Cu^{2+}$-doped ZnS Qdots (Chapter 4). The working principle is based on interactions between cellular components and the atomic states of the doped Qdots, as opposed to the literature known methods which are based primarily on electron transfer between Qdots and functional molecules bound to the Qdots surface. The as-synthesized chitosan stabilized $Cu^{2+}$-doped ZnS Qdots which did not exhibit any discernible emission (a weak emission peak at 420 nm), when treated with a reducing agent ($NaBH_4$ or citrate or ascorbate or glutathione), a new and intense peak appeared at 540 nm. On the other hand, upon addition of KPS to the $NaBH_4$-treated Qdots, the intensity went down immediately. It could be that the $Cu^{2+}$-doped ZnS Qdots reacted with the reducing agents and Cu(I) ions formed thereafter contributed to the green colored emission.

Additionally, when the as-prepared weakly- emissive composite nanoparticles of chitosan and the doped Qdots were added to mammalian cells (HeLa and HEK 293) green fluorescence was observed. Interestingly, pyrogallol (which is otherwise a reducing agent) was added to the cells containing the composite nanoparticles, the emission intensity went significantly down. Since pyrogallol is known to generate reactive oxygen species in the cells, the diminished fluorescence intensity indicated presence of oxidative stress in the intracellular environment.

Following tunable emission in singly doped Mn-doped ZnS and Cu-doped ZnS Qdots, the focus of the work reported in chapter 5 was to synthesize and study origin of fluorescence in double (Mn and Cu)-doped ZnS Qdots. It was found that the synthesized double doped ZnS Qdots emitted from the host lattice and from the $Mn^{2+}$ impurities. There was no emission from $Cu^{2+}$ state – similar to that reported in the previous chapter. However, when $Cu^{2+}$ was reduced to $Cu^{+}$, there was additional emission from $Cu^{+}$ in conjunction with the original emission.

The as-synthesized double-doped Qdots emitted orange, having dual peaks positioned at 592 nm and 460 nm. However, upon treatment with reducing agent, a new peak appeared at 520 nm, accompanied by increase in overall quantum yield. The emission largely appeared to be yellow upon addition of a reducing agent. This could be reversed by reaction with KPS. Further, addition of excess of KPS led to emission in blue (due to host only) with other emissions being turned off. The fluorescence results were interpreted in terms of change in oxidation states of the dopant ions upon reacting with redox reagents.

## 6.2. Concluding Remarks

In short, the essence of the current thesis is post-synthetic modification of optical properties of doped Qdots via chemical reaction of surface dopant ions. That electronic state of the dopant element possibly decides whether the atomic emission would be radiative or non-radiative can be considered to be a new finding.

It is important to mention here that all the Qdots referred to in my thesis involves synthesis in aqueous medium. Moreover, Qdots and the constituent ions are nontoxic or lowly cytotoxic. These have been pursued keeping in view of implications of using environmentally friendly constituents in the preparation of Qdots.

Furthermore, the present work could be extended by following ways.

## 6.3. Future Prospects

- Though the current thesis primarily dealt with redox tunable emission properties of binary doped Qdots, it could possibly be extended to other types of Qdots too, including doped-ternary alloy Qdots.

- With both copper and manganese being paramagnetic ions, the study of their magnetic properties in greater detail may reveal interesting phenomena hitherto unknown.

- Furthermore, double doped Qdots are not much investigated. Thus, synthesis and study of optical properties of double-doped Qdots other than copper-manganese such as cobalt-manganese doped, and nickel-manganese using different host materials could also be attempted.

- Electroluminescence and phosphorescence study could further aid understanding of the luminescence based on the redox states of the dopant ions.

At the end, I hope that the reported work in the thesis may be considered a worthy beginning of rich chemistry - in probing the reactions between Qdots and chemical reagents. Chemistry – considered as the central science – may provide plenty of new opportunity in the much sought world of Qdots and their applications in future technology.

# Appendix

# Appendix

**Etching of the Qdots with Strong Acid**

Different amounts of acid (HCl) were added to 2 samples containing 20 mL dispersions of QDots (the resultant pH: 3-4). The pH for sample 1 was 6.4, that of sample 2 was 3.9 and that of sample 3 was 3.2 at the stage of etching. After stirring for an hour, all of the samples were centrifuged and the pellets were redispersed in equal volume of water. As prepared Qdot solution along with these two samples were further digested with strong acid and diluted for AAS (atomic absorption spectroscopy) measurements for estimation of both Zn and Mn. The results are shown below in Table A2-1.

| | % Zn | % Mn |
|---|---|---|
| **Sample 1** (As prepared Qdot) | 88.9 | 11.1 |
| **Sample 2** (Etched Qdot) | 92.9 | 7.1 |
| **Sample 3** (Etched Qdot) | 94.6 | 5.5 |

**Table A2-1.** Mol % of zinc and manganese as obtained from AAS experimental data in as prepared Qdots and samples etched with different amount of HCl.

TEM images were recorded for the above samples (before digestion by strong acid). Sample 1 had average particle size of 4.0 $\pm$ 0.2 nm, as shown in Figure A2-1A, sample 2 (Figure A2-1B) had size 3.8 $\pm$ 0.2 nm and sample 3 (Figure A2-1C) had size 3.0 $\pm$ 0.5 nm.

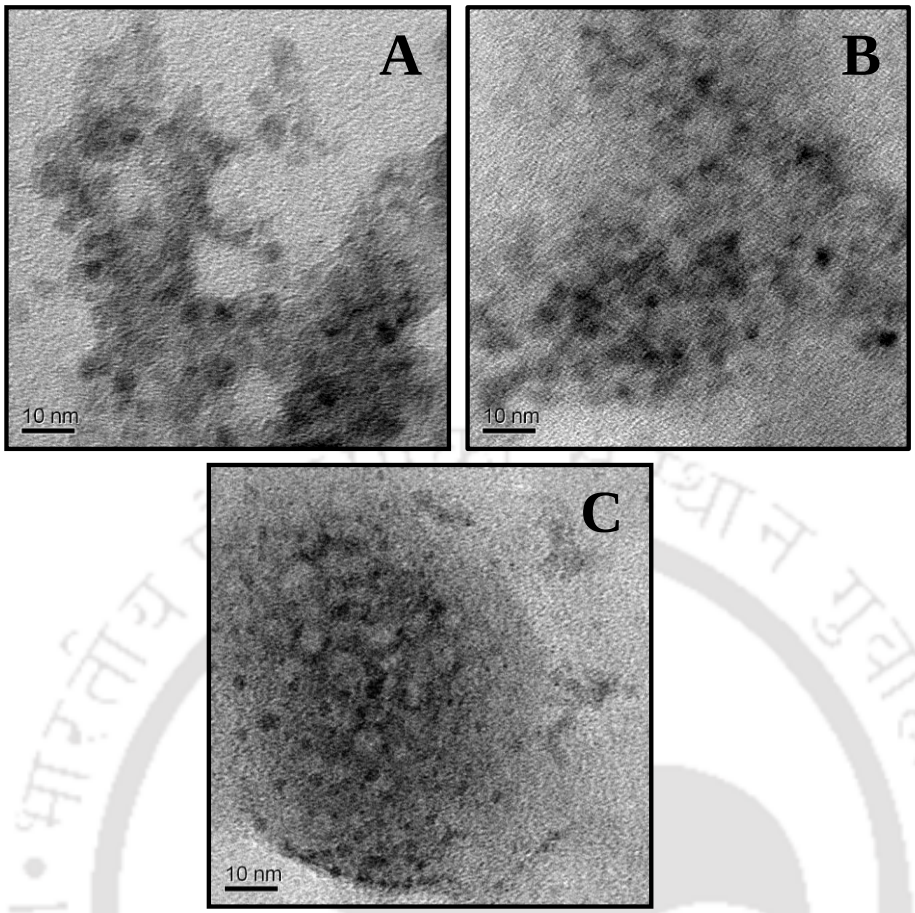


**Figure A2-1.** TEM image of (**A**) as-synthesized Qdots, and those of etched Qdots in (**B**) and (**C**).

UV-vis absorption spectra of the samples following etching for an hour were recorded. The spectra are shown in Figure A2-2.

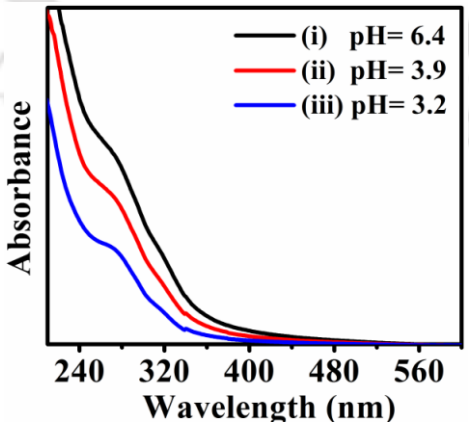


**Figure A2-2.** UV-vis absorption spectra of (**i**) as-synthesized Qdots and those of etched samples (**ii** and **iii**).

Fluorescence emission spectra of the samples were recorded immediately after addition of acid to the Qdots. The results are shown in Figure A2-3. It may again be mentioned here that the pH of as-synthesized Qdots was 6.4 and that of the etched samples (following addition of acid to the Qdots) were 3.9 and 3.2. It was observed that immediately after addition of dilute acid, there was no shift in wavelength maximum, although there was increase in intensity which could be because of removal of excess Mn ions similar to the observation of addition of CB. However, a maximum of 3 to 4 nm blue shift was observed when the spectrum of the same sample was recorded after 1 h of incubation.

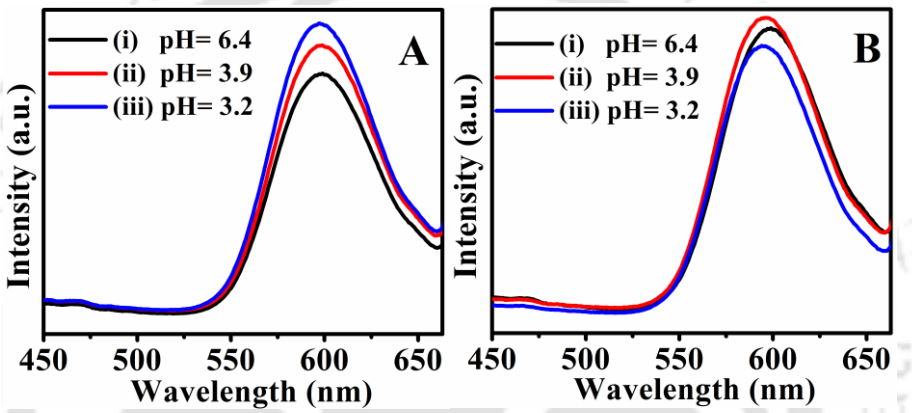


**Figure A2-3.** Fluorescence emission spectra of the Qdots following treatment with acid- The spectra in (**A**) represent samples for which the measurements were made following addition of the acid. On the other hand, the spectra in (**B**) are those of samples incubated with acid for 1 h. The legend (**i**) is for the as-synthesized Qdots and (**ii**) and (**iii**) are for the samples treated with acid. The pH of the medium for each sample is indicated in the legend.

ESR spectra of the Qdots measured following treatment with acid were similar to those of CB-treated samples. The results, shown in Figure A2-4, indicated that the Qdots were etched following incubation with acid and $Mn^{2+}$ ions were removed in the process. The spectra in conjunction with TEM results also indicated that significantly large percentage of $Mn^{2+}$ ions were either present on the surface of the Qdots or in their immediate vicinity.

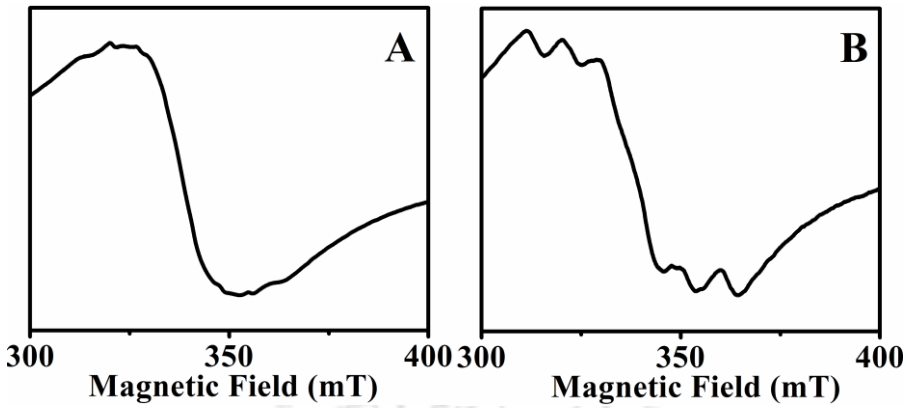


**Figure A2-4.** EPR spectra of (**A**) as-synthesized Qdots and (**B**) the etched sample (having 7% $Mn^{2+}$)

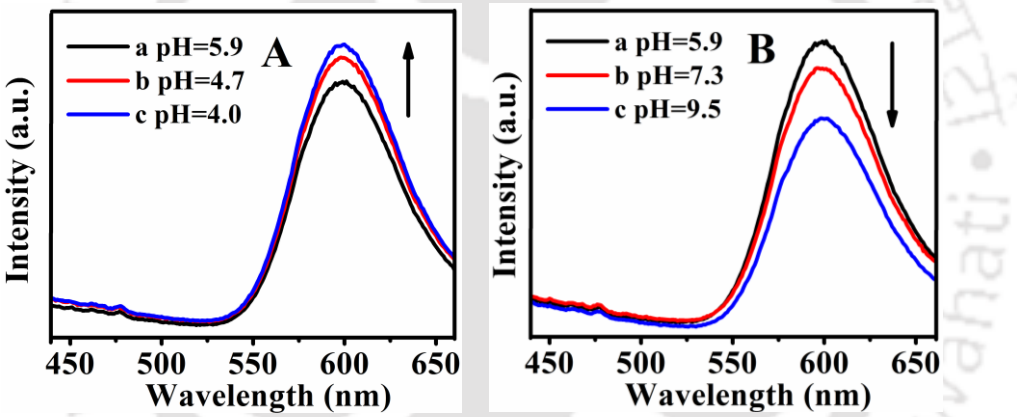


**Figure A3-1.** Effect of pH on the emission of the Qdots. Fluorescence emission spectra of (**A**): (**a**) as-synthesized Qdots and Qdots treated with acid (**b** and **c**). (**B**): (**a**) as-synthesized Qdots and the same treated with alkali (**b** and **c**). The pH of the medium after each addition is mentioned in the legend.

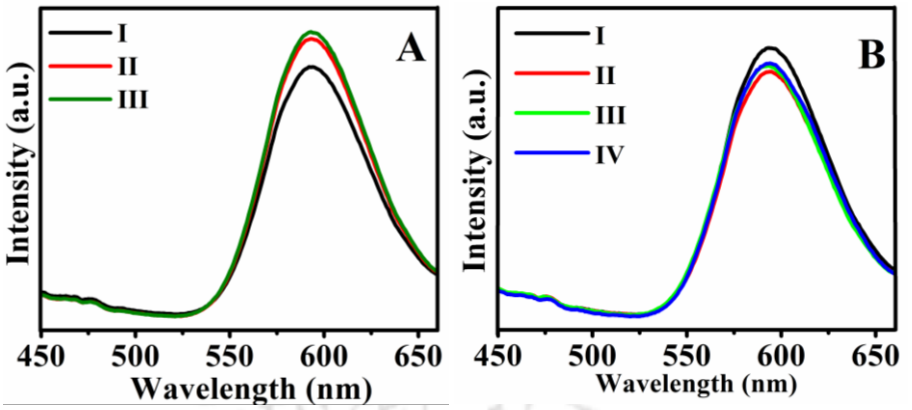


**Figure A3-2.** Fluorescence emission spectra of different dispersions as mentioned in the following. (**A**): (**I**) is that due to as-synthesized Qdots; (**II**) was recorded at 15 min after addition of 14.5 mM sodium citrate; while the spectrum in (**III**) was recorded after 2 h. (**B**): (**I**) is that due to as-synthesized Qdots; (**II**) was recorded at 15 min after addition of 9.7 mM $NaBH_4$; while spectra in (**III**) and (**IV**) were recorded after 2 h and 4 h respectively. The source of Mn of the Qdots was Mn-acetate.

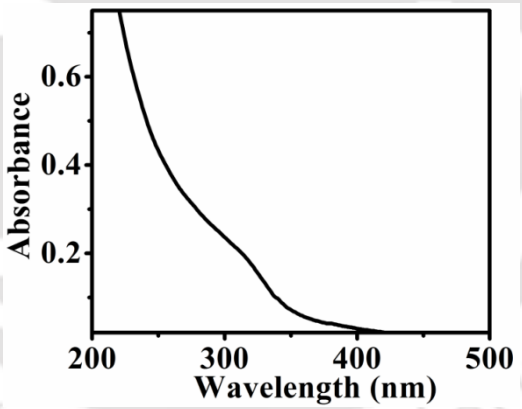


**Figure A3-3.** Optical absorption spectrum of as-synthesized Mn-doped ZnS Qdots (using $KMnO_4$ as the source of Mn).

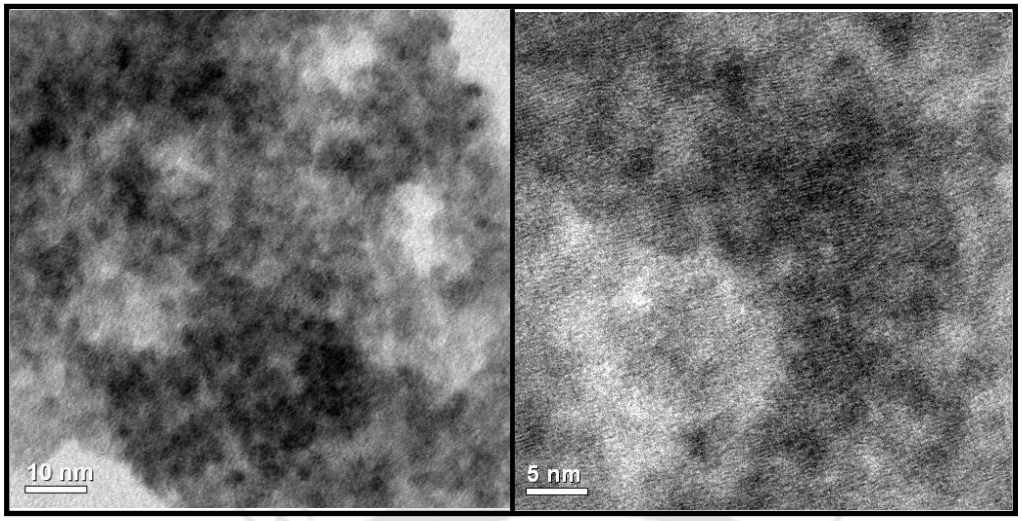


**Figure A3-4.** Transmission electron micrographs, at two resolutions, of as-synthesized Mn-doped ZnS Qdots prepared using $KMnO_4$ as the source of Mn.

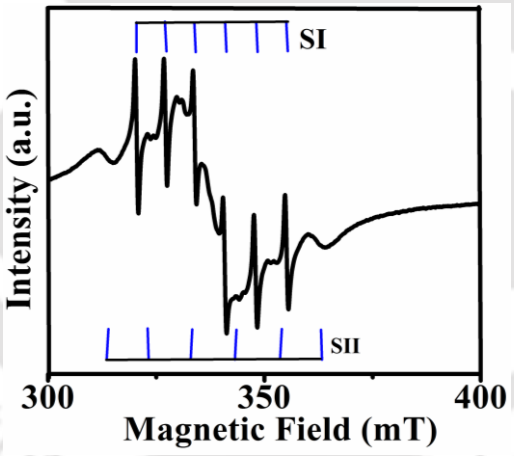


**Figure A3-5.** ESR spectrum of KPS-treated Mn-doped ZnS Qdots, indicating the presence of peaks due to $Mn^{2+}$ ions present both in the tetrahedral and octahedral sites of the crystals. The figure here corresponds to Figure 3-7AII.

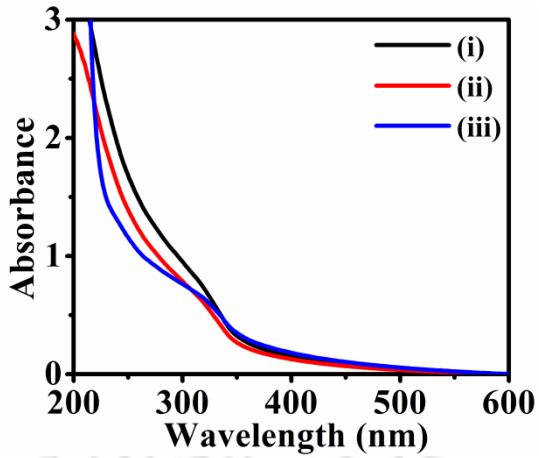


**Figure A4-1.** Absorption spectra of chitosan-stabilized (**i**) ZnS, (**ii**) $Cu^{2+}$-doped ZnS and (**iii**) $NaBH_4$ treated $Cu^{2+}$-doped ZnS.

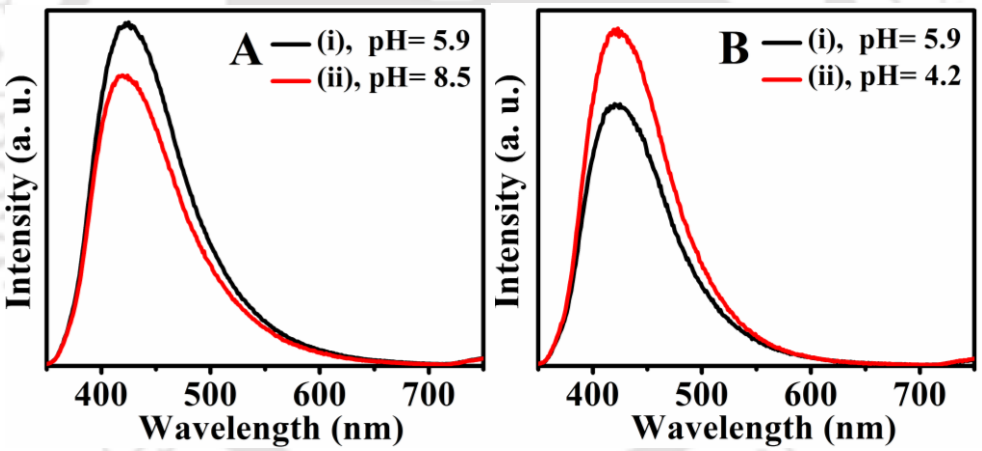


**Figure A4-2.** Emission spectrum of (**i**) as-synthesized Cu-doped ZnS Qdots at pH 5.9 those of sample treated with 25 uL of dilute (**A**) NaOH solutions and (**B**) HCl acid, also incubated for 1 h, respectively.

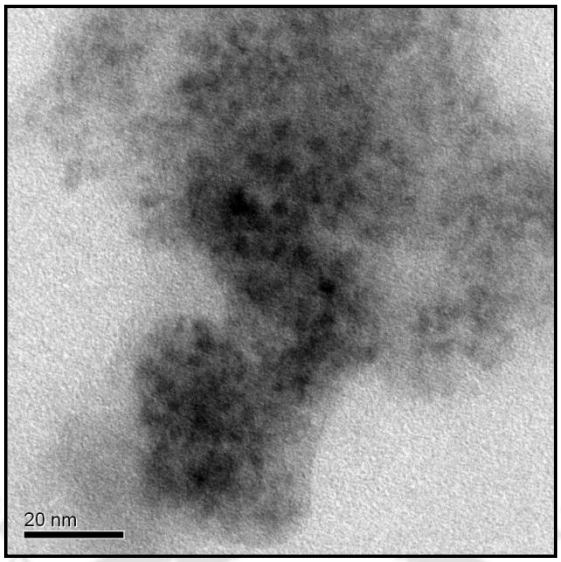


**Figure A4-3.** TEM image of chitosan-stabilized ZnS Qdots.

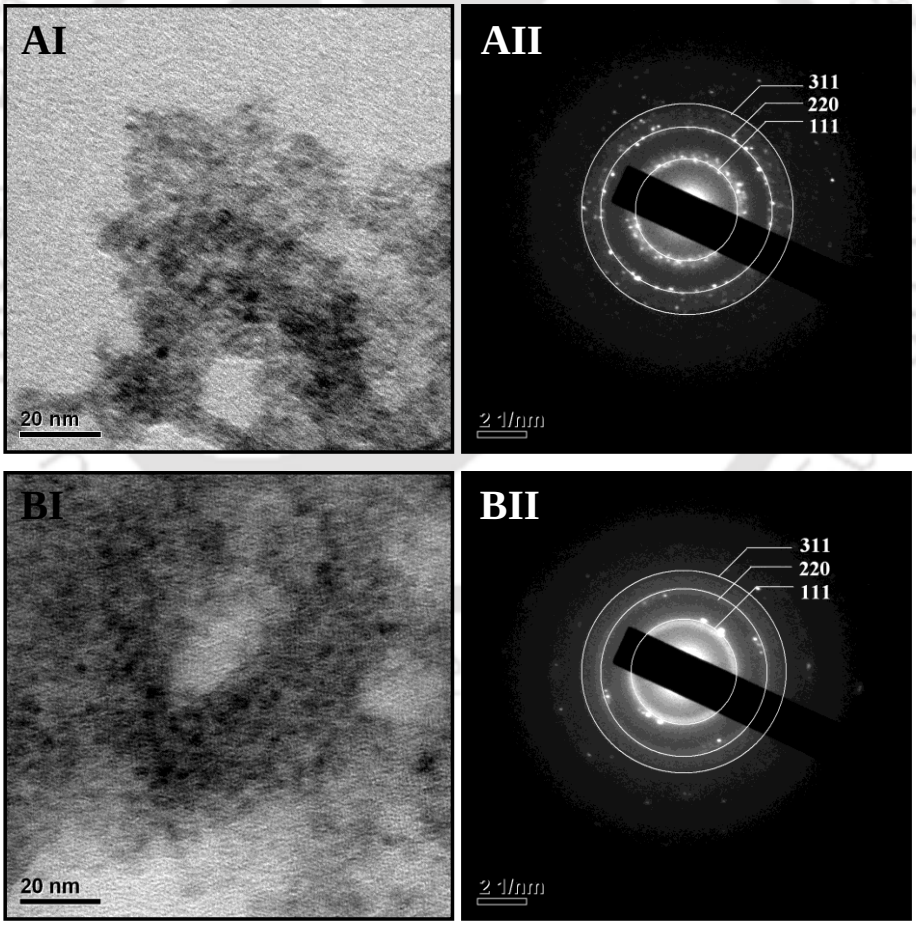


**Figure A4-4.** (**i**)TEM image and (**ii**) SAED pattern of (**A**) $NH_4SCN$ (**B**) trisodium citrate-stabilized $Cu^{2+}$ -doped ZnS Qdots. The diffraction corresponding to lattice planes are identified in Figure (**ii**).

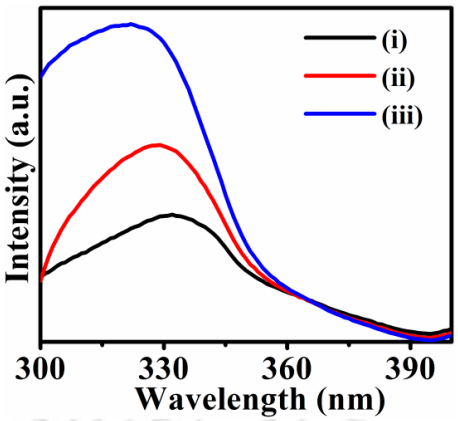


**Figure A4-5.** Excitation spectrum of (**i**) as-synthesized chitosan-stabilized Cu-doped ZnS Qdots; and the same upon treatment with $NaBH_4$ and incubation for (**ii**) 30 min and (**iii**) 1 h. The emission peak was set at 540 nm.

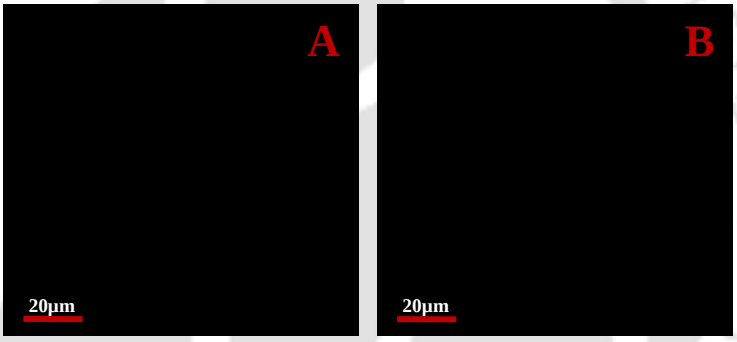


**Figure A4-6.** Fluorescence micrographs of composite NPs of chitosan and $Cu^{2+}$ doped ZnS Qdots treated with $NaBH_4$ captured using (**A**) blue emission filter (435-485 nm) and (**B**) of the same sample followed by KPS treatment, captured using green emission filter (515-555 nm); Scale bar: 20 µm.

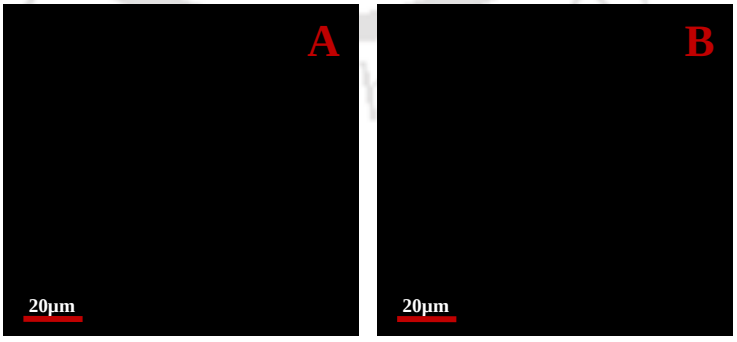


**Figure A4-7.** Fluorescence micrographs of (**A**) composite NPs of chitosan and ZnS Qdots and (**B**) the same treated with $NaBH_4$. Images were captured using a blue emission filter (435-485 nm); Scale bar: 20 µm.

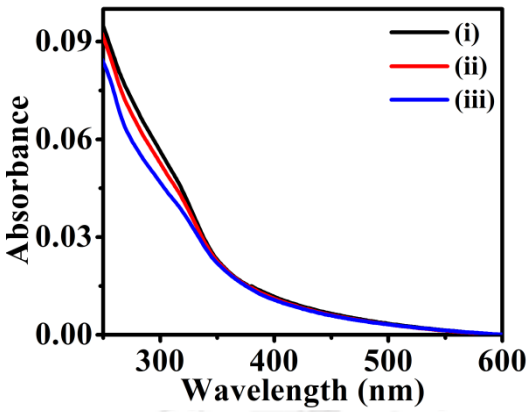


**Figure A5-1.** Absorption spectra of chitosan-stabilized (**i**) as-synthesized $Mn^{2+}$ and $Cu^{2+}$ (double) doped ZnS Qdots and of (**ii**) that obtained following treatment with 12 mM of $NaBH_4$; (**iii**) sample in (**ii**) treated with 0.2 mM of KPS.

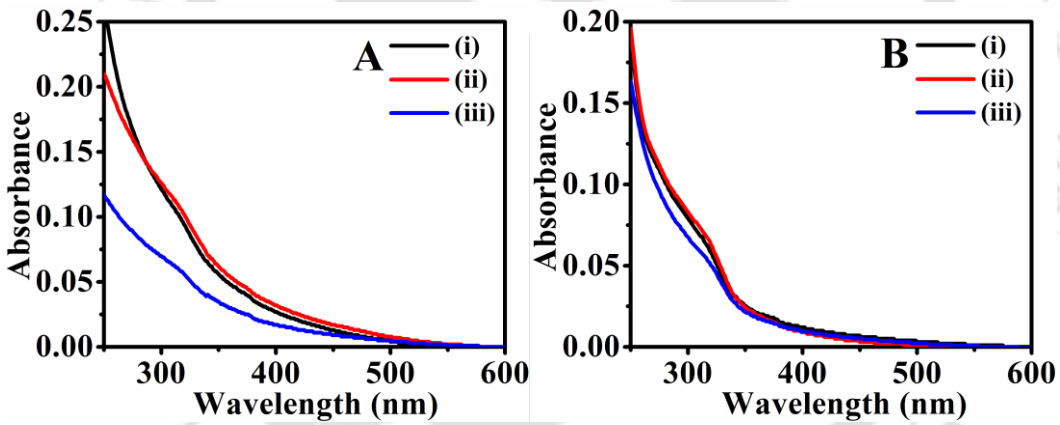


**Figure A5-2.** Absorption spectra of chitosan-stabilized (**A**) as-synthesized $Mn^{2+}$- doped ZnS and (**B**) $Cu^{2+}$ doped ZnS and the same upon treatment with (**i**) 12 mM of $NaBH_4$, (**ii**) following treatment with 0.2 mM of KPS with each being incubated for 10 min.

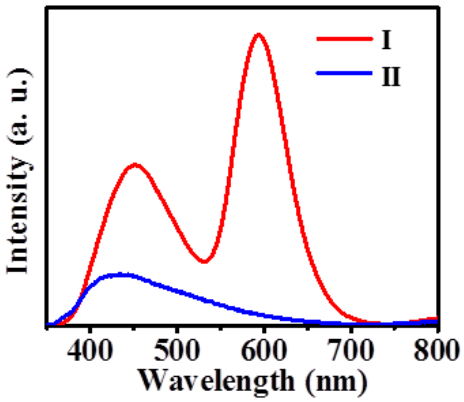


**Figure A5-3.** Emission spectrum of the as-synthesized (**I**) Mn and (**II**) Cu (singly) doped ZnS Qdots. Excitation wavelength was set at 320 nm.

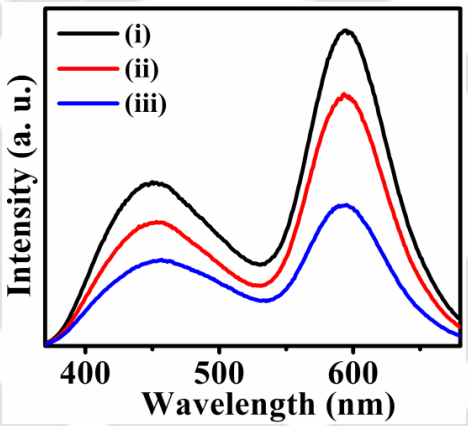


**Figure A5-4.** Time evolution of emission spectrum of (**i**) as synthesized $Mn^{2+}$ and $Cu^{2+}$ (double) doped ZnS Qdots treated with 0.2 mM of KPS and being recorded (**ii**) immediately and (**iii**) after 10 min. Excitation wavelength was set at 320 nm.

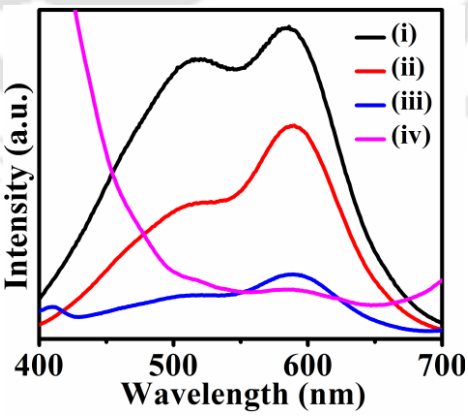


**Figure A5-5.** Fluorescence emission spectra of $NaBH_4$ treated $Cu^{2+}$ and $Mn^{2+}$ double doped ZnS Qdots upon excitation at wavelengths beyond the band edge of ZnS Qdots. The excitation wavelengths were (**i**) 320 nm, (**ii**) 340 nm, (**iii**) 360 nm and (**iv**) 380 nm.

# Publications and Presentations

# List of Publications

1) Begum, R.; Chattopadhyay, A. *J. Phys. Chem. Lett*. **2014**, 5, 126–130.

"Redox Tuned Three-color Emission in Double (Mn and Cu) Doped Zinc Sulphide Quantum Dots"

2) Begum, R.; Sahoo, A. K.; Ghosh, S. S.; Chattopadhyay, A. *Nanoscale* **2014** DOI:10.1039/C3NR05280J

"Recovering Hidden Quanta of $Cu^{2+}$-doped ZnS Quantum Dots in Reductive Environment"

3) Bhandari, S.; Begum, R.; Chattopadhyay, A. *RSC Adv*. **2013**, 3, 2885–2888.

"Surface Ion Engineering for Tuning Dual emission of Ternary Alloyed $Zn_XCd_{1-X}S$ Nanocrystals"

4) Begum, R.; Bhandari, S.; Chattopadhyay, A. *Langmuir* **2012**, 28, 9722–9728.

"Surface Ion Engineering of $Mn^{2+}$-Doped ZnS Quantum Dots Using Ion-Exchange Resins"

5) Begum, R.; Chattopadhyay, A. *Langmuir* **2011**, 27, 6433-6439.

"In Situ Reversible Tuning of Photoluminescence of $Mn^{2+}$-doped ZnS Quantum Dots by Redox Chemistry"

# List of Presentations

1) Poster presentation entitled “Tuning the Optical Properties of Quantum Dots by Chemical Means” at PFAM XXI held during 10-13 December, 2012 organized by Department of Mechanical Engineering, IIT Guwahati.

2) Oral presentation entitled “Chemical Reactions for Modulating Optical Properties of Quantum Dots” at Frontiers in Chemical Sciences (FICS) held during 2- 4 December, 2012 organized by Department of Chemistry, IIT Guwahati.

3) Poster presentation entitled “Chemical tuning of optical properties of Quantum Dots” at Young Scientists' Colloquium 2012" organized by Materials Research Society of India (MRSI) Kolkata Chapter on 8$^{th}$ August 2012 at Central Glass and Ceramic Research Institute (CGCRI), Kolkata.

4) Poster presentation entitled ‘Photoluminescence Tuning of $Mn^{2+}$-doped ZnS Quantum Dots by Redox Chemistry’ in International Conference on Nano Science and Technology (ICONSAT-2012) held during 20-23 January, 2012 in Hyderabad.

5) Oral presentation entitled ‘Tuning the Optical Properties of Quantum Dots by Chemical Means’ in International Conference on Advanced Nanomaterials and Nanotechnology (ICANN) held during 8- 10 December, 2011 in IIT Guwahati.

# Copyright Permissions

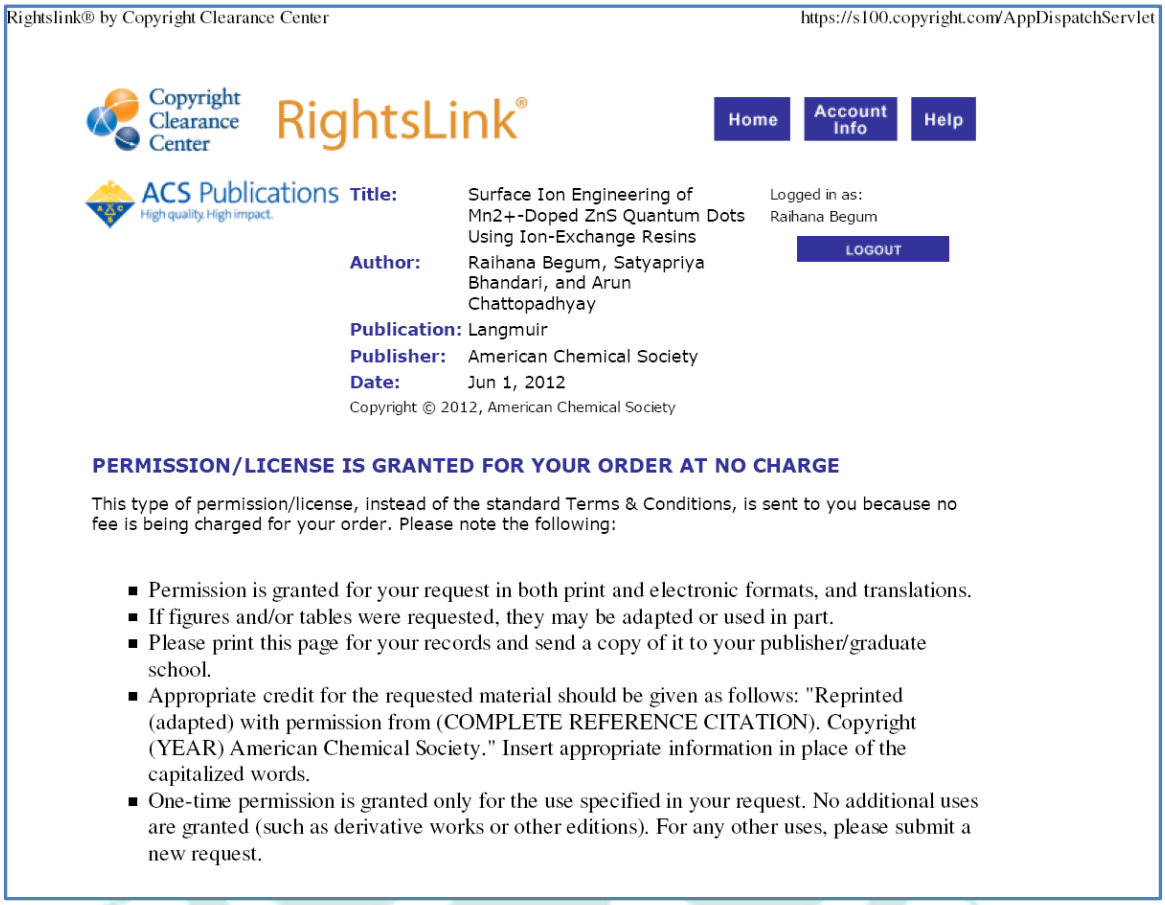

Rightslink® by Copyright Clearance Center https://s100.copyright.com/AppDispatchServlet

Copyright Clearance Center RightsLink®

Home | Account Info | Help

ACS Publications High quality. High impact.

**Title:** Surface Ion Engineering of Mn2+-Doped ZnS Quantum Dots Using Ion-Exchange Resins

**Author:** Raihana Begum, Satyapriya Bhandari, and Arun Chattopadhyay

**Publication:** Langmuir

**Publisher:** American Chemical Society

**Date:** Jun 1, 2012

Copyright © 2012, American Chemical Society

Logged in as: Raihana Begum

LOGOUT

**PERMISSION/LICENSE IS GRANTED FOR YOUR ORDER AT NO CHARGE**

This type of permission/license, instead of the standard Terms & Conditions, is sent to you because no fee is being charged for your order. Please note the following:

- Permission is granted for your request in both print and electronic formats, and translations.
- If figures and/or tables were requested, they may be adapted or used in part.
- Please print this page for your records and send a copy of it to your publisher/graduate school.
- Appropriate credit for the requested material should be given as follows: "Reprinted (adapted) with permission from (COMPLETE REFERENCE CITATION). Copyright (YEAR) American Chemical Society." Insert appropriate information in place of the capitalized words.
- One-time permission is granted only for the use specified in your request. No additional uses are granted (such as derivative works or other editions). For any other uses, please submit a new request.

## Copyright Permissions

RSC | Advancing the Chemical Sciences

Royal Society of Chemistry
Thomas Graham House
Science Park
Milton Road
Cambridge
CB4 0WF

Tel: +44 (0)1223 420 066
Fax: +44 (0)1223 423 623
Email: contracts-copyright@rsc.org

www.rsc.org

## Acknowledgements to be used by RSC authors

Authors of RSC books and journal articles can reproduce material (for example a figure) from the RSC publication in a non-RSC publication, including theses, without formally requesting permission providing that the correct acknowledgement is given to the RSC publication. This permission extends to reproduction of large portions of text or the whole article or book chapter when being reproduced in a thesis.

The acknowledgement to be used depends on the RSC publication in which the material was published and the form of the acknowledgements is as follows:

- For material being reproduced from an article in *New Journal of Chemistry* the acknowledgement should be in the form:
  - [Original citation] - Reproduced by permission of The Royal Society of Chemistry (RSC) on behalf of the Centre National de la Recherche Scientifique (CNRS) and the RSC
- For material being reproduced from an article *Photochemical & Photobiological Sciences* the acknowledgement should be in the form:
  - [Original citation] - Reproduced by permission of The Royal Society of Chemistry (RSC) on behalf of the European Society for Photobiology, the European Photochemistry Association, and RSC
- For material being reproduced from an article in *Physical Chemistry Chemical Physics* the acknowledgement should be in the form:
  - [Original citation] - Reproduced by permission of the PCCP Owner Societies
- For material reproduced from books and any other journal the acknowledgement should be in the form:
  - [Original citation] - Reproduced by permission of The Royal Society of Chemistry

The acknowledgement should also include a hyperlink to the article on the RSC website.

The form of the acknowledgement is also specified in the RSC agreement/licence signed by the corresponding author.

Except in cases of republication in a thesis, this express permission does not cover the reproduction of large portions of text from the RSC publication or reproduction of the whole article or book chapter.

A publisher of a non-RSC publication can use this document as proof that permission is granted to use the material in the non-RSC publication.

VAT Registration Number: GB 342 1764 71 Registered Charity Number: 207890

## Copyright Permissions

# Vitae

Raihana Begum was born in Sivasagar, Assam. She received her bachelor degree in Chemistry from Cotton College, Guwahati and subsequently master degree with specialization in Physical Chemistry from Gauhati University, Guwahati. She has qualified CSIR national eligibility test for junior research fellowship and presently works as a research scholar in the Department of Chemistry, Indian Institute of Technology Guwahati. She joined the department in July, 2008 as a PhD student under the supervision of Prof. Arun Chattopadhyay. Her area of research is chemical reactions involving transition metal doped quantum dots and has her works published in Langmuir, Nanoscale and the Journal of Physical Chemistry Letters. She has also received "MRSI Young Scientists' Award 2012" at "Young Scientists' Colloquium 2012" organized by Materials Research Society of India, Kolkata.